Newcastle University

Master of Philosophy Thesis

Numerical Cosmology

{Bubble Nucleation & Scalar Fields in Numerical Relativity}

Author:
Mario L. Gutierrez Abed

Supervisor(s):
Dr. Ian G. Moss
Dr. Gerasimos Rigopoulos

A thesis submitted in fulfillment of the requirements for the degree of Master of Philosophy

Cosmology and Quantum Gravity Research Group
School of Mathematics, Statistics & Physics

May 29, 2021

Declaration of Authorship

I, Mario L. Gutierrez Abed, declare that this thesis and the work presented in it are my own. I confirm that:

- This work was done wholly or mainly while in candidature for a research degree at this University.
- Where any part of this thesis has previously been submitted for a degree or any other qualification at this University or any other institution, this has been clearly stated.
- Where I have consulted the published work of others, this is always clearly attributed.
- Where I have quoted from the work of others, the source is always given. With the exception of such quotations, this thesis is entirely my own work.
- I have acknowledged all main sources of help.
- Where the thesis is based on work done by myself jointly with others, I have made clear exactly what was done by others and what I have contributed myself.

Signed: 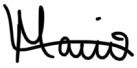

Date: 29/05/2021

"La filosofia è scritta in questo grandissimo libro che continuamente ci sta aperto innanzi a gli occhi (io dico l'universo), ma non si può intendere se prima non s'impara a intender la lingua, e conoscer i caratteri, ne' quali è scritto. Egli è scritto in lingua matematica, e i caratteri sono triangoli, cerchi, ed altre figure geometriche, senza i quali mezzi è impossibile a intenderne umanamente parola; senza questi è un aggirarsi vanamente per un oscuro labirinto."

Galileo Galilei (Il Saggiatore, 1623)

NEWCASTLE UNIVERSITY

Abstract

Mathematics MPhil
School of Mathematics, Statistics & Physics

Master of Philosophy

Numerical Cosmology
{Bubble Nucleation & Scalar Fields in Numerical Relativity}

by Mario L. Gutierrez Abed

Current measurements of the Higgs mass indicate that the Higgs potential develops a lower energy state than the electroweak vacuum, which implies that the quantum phenomenon known as *barrier penetration* (i.e., *quantum tunneling*) might lead to a disastrous decay of our universe's vacuum ([17], [23], [41]). However, one may be relieved to know that, at least according to the currently established Standard Model parameters, our vacuum's lifetime seems to greatly exceed the present age of the Universe. Therefore our vacuum is in a region of *metastability*; it is in a *false vacuum state*.

On the first part of this thesis we study the bubble nucleation and decay of a scalar field that posseses a multi-minima potential –one such minimum being a false vacuum and another the true, absolute vacuum state. We shall investigate both the zero-temperature (*instanton*) and finite-temperature (*caloron*) cases, where we will see how the effects of *quantum tunnelling* and *thermal fluctuations* enter the picture of the false vacuum decay. We present results in up to three spatial dimensions, ignoring gravitational effects and assuming spherical symmetry. Under such symmetry assumptions (and incorporating gravity into the picture), the system of the Einstein Field Equations (EFE's) coupled to matter (by which we mean a massive scalar field) can be reduced to a 1+1D system, and whence it is fairly understood. However, progress beyond spherical symmetry assumptions has been stifled due to the extremely high refinements required to study the stages of nucleation and evolution, which are magnified three-fold in full 3+1 codes. It is precisely the behaviour and evolution of these asymmetric scalar fields in the presence of a gravitational field that we are ultimately interested in studying. This is indeed quite the daunting task, which (unfortunately) we do not get to tackle in this thesis, but nevertheless we study and lay down the foundations of rather sophisticated 3+1 integration schemes in Part II. In particular, we shall present state-of-the-art numerical relativity (NR) techniques that we intend to employ in future work, once computational resources become available. It is only through the use of these advanced methods that we will be able to study the fully asymmetric settings, which are much less understood.

Acknowledgements

I would like to thank first and foremost my supervisors, Ian G. Moss and Gerasimos Rigopoulos, not only for all the knowledge shared and for the invaluable time dedicated to supervising my thesis, but also for all their moral support and for making sure that Newcastle felt like home for my family and I. I thank them for sharing with me their work, ideas, and potential projects, and for helping me understand the physical interpretations of my numerical results (which is the hardest bit for someone like myself whose background is mainly in mathematics, rather than physics!). I have benefited greatly from our time working together.

The acknowledgement is extended to the rest of our Theoretical Cosmology group, for all the great interactions –both on- and off-topic– (the latter, of course, being largely attributed to Marios Bounakis's Brexit rants :P). In particular, I would like to acknowledge Paul McFadden for all his sound academic advice and for his invaluable aid in proof-reading and spotting mistakes in my work; I simply cannot thank him enough. I would also like to thank the entire staff of the School of Mathematics, Statistics & Physics at Newcastle University, for keeping this well-oiled machine running, despite all the recent arduous events. To my office mates, I appreciate you, and I will always miss you. The theorem $\lim_{\star\to\infty}\{\mathrm{Mario}\} = i$ will forever live on [inside joke]. Last but certainly not least, I would like to express my gratitude to my entire family, especially my mother and my wife, for their constant support through thick and thin. You give me the strength and willpower to always push forward, and I cannot overstate how much I appreciate you both for it.

Mario Luis Gutierrez Abed

Contents

Dedicado a mis padres, mi esposa Laura y a mi precioso bebé Alessandro. …

Preface

The present thesis covers material from two seemingly unrelated topics: numerical relativity and false vacuum decay. The former is required in order to solve the Einstein Field Equations (EFE's) of General Relativity (GR) in the absence of significant symmetries, whilst the latter provides some insight into the technicalities of first-order phase transitions in the very early universe. A prominent link between these two active areas of investigation may be established by considering the relevance of scalar field models to cosmology.

As proposed in [12], seeded bubble nucleation can be studied in a laboratory cold-atom analogue of cosmological vacuum decay [25]. Whilst, traditionally, analogue systems have mostly been employed to test ideas in perturbative quantum field theory, there has been recent interest in using such analogue "table-top" experiments on nonperturbative phenomena such as bubble nucleation. Through "modelling the universe in the lab" we hope to gain a better understanding of the process of vacuum decay and the role of the instanton. This is particularly relevant nowadays in light of the recent measurements of the Higgs mass, which currently indicate that our universe's vacuum is in a region of metastability.

In semi-classical studies of the false vacuum decay, one considers the decay rate of an *instanton*, i.e., of a field solution to the imaginary-time classical equations of motion. Such solutions are subject to a quantum effect known as *barrier penetration* (or *quantum tunneling*), which is forbidden at the classical level but are very much present in the quantum realm. It turns out that the nucleation and decay of such scalar field solutions may just have played a significant role during first-order phase transitions in the early universe; thus analysing the transition from *vacuum decay* to *thermal decay* of these instantons is of great importance. Such transitions are associated with supercooled states and the nucleation of bubbles. They arise in a wide range of applications, from the condensation of water vapour to the vacuum decay of fundamental quantum fields. In cosmology, bubbles of a new matter phase would produce huge density variations, and (unsurprisingly) first-order phase transitions have been proposed as sources of gravitational waves [19, 32] and of primordial black holes [24, 31]. In a cosmological context, the temperature is falling as the universe expands, and at some stage the rate for the first-order phase transition becomes smaller than the rate of vacuum decay. New numerical methods developed in this thesis will allow the vacuum-thermal crossover to be studied in detail for the first time, since traditional shooting methods break down in the thermal case due to the lack of rotational symmetry of the bubble.

On the other side of the spectrum, at the purely-classical level, we have scalar fields that obey the (non-imaginary) classical equation of motion (i.e., the Klein Gordon equation). Such a classical field solution may then be coupled with the EFE's to study the scalar field's behaviour under the influence of gravity in many cosmologically-relevant scenarios. For instance, we may be interested in investigating the gravitational collapse of cold dark matter (CDM) candidates known as *axions* (or *axion-like particles* (ALP's)). Two important situations that arise in such settings are the formation of galaxies from dark matter and the collapse of black holes. The galaxy formation case can be analysed using just

Newtonian gravity with novel forms of scalar field matter (e.g., self-interacting or superfluid phonon analogues). The black hole case, on the other hand, needs to be addressed with the full might of Numerical Relativity (NR). Recent work on the non-rotating case [39] points the way to the new results on the rotating case, which is the most interesting scenario since dark matter collapse inevitably involves rotation. Part II of this thesis lays the foundation for future research work in which gravity will be incorporated in order to study the full evolution of asymmetric scalar fields and their applications to cosmology.

To summarise, the main objective of our work is to use both analytical techniques and numerical modelling based on general relativity and scalar boson models to investigate the central role that scalar fields play in solving the dark matter problem of cosmology. Nucleation and decay of scalar field bubbles, as well as the dynamics of such fields in the presence of non-negligible gravitational effects, are two cornerstones of modern cosmology that we are interested in investigating, mostly in the fully asymmetric setting using numerical techniques. The novel investigations presented by [16] hints at the bridge between the two topics covered on this thesis. The paper proposes an alternative picture of vacuum decay, in which the classical evolution (as opposed to the instanton's imaginary-time evolution) of the field from some initial realization of the false vacuum fluctuations leads to the emergence of bubbles. This method, however, has not yet been extended to the thermal decay. The relaxation technique that we present on this thesis does apply to the thermal case, although this is in the semi-classical, instanton picture. A numerical method that successfully tackles thermal decay in the classical scene would be a nice extension to the work presented both in [16] and on this thesis.

Part I

Bubble Decay

Chapter 1

Theoretical Background

Even though at the very beginning of the existence of our universe the structure of spacetime consisted mostly of large scale homogeneity with only small-scale perturbative fluctuations, there is plenty of evidence that suggests that, in occasion, non-perturbative effects may have also played an important role during first-order phase transitions. Amongst the latter, the formation and decay of bubbles has been of much interest to the cosmology community ever since the publication of the classical papers by Coleman & Callan ([17], [23]). The presentation of this thesis consists of a novel numerical approach to the semiclassical treatment of the false vacuum decay studied in these original papers, with particular interest in the intersection of zero-temperature (vacuum) and finite nonzero-temperature (thermal) nucleation. Both instances are described in terms of an ***instanton***, i.e., a scalar field that is a solution of the imaginary-time classical equations of motion (in the thermal case the field is also usually called a ***caloron***). The motivation for choosing to model an instanton over a classical scalar particle satisfying the Klein-Gordon equation (c.f., Eq. (5.49)) is made clear in Figure 1.1: a classical particle does not penetrate a potential barrier, whilst an instanton can be used to calculate the transition probability for a quantum mechanical particle to undergo the phenomenon commonly known as *tunneling*, or *barrier penetration*.

It is, in fact, this transition probability what we are ultimately interested in computing. The ***probability of decay*** per unit time per unit volume, Γ/V, of the false vacuum (FV), is given by

$$\Gamma/V = Ae^{-B/\hbar}[1 + \mathcal{O}(\hbar)], \tag{1.1a}$$

where A and B are quantities that reflect the underlying physics. As in the rest of this thesis, we are using geometrised units ($\hbar = c = k_B = 1$),[1] so we may write (1.1a) as

$$\Gamma/V \approx Ae^{-B}. \tag{1.1b}$$

A numerical treatment of the coefficient B is the focus of the present work. Analytically, it is presented in the original paper [23] as the total Euclidean action $S_E = iS$:

$$B = S_E = \int \left[\frac{1}{2}\mathring{\nabla}^a\phi\mathring{\nabla}_a\phi + U(\phi)\right] \mathrm{d}\tau\, \mathrm{d}\vec{x}. \tag{1.2}$$

Here the scalar field $\phi = \phi(\tau, \vec{x})$ is the instanton, which varies in the spatial coordinates $\vec{x}$ and *imaginary time* $\tau = it$, and $\mathring{\nabla}_a\phi$ is the spatial gradient $D_a\phi$ plus the τ-gradient (in Cartesian coordinates, $\mathring{\nabla}_a\phi = \partial_\tau\phi + \partial_{\vec{x}}\phi$). Meanwhile the quantity U is a multi-minima potential; for instance we may set

$$U(\phi) = \frac{1}{2}\lambda^2 \sin^2\phi - \cos\phi - 1, \tag{1.3}$$

[1] Furthermore, in all the work presented in Part I we are ignoring gravitational effects, thus we are dealing with a flat Riemannian metric.

which exhibits a ***false vacuum*** at $\phi_{\mathrm{FV}} \equiv \pi$ and the ***true vacuum*** at $\phi_{\mathrm{TV}} \equiv 0$ (see figure (1.1)). The parameter λ shows a dependence on temperature in the thermal case (this shall be illustrated later on in Chapter 2); in an early universe setting, this effect plays an important role in placing the field in the false vacuum as the universe supercools. Moreover, we will suppose that at zero temperature the potential barrier is still present, so in this case the temperature dependence of the potential plays less of a role and we will take λ to be constant.

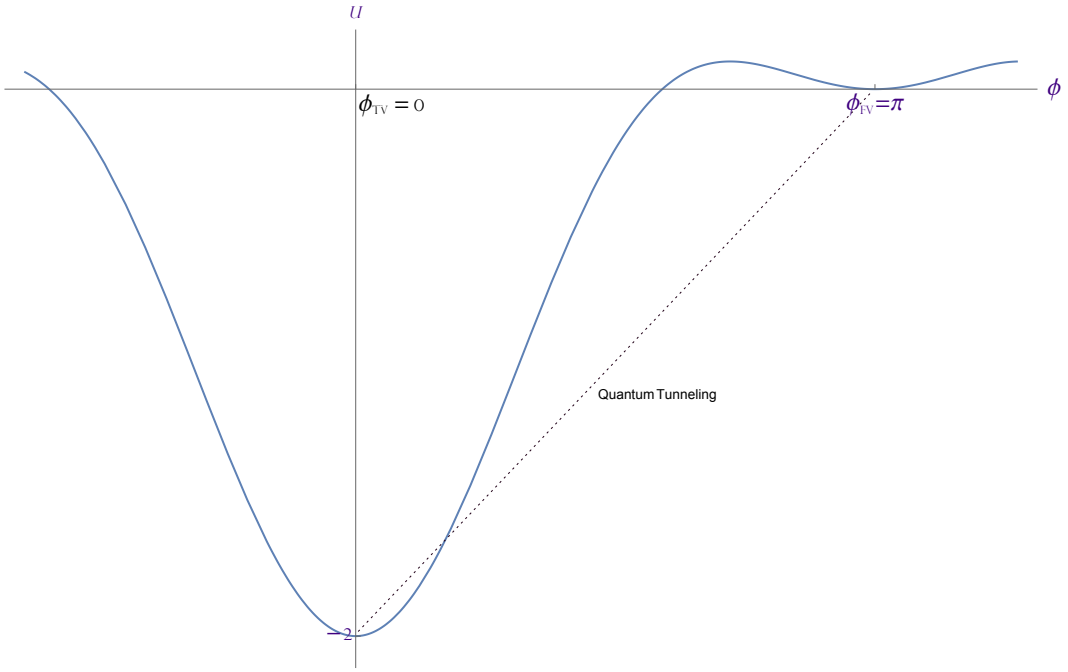

FIGURE 1.1: In classical field theory, the state for which $\phi = \phi_{\mathrm{TV}}$ is the unique classical state of lowest energy, and corresponds to the unique (true) vacuum state of the quantum theory of the field. As for $\phi = \phi_{\mathrm{FV}}$, however, the quantum and classical theories differ in that for the latter ϕ_{FV} is a stable classical equilibrium state, whereas for the quantum case ϕ_{FV} is rendered unstable by barrier penetration (i.e., quantum tunneling). For this reason, in quantum theory ϕ_{FV} is known as a false vacuum.

We note that, since there may be multiple field solutions $\{\phi_i\}$ that satisfy the field equations, we must sum the contributions to Γ/V of all such fields. At non-zero temperature,

$$\mathcal{Z} = \mathrm{Tr}(e^{-\beta\hat{H}}) = \int D\phi\, e^{-S_E[\phi]}, \tag{1.4}$$

where Tr denotes a *trace* over all quantum states, $\hat{H}$ is a *Hamiltonian operator*, and

$$\beta \equiv \frac{\hbar}{k_B T} = \frac{1}{T} \qquad (T = \text{temperature}). \tag{1.5}$$

The thermal aspect of the bubble decay is represented by a periodicity imposed in the τ-coordinate, with period β. At low temperatures, the size of the bubble is small compared to β and thermal effects appear mostly through the form of the effective potential [37]. On the other hand, at higher temperatures –provided the effective potential still has a potential barrier– the instanton solution

becomes constant in the τ-direction. In between there is a cross-over region were instanton solutions become distorted; we see this transition in detail in Figures 1.2 & 2.3). When the temperature is very low (β is very large), the τ-direction is identical to the space directions, and we can expect that the solution has $O(D)$ symmetry (i.e., rotational symmetry of the full D-dimensional configuration). Such a solution (shown on the left of Figs. 1.2 & 2.3) is said to describe *quantum tunnelling*. Conversely, with increasing temperatures (decreasing β), the D-volume becomes "squeezed", and this reshapes the profile of the bubble solution (middle of Figs. 1.2 & 2.3). In this case we say that both *quantum tunnelling* and *thermal fluctuations* play a role. Lastly, for very large T (even smaller β) the bubble profile becomes very squeezed, and we expect that the solution only respects $O(D-1)$ symmetry. [2] Such *classical thermal fluctuation* is shown on the right of Figs 1.2 & 2.3.

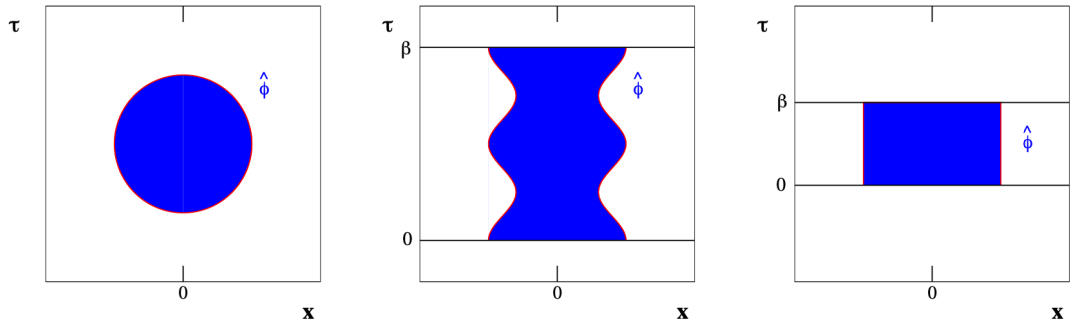

FIGURE 1.2: Transition from vacuum to thermal case. The figure shows the nontrivial bubble solution ϕ_b (here denoted $\hat{\phi}$) in various regimes: at zero (left), intermediate (middle), and high (right) temperatures. The image is taken from [35]; our numerical results shown in Fig 2.3 also show this transition.

We note that we shall not make any use whatsoever of the coefficient A in what follows; the interested reader is advised to consult the original work [17], where it is shown that

$$A = \left| \frac{\det' S_E''[\phi_b]}{\det S_E''[\phi_{FV}]} \right|^{-1/2} \left(\frac{S_E[\phi_b]}{2\pi} \right)^{N/2}. \tag{1.6}$$

Here ϕ_b is the ***bubble*** (or "***bounce***") solution to the equations of motion presented below (c.f., Eq. (1.7)), ϕ_{FV} is the value of the field in the false vacuum ($= \pi$), S_E'' denotes the second functional derivative of the Euclidean action (1.2), and lastly $\det'$ denotes omission of $N = n+1$ zero modes from the functional determinant of the operator in the vacuum case and $N = n$ zero modes for the thermal case.

From variational principles, setting $\delta S_E = 0$ yields the *equation of motion*

$$\mathring{\nabla}^2 \phi - \partial_\phi U = 0. \tag{1.7}$$

[2] It is precisely because of this breaking of symmetry in the thermal case that we have endeavored to find a new numerical technique that solves the equation of motion of the caloron, since the usual shooting methods found in the literature are only applicable to the vacuum case (see full discussion on Chapter 2).

(From a quantum theory perspective, solutions to this equation of motion may be thought of as critical points of the action (1.2).) The term containing the gradient of the potential makes what would otherwise be a straightforward computation (a simple Laplacian) into an equation that is actually very difficult to tackle head on; we must thus resort to numerical methods. In light of the ineffectiveness of shooting methods when dealing with thermal fluctuations, we have developed from scratch a new relaxation scheme that has proven effective in both the vacuum and thermal cases. We shall present all our results in the following chapter, for up to three spatial dimensions. [3]

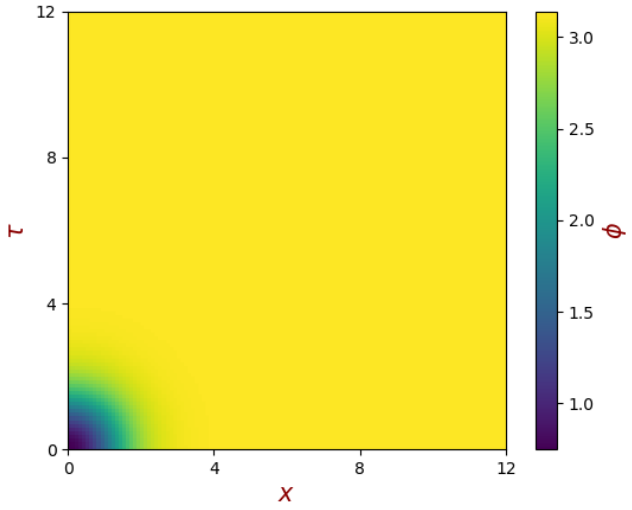

FIGURE 1.3: Initial data (one spatial dimension; vacuum case) given by Eq. (1.9), with $R = \varpi = 1$ and $\mathfrak{e} = 0$. Because of the symmetry assumptions on our bubble, there is no loss of generality in plotting just one quadrant ($x \geq 0, \tau \geq 0$). Note that away from the bubble, which is caused by quantum fluctuations, the false vaccuum persists (this is manifest in the boundary condition (1.8a) and $\lim_{\tau\to\pm\infty}\phi = \phi_{\mathrm{FV}} = \pi$, which holds true in the vacuum case.).

In the vacuum case, the field approaches the false vacuum value $\phi_{\mathrm{FV}} = \pi$ as $\tau \to \pm\infty$, whilst in the thermal case an initial thermal ensemble is represented by solutions that are periodic in τ with periodicity $\beta = 1/T$. Thus we may sum up the boundary conditions for the PDE (1.7) as [4]

$$\lim_{\|\vec{x}\|\to\infty} \phi = \phi_{\mathrm{FV}} = \pi \tag{1.8a}$$

$$\partial_{\vec{x}}\phi(\tau, \vec{x}_{\min}) = 0 \tag{1.8b}$$

$$\partial_\tau\phi(\tau_{\max}, \vec{x}) = \partial_\tau\phi(\tau_{\min}, \vec{x}) = 0. \tag{1.8c}$$

In our numerical implementations we shall use $\tau_{\min} = \vec{x}_{\min} = 0$ and $\vec{x}_{\max} = 12$, whilst $\tau_{\max}$ will be varied in order to consider a range of different temperatures. An approximate bubble solution (see Figure 1.3) we shall use later is given by [5]

$$\phi = \frac{\pi}{2}\left(2 + \tanh\frac{\mathfrak{d} - \mathfrak{R}}{\varpi} - \tanh\frac{\mathfrak{d} + \mathfrak{R}}{\varpi}\right), \tag{1.9}$$

where $\mathfrak{R}$ and ϖ are the radius and wall thickness (i.e., width), respectively, of the bubble. Moreover, we have $\mathfrak{d} = \sqrt{\mathfrak{a}\tau^2 + \mathfrak{b}\vec{x}^2}$, with the parameters $\mathfrak{a} = 1 - \mathfrak{e}^2$ and $\mathfrak{b} = 1 + \mathfrak{e}^2$ determined by the *ellipticity* $0 \leq \mathfrak{e} \leq 1$.

[3] In all cases we assume rotational symmetry of the spatial coordinates; the full 3+1 asymmetric case will be considered in future developments which shall include gravity.

[4] A bit of thought should convince the reader that the last condition (1.8c) suits both the vacuum and thermal cases.

[5] This approximation is the "guess" that we use as initial conditions for the relaxation technique we will present in the next chapter.

In the case where $\mathfrak{e} = 0$ we shall refer to our field as the ***non-static instanton*** and for $\mathfrak{e} = 0.99$ (where the field is (nearly) independent of τ) we will call it the ***quasi-static instanton*** (these are the instances of most importance to our work). In the special case when the field is completely independent of τ (i.e., it is fully static, $\mathfrak{e} = 1$) the equation of motion (1.7) (in Cartesian coordinates) reduces to

$$\partial_{\vec{x}}^2 \phi - \partial_\phi U = 0 \tag{1.10}$$

or, in one spatial dimension,

$$\frac{\mathrm{d}^2\phi}{\mathrm{d}x^2} - \partial_\phi U = 0. \tag{1.11}$$

Here we can easily find a closed-form solution: we have

$$\frac{\mathrm{d}\phi}{\mathrm{d}x} = \sqrt{2U}, \tag{1.12}$$

with the solution bouncing off the potential at $\phi_r = \arccos(1 - 2/\lambda^2)$. [6] The action (1.2) is then reduced to

$$S_E = 2\beta \int_{\phi_r}^{\phi_{\mathrm{FV}}} \sqrt{2U}\, \mathrm{d}\phi, \tag{1.13}$$

which can be obtained in closed-form,

$$S_E = 4\beta \left[\sqrt{\lambda^2 - 1} - \frac{1}{\lambda} \log\left(\sqrt{\lambda^2 - 1} + \lambda \right) \right]. \tag{1.14}$$

Finding such a nice, exact solution for (1.10) in higher spatial dimensions is not feasible, except for when the potential barrier is relatively large (large λ) in the so-called *thin-wall approximation* ([1], [23]). Thus, in the general case, we must turn to numerical solutions; this is precisely what set out to accomplish in the next chapter.

[6] $U(\phi_r) = \frac{1}{2}\lambda^2 \left(1 - \cos^2 \phi_r\right) - \cos\phi_r - 1 = \frac{1}{2}\lambda^2 \left[1 - \left(1 - \frac{2}{\lambda^2}\right)^2\right] - \left(1 - \frac{2}{\lambda^2}\right) - 1 = 0.$

Chapter 2

Numerical Results

A thorough comparison of the theory of bubble nucleation with the proposed table-top experiments in laboratory Bose-Einstein condensates ([16], [25]) requires precise numerical modeling. Such computations of bubble nucleation rates in cosmology are usually obtained using *shooting methods* (e.g., [6], [38]), an option that is viable thanks to the $O(D)$ symmetry enjoyed by the instanton solution in the vacuum case; under such symmetry assumptions the equation of motion can be reduced to an ODE that is easily solved using such methods. This symmetry, however, is not a feature present in the thermal case (as we clearly saw on Fig. 1.2), and as a consequence we need to find an alternative approach [1]. We do, indeed, present in what follows a new numerical method that is valid for calculating nucleation exponents for both thermal and vacuum decay.

2.1 Relaxation Methods

The numerical method we employ in our work is a kind of *relaxation technique*. In the typical relaxation method we start with a guessed solution that satisfies the required boundary conditions and then is gradually modified to satisfy the difference equation within a given tolerance. The classic example is an elliptic PDE such as the Laplace equation (say, in two spatial dimensions),

$$D^2\varphi = \partial_x^2\varphi + \partial_y^2\varphi = 0 \tag{2.1}$$

which, using standard FDM techniques with equidistant spacing $\mathrm{h} = \Delta x = \Delta y$, is rewritten as

$$\frac{\varphi(x+\mathrm{h},y) - 2\varphi(x,y) + \varphi(x-\mathrm{h},y)}{\mathrm{h}^2} + \frac{\varphi(x,y+\mathrm{h}) - 2\varphi(x,y) + \varphi(x,y-\mathrm{h})}{\mathrm{h}^2} = 0. \tag{2.2}$$

Rearranging, and writing in standard FDM notation ($\varphi_{i,j} \equiv \varphi(x,y)$; $\varphi_{i\pm1,j} \equiv \varphi(x\pm\mathrm{h},y)$; $\varphi_{i,j\pm1} \equiv \varphi(x,y\pm\mathrm{h})$), we have

$$\varphi_{i,j} = \frac{\varphi_{i+1,j} + \varphi_{i-1,j} + \varphi_{i,j+1} + \varphi_{i,j-1}}{4}. \tag{2.3}$$

This shows the rather surprising property of the solution to Laplace's equation at any given point on the grid given as the average of the values at the four neighbouring points. From (2.3) we may find an iterative scheme for finding solutions to the Laplace equation.

As we alluded to above, we start with some initial ansatz/guess, [1] and then sweep across the grid updating the value at each point (per Eq. (2.3)). This process is then repeated over and over until we converge to a solution. How do we know we have reached the desired solution? When the change from one iteration to the next is less than some specified tolerance, we declare the solution converged and break the loop. Of course, in theory we would like this change in solution to be zero, but such exact nature is not amenable to numerical computations. Instead we settle for a *residual*

$$r := \frac{\varphi_{i+1,j} + \varphi_{i-1,j} + \varphi_{i,j+1} + \varphi_{i,j-1}}{4} - \varphi_{i,j}$$

to reach a small-enough threshold $r \leq \epsilon$ at which the loop breaks. Intuitively, we may recast this as an evolution-boundary-value problem; start by turning (2.1) into a heat equation

$$\partial_t \varphi = \partial_x^2 \varphi + \partial_y^2 \varphi. \tag{2.4}$$

Then, writing $\varphi_{i,j}^n$ to denote the value of the function φ at the grid point $(x, y) = (i\mathrm{h}, j\mathrm{h})$ at time step $t = n$, the FDA of Eq. (2.4) is

$$\frac{\varphi_{i,j}^{n+1} - \varphi_{i,j}^n}{\Delta t} = \frac{\varphi_{i+1,j}^n + \varphi_{i-1,j}^n + \varphi_{i,j+1}^n + \varphi_{i,j-1}^n - 4\varphi_{i,j}^n}{\mathrm{h}^2}. \tag{2.5}$$

If we now choose (for simplicity) time stepping $\Delta t = \mathrm{h}^2/4$, we end up with

$$\varphi_{i,j}^{n+1} = \frac{\varphi_{i+1,j}^n + \varphi_{i-1,j}^n + \varphi_{i,j+1}^n + \varphi_{i,j-1}^n}{4}, \tag{2.6}$$

which is precisely the iteration described by (2.3), though now with a "time" label. In other words, we can think of our relaxation ploy as a time evolution scheme that searches for a *steady-state* configuration that satisfies Laplace's equation.

As to how exactly we perform the sweep across the grid, there are quite a few options to work with. Our implementation will be the so-called *Jacobi method*, in which we compute all the new values for ϕ at all grid points before moving on to the next iteration. Admittedly, a method such as the *Gauss-Seidel* relaxation –in which we immediately use the updated values to compute the new values at the neighbouring points– is much faster than using Jacobi, but the latter suffices for our needs in the problem at hand.

Back to our main task. By using $\tau = it$ instead of coordinate time t, our equation of motion (1.7) is treated as a boundary value problem (BVP) as opposed to an initial value problem (IVP). In such setting, a relaxation scheme is quite appropriate; thus we proceed by introducing an extra "time" dimension s and an auxiliary scalar $\Phi(s, \tau, x)$. At this point we may naïvely attempt to solve Eq. (1.7) by using a relaxation method as discussed above:

$$\frac{\mathrm{d}\Phi}{\mathrm{d}s} = \mathcal{O}\mathscr{F}, \tag{2.7a}$$

[1] The final solution should not depend on the initial values we guess, but the solution may converge more rapidly if we start with a good ansatz from the onset (i.e., if our guess is reasonably close to the final solution).

where $\mathscr{F}[\Phi] \equiv -S_E'[\Phi]$ is the *residual*

$$\mathscr{F} = \mathring{\nabla}^2\Phi - \partial_\Phi U, \tag{2.8}$$

and the operator $\mathcal{O}$ is introduced to ensure that the scheme converges to the desired solution ϕ_b (i.e., to ensure that $\lim_{s\to\infty} \Phi(s,\tau,x) = \phi_b(\tau,x)$). The simplest such operator is the identity operator, which yields

$$\frac{\mathrm{d}\Phi}{\mathrm{d}s} = \mathscr{F}. \tag{2.7b}$$

We now proceed using one spatial dimension, writing $\Phi^n_{i,j}$ for the value of the field Φ at the grid point $(\tau, x) = (i\mathrm{h}, j\mathrm{h})$ at the time step $s = n$. Discretising (2.7b),

$$\frac{\Phi^{n+1}_{i,j} - \Phi^n_{i,j}}{\Delta s} = \frac{\Phi^n_{i+1,j} + \Phi^n_{i-1,j} + \Phi^n_{i,j+1} + \Phi^n_{i,j-1} - 4\Phi^n_{i,j}}{\mathrm{h}^2} - \frac{\lambda^2}{2}\sin(2\Phi^n_{i,j}) + \sin\Phi^n_{i,j} \tag{2.9a}$$

or, rearranging,

$$\begin{aligned}\Phi^{n+1}_{i,j} = \varsigma\left[\Phi^n_{i+1,j} + \Phi^n_{i-1,j} + \Phi^n_{i,j+1} + \Phi^n_{i,j-1}\right] + \Phi^n_{i,j}\left[1 - 4\varsigma\right] \\ - \Delta s\left[\frac{\lambda^2}{2}\sin(2\Phi^n_{i,j}) + \sin\Phi^n_{i,j}\right]\end{aligned} \tag{2.9b}$$

with

$$\varsigma \equiv \frac{\Delta s}{\mathrm{h}^2}. \tag{2.10}$$

Thus, Equation (2.9b) yields an expression for Φ at the the next "s" time step in terms of the current "s" time step; since this is an *explicit* scheme, we need to be mindful of the Courant-Friedrichs-Lewy (CFL) condition (we have found that $\varsigma \lesssim 1/2$ works). However, there is a problem with this particular relaxation method: regardless of which value we pick for ς, the algorithm does not remain stable for long (this has to do with the spectrum of $\mathscr{F}$; more on this shortly). Hence, after not many interations, Eq. (2.9b) will always relax to a vacuum state, be it the false or the true vacuum (whether we end up with ϕ_{FV} or ϕ_{TV} depends heavily on the length of the potential barrier, and hence on the parameter λ).

The procedure just presented outlines the methodology we are to employ in our work. However, moving forward there are a couple of changes that need to be made, as evident by the instability of Eq. (2.9b). Let us examine the response of the field near the solution Φ_b under the effect of a slight perturbation $\delta\Phi$:

$$\frac{\mathrm{d}\Phi}{\mathrm{d}s} = \frac{\mathrm{d}}{\mathrm{d}s}\left(\Phi_b + \delta\Phi\right) = \underbrace{\frac{\mathrm{d}\Phi_b}{\mathrm{d}s}}_{=0} + \frac{\mathrm{d}(\delta\Phi)}{\mathrm{d}s} = \frac{\mathrm{d}(\delta\Phi)}{\mathrm{d}s}. \tag{2.11}$$

Hence the behaviour of the system close to the bubble solution Φ_b is governed by a second-order operator $\mathscr{F}'[\Phi_b] \equiv \delta\mathscr{F}[\Phi_b]/\delta\Phi$ $(\equiv -S_E''[\Phi_b])$, which is given from Eq. (2.7a) by

$$\frac{\mathrm{d}(\delta\Phi)}{\mathrm{d}s} = \mathcal{O}\mathscr{F}'\delta\Phi. \tag{2.12}$$

Now, choosing $\mathcal{O}$ in such a way that $\mathcal{O}\mathscr{F}'$ has a positive spectrum leads to convergence in a neighbourhood of the solution Φ_b. However note that, since the operator $\mathscr{F}'$ has negative eigenvalues, we are barred from choosing $\mathcal{O}$ to be a multiple of the identity (as we did earlier). Two obvious choices that fulfill the positive spectrum requirement of $\mathcal{O}\mathscr{F}'$ are $\mathcal{O} = (\mathscr{F}')^{-1}$ and $\mathcal{O} = (\mathscr{F}')^\dagger$. The former gives convergence, but it requires a matrix inversion step that may itself be problematic due to small eigenvalues of $\mathscr{F}'$. That leaves $(\mathscr{F}')^\dagger$ as the best choice, which we denote by $\Delta^\dagger$; its action on $\mathscr{F}$ is given by

$$\Delta^\dagger \mathscr{F} \equiv (\mathscr{F}')^\dagger \mathscr{F} = -\mathring{\nabla}^2 \mathscr{F} + \partial_\Phi^2 U \mathscr{F}. \tag{2.13}$$

We plug this back into Eq. (2.7a):

$$\frac{\mathrm{d}\Phi}{\mathrm{d}s} = \Delta^\dagger \mathscr{F}. \tag{2.14a}$$

However, we are not entirely out of the woods just yet; as the von Neumann stability analysis that we will perform shortly reveals, the choice $\mathcal{O} = \Delta^\dagger$ requires a very small numerical relaxation time step ($\Delta s \sim O(\mathrm{h}^4)$; c.f.,Proposition 1). How do we get around this problem? It turns out that recasting (2.14a) as a second-order, damped-oscillator equation in relaxation time,

$$\frac{\mathrm{d}^2\Phi}{\mathrm{d}s^2} + k\frac{\mathrm{d}\Phi}{\mathrm{d}s} = \Delta^\dagger \mathscr{F} \tag{2.14b}$$

provides a stable algorithm that only requires $\Delta s \sim O(\mathrm{h}^2)$ (c.f.,Proposition 2) for stability (provided we use central differencing for the relaxation time derivatives). We now comment on the damping coefficient k: the convergence of (2.14b) is related to the eigenvalue spectrum of $\mathscr{F}'[\phi]$. If we consider a single mode with eigenvalue η, then the amplitude $\delta\phi_\eta$ of the mode decays exponentially,

$$\delta\phi_\eta \propto e^{-ks + \sqrt{k^2 - |\eta|^2}s}. \tag{2.15}$$

For large values of $|\eta|$, the convergence is determined by k, and for small $|\eta|$ by $|\eta|^2/(2k)$. Thus, the optimal value of k would be $k \approx |\eta_{\min}|$, where $\eta_{\min}$ is the eigenvalue with smallest modulus. In practice we ended up only using $k = 1$ in our code.

Finite-differencing Eq. (2.14b), we get

$$\boxed{\Phi_{i,j}^{n+1} = \frac{1}{1+\frac{k}{2}\Delta s}\left\{2\Phi_{i,j}^n - \Phi_{i,j}^{n-1}\left[1 - \tfrac{k}{2}\Delta s\right] + \Delta^\dagger \mathscr{F}(\Phi_{i,j}^n)\Delta s^2\right\}.} \tag{2.16}$$

This algorithm has proven to be quite robust in all cases tested. Note that the $\Phi_{i,j}^{n-1}$ term mandates that we know the value of the field Φ at the $s = -1$ step; we set $\Phi_{i,j}^{-1} = \Phi_{i,j}^0$, since the solutions are damped oscillations and this boundary condition fixes the phase of the oscillation.

2.1.1 von Neumann Analysis

The von Neumann stability analysis of a time-dependent PDE is based on the assumptions that the PDE has constant coefficients (or at the very least the coefficients vary so slowly as to be considered constant), and that the PDE is subject to periodic boundary conditions. Despite the latter, the analysis

actually proves useful even in cases where the boundary conditions are nonperiodic, so we may apply it in all our cases of interest (static, quasi-static, thermal, vacuum). Throughout this subsection we will suppress the spatial dimension for clarity, since the expressions dependent on τ are identical to the expressions dependent on x; i.e., a stability analysis on $\Phi(s,\tau)$ is trivially extended to $\Phi(s,\tau,x)$. To that end we shall write Φ_i^n in place of $\Phi_{i,j}^n$.

The analysis is usually written in terms of the roundoff error

$$\varepsilon_i^n \equiv \tilde{\Phi}_i^n - \Phi_i^n, \tag{2.17}$$

where Φ_i^n is our numerical solution and $\tilde{\Phi}_i^n$ is the finite-precision solution. Then for periodic boundary conditions over some domain $[0, L]$, the error can be represented as a discrete Fourier series

$$\varepsilon(s,\tau) = \sum_m A_m e^{\iota\omega_m\tau}, \tag{2.18}$$

where $\omega_m = (2\pi m)/L$ is the wave number. (Note also that we are using ι to denote the imaginary number $\sqrt{-1}$ to avoid any confusions with the index i.) In our grid then (2.18) takes the form

$$\varepsilon_i^n = \sum_m A_m^n e^{\iota\omega_m\tau_i}, \tag{2.19}$$

where A_m^n is the value of the Fourier coefficient A_m at $n\Delta s$, i.e., at the "time step" n. Moving forward we shall focus our analysis only on one term of the full series, since (by the linearity of our FDAs) it is enough to consider the growth of error of a single Fourier harmonic term. Moreover, instead of writing everything in terms of the error ε, we shall instead write out the analysis in terms of the actual numerical solution $\Phi(s,\tau)$. Hence, from now on we will replace (2.19) with

$$\Phi_i^n = A^n e^{\iota\omega\tau_i}. \tag{2.20}$$

The *von Neumann stability criterium* states that the FDA of the PDE being analysed is stable, provided that

$$|\alpha| \leq 1, \tag{2.21}$$

where α is the *amplification factor*

$$\alpha \equiv \frac{A^{n+1}}{A^n}. \tag{2.22}$$

We are now ready to prove the following stability claims we made earlier:

Proposition 1. *The numerical relaxation time step Δs of the FDA (2.14a) is of order $\sim O(\mathrm{h}^4)$.*

Proposition 2. *The numerical relaxation time step Δs of the FDA (2.14b) is of order $\sim O(\mathrm{h}^2)$.*

Note what the propositions actually state; we are not doing a full stability analysis, but rather searching for some guidance to determine what Δs steps might work with the code. A more thorough analysis is outside our scope. To that end in the proofs we shall use a truncated $\Delta^\dagger\mathscr{F}$ term; expanding (2.13), we have

$$\Delta^\dagger\mathscr{F} = -\partial_\tau^4\Phi - \partial_x^4\Phi + \Upsilon(U), \tag{2.23a}$$

where $\Upsilon(U)$ is an expression containing gradients of the potential that we exclude from our stability analysis. Moreover, the gradient $-\partial_x^4\Phi$ is also excluded because of the omission of the spatial coordinate (we discussed the grounds for doing this at the beginning of this subsection). Hence we shall work instead with

$$\Delta^\dagger \mathscr{F} = -\partial_\tau^4 \Phi. \tag{2.23b}$$

Proof of Proposition 1. Equation (2.14a) is now written as

$$\frac{\mathrm{d}\Phi}{\mathrm{d}s} = -\partial_\tau^4 \Phi, \tag{2.24}$$

which FDA is

$$\frac{\Phi_i^{n+1} - \Phi_i^{n-1}}{2\Delta s} = -\frac{\Phi_{i+2}^n - 4\Phi_{i+1}^n + 6\Phi_i^n - 4\Phi_{i-1}^n + \Phi_{i-2}^n}{\mathrm{h}^4}. \tag{2.25}$$

Writing $\Sigma \equiv \Delta s/\mathrm{h}^4$ and rearranging, we get

$$\Phi_i^{n+1} = -2\Sigma\left\{\Phi_{i+2}^n - 4\Phi_{i+1}^n + 6\Phi_i^n - 4\Phi_{i-1}^n + \Phi_{i-2}^n\right\} + \Phi_i^{n-1}, \tag{2.26}$$

and then using (2.20),

$$\begin{aligned} A^{n+1}e^{\imath\omega\tau_i} = &-2\Sigma\left\{A^n e^{\imath\omega\tau_{i+2}} - 4A^n e^{\imath\omega\tau_{i+1}} + 6A^n e^{\imath\omega\tau_i} - 4A^n e^{\imath\omega\tau_{i-1}} + A^n e^{\imath\omega\tau_{i-2}}\right\} \\ &+ A^{n-1}e^{\imath\omega\tau_i}. \end{aligned} \tag{2.27}$$

We now divide both sides by $A^n e^{\imath\omega\tau_i}$, noting that $e^{\imath\omega\tau_{i\pm1}} = e^{\imath\omega\tau_i}e^{\pm\imath\omega\mathrm{h}}$ and that $A^{n-1}/A^n = A^n/A^{n+1} = \alpha^{-1}$:

$$\alpha = -2\Sigma\left\{e^{2\imath\omega\mathrm{h}} - 4e^{\imath\omega\mathrm{h}} + 6 - 4e^{-\imath\omega\mathrm{h}} + e^{-2\imath\omega\mathrm{h}}\right\} + \frac{1}{\alpha}. \tag{2.28}$$

Then we multiply through by α, and use the identities

$$\cos\varphi = \frac{e^{\imath\varphi} + e^{-\imath\varphi}}{2} \quad \text{and} \quad \cos(2\varphi) = 2\cos^2\varphi - 1, \tag{2.29}$$

to get

$$\begin{aligned} \alpha^2 &= -2\alpha\Sigma\left\{\left(e^{2\imath\omega\mathrm{h}} + e^{-2\imath\omega\mathrm{h}}\right) - 4\left(e^{\imath\omega\mathrm{h}} + e^{-\imath\omega\mathrm{h}}\right) + 6\right\} + 1 \\ &= -2\alpha\Sigma\left\{2\cos(2\omega\mathrm{h}) - 8\cos(\omega\mathrm{h}) + 6\right\} + 1 \\ &= -4\alpha\Sigma\left\{2\cos^2(\omega\mathrm{h}) - 4\cos(\omega\mathrm{h}) + 2\right\} + 1 \\ &= -8\alpha\Sigma\left\{\cos^2(\omega\mathrm{h}) - 2\cos(\omega\mathrm{h}) + 1\right\} + 1 \\ &= -8\alpha\Sigma\left[\cos(\omega\mathrm{h}) - 1\right]^2 + 1. \end{aligned} \tag{2.30}$$

The sinusoidal term comes up again in our analysis; let us denote it as

$$\Theta \equiv \left[\cos(\omega\mathrm{h}) - 1\right]^2. \tag{2.31}$$

Thus we have an equation quadratic in α,

$$\alpha^2 + 8\Sigma\Theta\alpha - 1 = 0. \tag{2.32}$$

Our goal is not to solve this equation, but rather use the von Neumann stability criterion (2.21) to find the order of Δs. Plugging in either 1 or -1 for α in (2.32) does not help since the whole expression vanishes. Let us instead use, say $\alpha = 9/10$. Then

$$\frac{81}{100} + \frac{720}{100}\Sigma\Theta = 1 \implies \Delta s = \frac{19\mathrm{h}^4}{720\Theta}.$$

This shows that $\Delta s \sim O(\mathrm{h}^4)$, as we set out to prove. □

Proof of Proposition 2. Now we check for the stability of the damped-oscillator equation (2.14b):

$$\frac{\mathrm{d}^2\Phi}{\mathrm{d}s^2} + k\frac{\mathrm{d}\Phi}{\mathrm{d}s} = -\partial_\tau^4\Phi, \tag{2.33}$$

which FDA is

$$\frac{\Phi_i^{n+1} - 2\Phi_i^n + \Phi_i^{n-1}}{\Delta s^2} + k\frac{\Phi_i^{n+1} - \Phi_i^{n-1}}{2\Delta s} = -\frac{\Phi_{i+2}^n - 4\Phi_{i+1}^n + 6\Phi_i^n - 4\Phi_{i-1}^n + \Phi_{i-2}^n}{\mathrm{h}^4}. \tag{2.34}$$

We can rewrite this (c.f., (2.16)) as

$$\begin{aligned}\Phi_i^{n+1} &= \frac{1}{1+\frac{k}{2}\Delta s}\left\{2\Phi_i^n - \Phi_i^{n-1}\left[1 - \frac{k}{2}\Delta s\right] - \left(\Phi_{i+2}^n - 4\Phi_{i+1}^n + 6\Phi_i^n - 4\Phi_{i-1}^n + \Phi_{i-2}^n\right)\varsigma^2\right\} \\ &= \frac{1}{1+\frac{k}{2}\Delta s}\left\{\Phi_i^n\left[2 - 6\varsigma^2\right] - \Phi_i^{n-1}\left[1 - \frac{k}{2}\Delta s\right] + \left(4(\Phi_{i+1}^n + \Phi_{i-1}^n) - \Phi_{i+2}^n - \Phi_{i-2}^n\right)\varsigma^2\right\},\end{aligned} \tag{2.35}$$

where ς is given by (2.10). As before we write everything as Fourier harmonic terms,

$$\begin{aligned}A^{n+1}e^{\iota\omega\tau_i} = \frac{1}{1+\frac{k}{2}\Delta s}\{&A^n e^{\iota\omega\tau_i}\left[2 - 6\varsigma^2\right] - A^{n-1}e^{\iota\omega\tau_i}\left[1 - \frac{k}{2}\Delta s\right] + \\ &\left(4(A^n e^{\iota\omega\tau_{i+1}} + A^n e^{\iota\omega\tau_{i-1}}) - A^n e^{\iota\omega\tau_{i+2}} - A^n e^{\iota\omega\tau_{i-2}}\right)\varsigma^2\}\end{aligned} \tag{2.36}$$

which, dividing by $A^n e^{\iota\omega\tau_i}$, becomes

$$\alpha = \frac{1}{1+\frac{k}{2}\Delta s}\{2 - 6\varsigma^2 - \frac{1}{\alpha}\left[1 - \frac{k}{2}\Delta s\right] + \left(4(e^{\iota\omega\mathrm{h}} + e^{-\iota\omega\mathrm{h}}) - (e^{2\iota\omega\mathrm{h}} + e^{-2\iota\omega\mathrm{h}})\right)\varsigma^2\}. \tag{2.37}$$

Mutiplying through by α and using (2.29) and (2.31), we get the following quadratic equation after rearranging terms:

$$\alpha^2\left(1 + \frac{k}{2}\Delta s\right) - 2\left(1 - 2\varsigma^2\Theta\right)\alpha + 1 - \frac{k}{2}\Delta s = 0. \tag{2.38}$$

Letting $\alpha = 1$ makes the whole expression vanish; let us instead try $\alpha = -1$:

$$\left(1 + \frac{k}{2}\Delta s\right) + 2\left(1 - 2\varsigma^2\Theta\right) + 1 - \frac{k}{2}\Delta s = 0 \quad \implies \quad \Delta s = \frac{\mathrm{h}^2}{\sqrt{\Theta}}.$$

Thus we have shown that $\Delta s \sim O(\mathrm{h}^2)$, which makes (2.14b) the more desirable algorithm. □

2.2 Results & Conclusions

We now show all the relevant numerical results obtained from the equation of motion of our instanton. Let us start with the the Euclidean action of the field (1.2). In the 1+1D case, we have

$$S_E = \int \left\{ \frac{1}{2} \left[(\partial_\tau \Phi)^2 + (\partial_x \Phi)^2 \right] + U \right\} \mathrm{d}\tau \, \mathrm{d}x. \tag{2.39a}$$

To numerically evaluate this double integral we implement a 2D composite Simpson method (see § C.1) which, for uniform grid spacing h, is given by the *Frobenius inner product* [2]

$$S_E \approx \frac{\mathrm{h}^2}{9} \boldsymbol{S} \otimes_F \mathcal{L} \equiv \frac{\mathrm{h}^2}{9} \sum_{i=\tau_{\min}}^{\tau_{\max}} \sum_{j=x_{\min}}^{x_{\max}} S_{ij} \, \mathcal{L}_{ij}. \tag{2.40}$$

Here $\boldsymbol{S}$ is the Simpson coefficient matrix (c.f., Eq. (C.20)) and $\mathcal{L}_{ij}$ is the FDA of the Lagrangian

$$\mathcal{L} = \frac{1}{2} \left[(\partial_\tau \Phi)^2 + (\partial_x \Phi)^2 \right] + U. \tag{2.41}$$

The extension of this calculation to two and three spatial dimensions (with $O(D)$ symmetry) is straightforward. In these cases the action (1.2), rewritten in spherical coordinates, takes the form

$$^{2D}S_E = 2\pi \int \left\{ \frac{1}{2} \left[(\partial_\tau \Phi)^2 + (\partial_r \Phi)^2 \right] + U \right\} r \, \mathrm{d}\tau \, \mathrm{d}r \tag{2.39b}$$

$$^{3D}S_E = 4\pi \int \left\{ \frac{1}{2} \left[(\partial_\tau \Phi)^2 + (\partial_r \Phi)^2 \right] + U \right\} r^2 \, \mathrm{d}\tau \, \mathrm{d}r, \tag{2.39c}$$

where $r \equiv \sqrt{\sum_i (x^i)^2}$ is the radial coordinate. The only other consideration that we must take into account is how the gradients $\mathring{\nabla}_a \Phi$ change when written in the new coordinates. In such cases the residual (2.8) is written as

$$^{2D}\mathscr{F}(\Phi) = \partial_\tau^2 \Phi + \partial_r^2 \Phi + \frac{1}{r} \partial_r \Phi - \partial_\Phi U \tag{2.42a}$$

$$^{3D}\mathscr{F}(\Phi) = \partial_\tau^2 \Phi + \partial_r^2 \Phi + \frac{2}{r} \partial_r \Phi - \partial_\Phi U. \tag{2.42b}$$

To work around the coordinate singularity at $r = 0$ we Taylor-expand Φ in a neighbourhood of $r = 0$,

$$\begin{aligned} \Phi(s, \tau, r) &= \Phi(s, \tau, 0) + (r - 0) \cancelto{0}{\partial_r \Phi(s, \tau, 0)} + \frac{(r-0)^2}{2!} \partial_r^2 \Phi(s, \tau, 0) + O(r^3) \\ &\approx \Phi(s, \tau, 0) + \frac{r^2}{2} \partial_r^2 \Phi(s, \tau, 0), \end{aligned} \tag{2.43}$$

[2] Of course, since in our code we are using only one quadrant of the whole grid, (2.40) must be multiplied by 4 in order to get the full action.

where $\partial_r\Phi(s,\tau,0)$ vanished because of the boundary condition (1.8b). Taking the r-derivative of this expression, [3]

$$\begin{aligned}\partial_r\Phi(s,\tau,r) &\approx \partial_r\left(\Phi(s,\tau,0)+\frac{r^2}{2}\partial_r^2\Phi(s,\tau,0)\right)\\ &= \cancelto{0}{\partial_r[\Phi(s,\tau,0)]} + r\,\partial_r^2\Phi(s,\tau,0) + \frac{r^2}{2}\cancelto{0}{\partial_r[\partial_r^2\Phi(s,\tau,0)]}\\ &= r\,\partial_r^2\Phi(s,\tau,0).\end{aligned} \tag{2.44}$$

Hence, in a neighbourhood of $r=0$, we have

$$\frac{1}{r}\partial_r\Phi(s,\tau,r) \approx \partial_r^2\Phi(s,\tau,0).$$

Thus, we rewrite (2.42) as

$${}^{2D}\mathscr{F}(\Phi) = \begin{cases}\partial_\tau^2\Phi + 2\partial_r^2\Phi - \partial_\Phi U & \text{if } r=0,\\ \partial_\tau^2\Phi + \partial_r^2\Phi + \frac{1}{r}\partial_r\Phi - \partial_\Phi U & \text{otherwise;}\end{cases} \tag{2.42c}$$

$${}^{3D}\mathscr{F}(\Phi) = \begin{cases}\partial_\tau^2\Phi + 3\partial_r^2\Phi - \partial_\Phi U & \text{if } r=0,\\ \partial_\tau^2\Phi + \partial_r^2\Phi + \frac{2}{r}\partial_r\Phi - \partial_\Phi U & \text{otherwise.}\end{cases} \tag{2.42d}$$

Figure 2.1 shows the relation between action and temperature for both non-static and quasi-static initial conditions, in all three dimensional cases. Two curious observations are *a)* that we did not find any evidence for a non-static solution with higher action than the quasi-static solution, and *b)* that the critical temperature at which the transition takes place decreases with increasing dimensions.

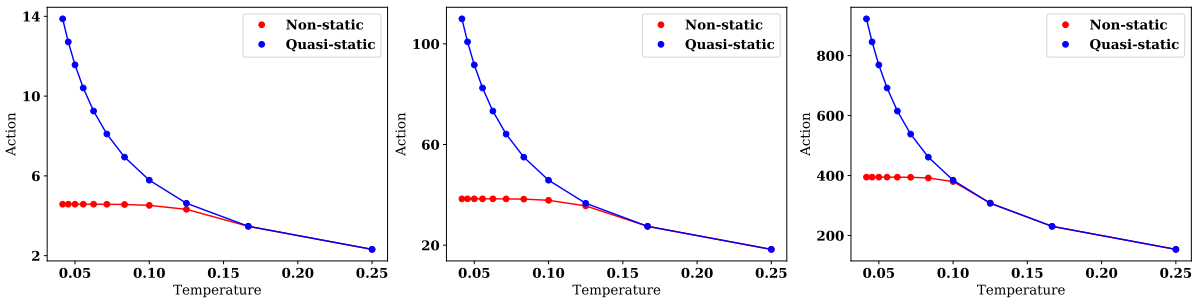

FIGURE 2.1: The plots show the dependence of the Euclidean action on temperature for non-static and quasi-static instantons. From left to right we show one, two, and three spatial dimensions. In all cases $\lambda = 1.2$.

[3] Do note the subtlety in notation; $\partial_r\Phi(s,\tau,0)$ vanished because of the boundary condition (1.8b), whereas $\partial_r[\Phi(s,\tau,0)]$ vanishes because we are taking the r-derivative of a constant expression ($\Phi(s,\tau,0)$).

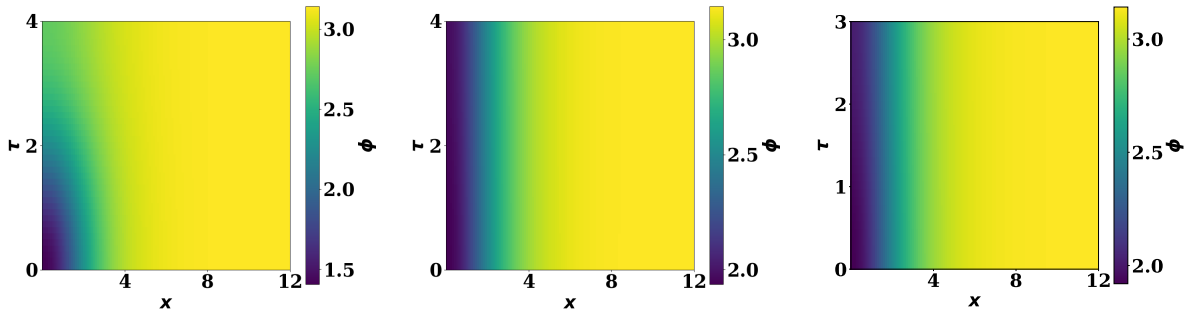

FIGURE 2.2: At $T = 0.125$, the non-static instanton (left) becomes distorted in the imaginary time direction. In the middle figure we show the quasi-static instanton at that very same temperature. Pushing the non-static field to a higher temperature $T = 0.17$ breaks its $O(2)$ symmetry even further and its profile (right) becomes identical to the quasi-static field shown in the middle.

Let us inspect the situation closer near the critical transitional temperature...Consider, for instance, the 1+1D case (left canvas on Fig. 2.1). At around $T = 0.125$ the non-static instanton is becoming distorted and is starting to look a lot like the quasi-static bubble. If we push the temperature just a bit further to, say, $T = 0.17$, the profiles of the non-static and quasi-static fields become indistinguishable (see Fig. 2.2). Focusing strictly on the non-static instanton, we see this transition from vacuum to thermal fluctuations on Figure 2.3 (compare this figure to Fig. 1.2).

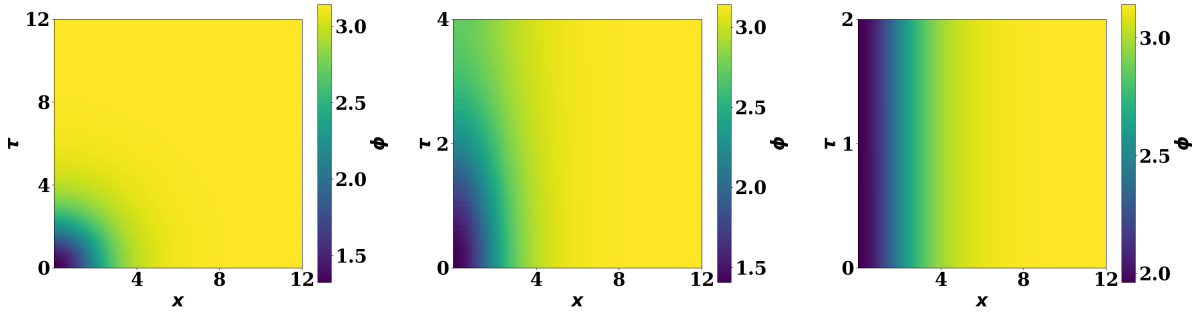

FIGURE 2.3: Transition from vacuum to thermal case of the non-static ($\mathfrak{e} = 0$) instanton, and the breaking of its $O(2)$ symmetry (one spatial dimension). The figure shows minimum [$T \approx 0.04$] (left), medium [$T = 0.125$] (middle), and high [$T = 0.25$] (right) temperatures. We can see how the rotational symmetry of the bubble is broken as temperatures increase. In all cases $\lambda = 1.2$.

The action also shows a dependence on the height of the potential barrier, which is given by the parameter λ; we show this relation on Fig. 2.4. We can quantify this relation through a least squares fitting; let us consider the case with quasi-static initial conditions. From our data (see Table 2.1) we can infer an ansatz $S_E \approx \alpha/(2T)$ for some constant α; let us instead absorb this factor of 2 in α and proceed with a fitting for the ansatz

$$S_E = \frac{\alpha}{T}. \tag{2.45}$$

	T	S_E	
x_0	0.0416667	13.8767	y_0
x_1	0.0454545	12.7177	y_1
x_2	0.05	11.567	y_2
x_3	0.0555556	10.4083	y_3
x_4	0.0625	9.25161	y_4
x_5	0.0714286	8.09933	y_5
x_6	0.0833333	8.09933	y_6
x_7	0.1	5.78424	y_7
x_8	0.125	4.62776	y_8
x_9	0.166667	3.47151	y_9
x_{10}	0.25	2.31488	y_{10}

TABLE 2.1: Relation between action and temperature for the quasi-static, 1+1D instanton.

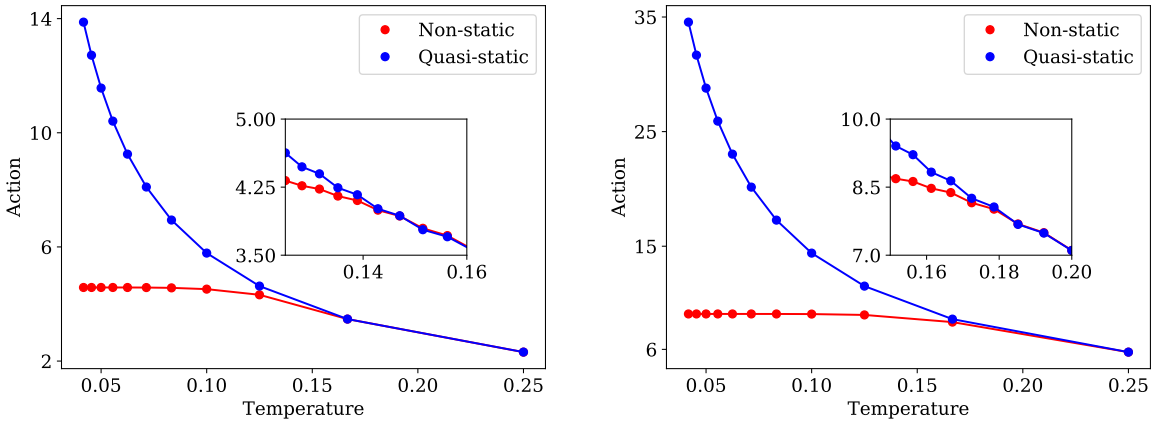

FIGURE 2.4: The plots show the dependence of the Euclidean action on temperature for non-static and quasi-static instantons with different potential barrier heights (left: $\lambda = 1.2$; right: $\lambda = 1.4$).

Then, via a least-squares fitting (§ C.2), α is furnished from

$$\alpha = \frac{\sum_i \frac{y_i}{x_i}}{\sum_i x_i^{-2}}. \tag{2.46}$$

Figure 2.5 shows the fitting of α with the action of quasi-static instanton for all three dimensional cases, as well as the (surprisingly linear!) relation between α and the potential barrier parameter λ.

This brings us to the conclusion of our study. We have investigated the cross-over regime of bubble nucleation, where the tunnelling instantons that dominate the nucleation rate lose one degree of symmetry in the presence of non-zero temperatures. The numerical results were obtained using a new relaxation technique that is amenable to both vacuum and thermal ensembles, and we found that the distorted instantons merge smoothly into quasi-static instantons.

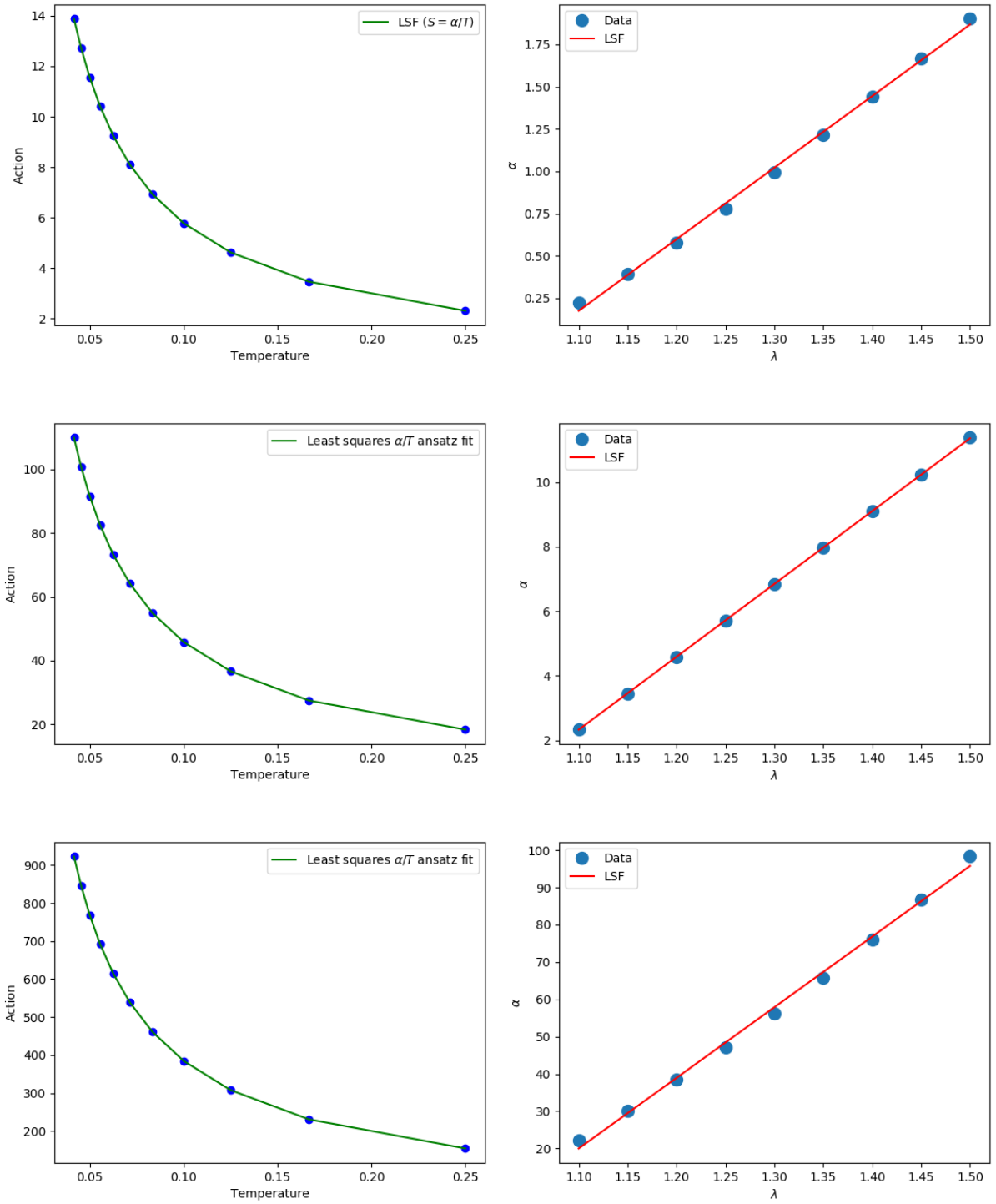

FIGURE 2.5: Least-squares fitting for $S_E = \alpha/T$ (left). This value of α is saved for different values of λ, from which we discover a surprisingly linear relation between α and λ (right), and consequently shows λ's dependence on T. The figure shows results for one (top), two (middle), and three (bottom) spatial dimensions.

Part II

Basics of 3+1 Numerical Relativity

Conventions & Notation

Metric signature	"Mostly plus" $(-+\cdots+)$
Einstein summation	"Downstairs" and "upstairs" indices are summed over, e.g., $X^i e_i = \sum_i X^i e_i$
Index convention	Standard convention whereby the letters $a-h$ and $o-z$ are used for 4-dimensional spacetime indices that run from 0 to 3, whereas the letters $i-n$ are reserved for 3-dimensional spatial indices that run from 1 to 3. Lowercase Greek letters are reserved for components in a chosen basis (see [50] for reference).
Dimensionless units	$G = c = \hbar = 1$ (unless otherwise stated)
Cosmological constant	$\Lambda = 0$
Riemann curvature	$R(X,Y)Z = \nabla_X \nabla_Y Z - \nabla_Y \nabla_X Z - \nabla_{[X,Y]} Z$
(In components)	$R^d{}_{abc} = \partial_b \Gamma^d_{ac} - \partial_c \Gamma^d_{ab} + \Gamma^e_{ac}\Gamma^d_{eb} - \Gamma^e_{ab}\Gamma^d_{ec}$
Ricci tensor	$R(X,Y) = \langle f^a, R(e_a,Y)X\rangle$ (f^a is a basis covector and e_a is a basis vector)
(In components)	$R_{ab} = R^d{}_{adb} = \partial_d \Gamma^d_{ab} - \partial_b \Gamma^d_{ad} + \Gamma^e_{ab}\Gamma^d_{ed} - \Gamma^e_{ad}\Gamma^d_{eb} = 2\Gamma^d_{a[b,d]} + 2\Gamma^d_{e[d}\Gamma^e_{b]a}$
Ricci scalar	$R = g^{ab}R_{ab} = R^b{}_b = 2g^{ab}\left(\Gamma^d_{a[b,d]} + \Gamma^d_{e[d}\Gamma^e_{b]a}\right)$
Einstein tensor	$G_{ab} = R_{ab} - \frac{1}{2}Rg_{ab}$
Einstein field equations	$G_{ab} = 8\pi T_{ab}$

Chapter 3

The ADM Formalism

The present chapter introduces the Cauchy 3+1 formalism of numerical relativity (NR), which provides an intuitive and efficient approach to solving the equations of the gravitational field. These equations, which are known as the Einstein Field Equations (EFEs), are nonlinear coupled partial differential equations (PDEs) which, with the exception of a few idealised cases characterised by high degrees of symmetry, simply cannot be obtained analytically;[1] we need a computer to do the heavy lifting for us. That being said, computers (for better or worse) lack a sense of humour; if you feed them nonsense, they *will* calculate nonsense. Therefore, we will not get too far in cracking the mysteries of the universe if we are not capable of somehow prescribing the right numerical recipe to the machine.

There are in fact quite a few different variations of recipes that we can cook with, in order to cast Einstein's equations in a convenient form for numerical purposes. These schemes can be roughly distinguished by the level set of hypersurfaces adopted to the foliation of the ambient spacetime (more on this later) and whether this spacetime is the physical one or a "larger" one where the physical description is obtained *a posteriori* by a rather straightforward restriction. A notion of "time" is then defined by a chosen foliation of the spacetime (physical or not) which is parametrised by a global parameter t. The character of the normal vector field $\nabla^a t$ (normal to the t = constant surfaces) characterises the different approaches. For instance, the so-called *Cauchy* approach corresponds to $\nabla^a t$ being timelike, whilst the *characteristic* approach is characterised by $\nabla^a t$ being null.

Whilst different approaches are naturally suited for different problems (and thus it is a good idea to be verse in all variations!), it is ultimately the 3+1 implementation the one that is arguably the most powerful one across the board, and as such it shall be the preferred flavour to be used in our future work on the evolution of (asymmetric) scalar fields in the presence of a gravitational field.

3.1 Basics of the 3+1 Setting

In General Relativity (GR), the evolution of the gravitational field can be posed as an *initial value problem* (or *Cauchy problem*) with constraints (see the original breakthrough paper [26]). In this so-called "3+1 formalism," the EFEs can be determined in two steps:

i) specify the spacetime metric tensor g_{ab} and its time-derivative $\partial_t g_{ab}$ (actually, it will be related quantities) for some initial 3D spacelike hypersurface Σ_0 that has a fixed time coordinate $x^0 = t =$ constant;

[1] Even in cases where there are high levels of symmetry we run into major problems! A textbook example of this issue is the question of the non-perturbative stability of the Kerr solution –it is still unknown whether the exterior Kerr solution is stable; a difficulty that arises due to the high non-linearity of the EFE's, which defies perturbative approaches.

ii) provided that we can obtain expressions for second-time derivatives of the 4-metric g_{ab} at all points on the hypersurface from the EFEs, we then integrate forward in time the metric quantities from step i).

However, even though this seems like a straightforward proposal, we immediately face the problem that in GR –unlike in other standard dynamical systems– space and time are two sides of the same coin; these two entities are treated on equal footing. This makes the space-time split that we are so accostumed to seeing in non-relativistic Cauchy problems a much more complicated endeavour. A further complication is the *constraints* of the system; while the EFEs consist of ten coupled PDEs, not all of them are evolution equations:

By the (contracted) *Bianchi identities*,

$$\begin{aligned} 0 &= \nabla_b {}^{(4)}G^{ab} \\ &= \partial_0 {}^{(4)}G^{a0} + \partial_i {}^{(4)}G^{ai} + {}^{(4)}G^{bc}\,{}^{(4)}\Gamma^{a}{}_{bc} + {}^{(4)}G^{ab}\,{}^{(4)}\Gamma^{c}{}_{bc}, \end{aligned}$$

we get

$$\partial_t {}^{(4)}G^{a0} = -\partial_i {}^{(4)}G^{ai} - {}^{(4)}G^{bc}\,{}^{(4)}\Gamma^{a}{}_{bc} - {}^{(4)}G^{ab}\,{}^{(4)}\Gamma^{c}{}_{bc}. \tag{3.1}$$

The quantities ${}^{(4)}\Gamma^{a}{}_{bc}$ are the so-called *Christoffel symbols* (or *connection coefficients*) of the 4-metric g_{ab}. Here (and throughout this paper) we use the convention of identifying the time-component with the zeroth index, as well as the widely adopted Einstein summation convention (refer to the Conventions page for details). Because there is no third-time derivatives (or higher) on the RHS of (3.1), this implies that there are no second-time derivatives contained in ${}^{(4)}G^{a0}$, and thus the four equations

$${}^{(4)}G^{a0} = 8\pi T^{a0} \tag{3.2}$$

do not yield any information whatsoever on how the fields evolve in time. Instead, they function as four *constraints* that must be satisfied from the onset on the initial hypersurface at $x^0 = t$ (and remain satisfied throughout the entire evolution!) if we are to have a physically-meaningful system. Thus, we can see that the only true dynamical (*evolution*) equations are encoded in the remaining six field equations

$${}^{(4)}G^{ij} = 8\pi T^{ij}. \tag{3.3}$$

We will see later on that certain projections of (3.2) and (3.3) onto the hypersurfaces will indeed yield the desired constraint and evolution equations of the system.

Hence, according to our discussion above, our first order of business is to somehow find a way to define the role played by space and time, as (somewhat) separate entities. Of course, by this we do not mean "forget about GR and go back to Newtonian/Galilean gravity!" It turns out that there is a special class of spacetimes, known as *globally hyperbolic* spacetimes, that will allow us this sought-after time/space split. First recall that a *Cauchy surface* is a spacelike hypersurface Σ embedded in an ambient manifold $\mathcal{M}$ such that each causal curve without endpoint in $\mathcal{M}$ intersects Σ exactly once. An equivalent way of saying this is that a Cauchy surface for a spacetime $\mathcal{M}$ is an *achronal* subspace $\Sigma \subset M$ (i.e., a subspace Σ in which no two points are timelike-related) which is transversed by every inextendible causal curve in $\mathcal{M}$. Now we properly define the concept of global hyperbolicity:

Definition 1. *A spacetime $\mathcal{M}$ is said to be **globally hyperbolic** if it admits a Cauchy surface. Equivalently, $\mathcal{M}$ is globally hyperbolic if it satisfies the strongly causal condition (i.e., if every $p \in \mathcal{M}$ has arbitrarily small neighborhoods U in which every every causal curve with endpoints in U is entirely contained in U) and if the "causal diamonds" $J^+(p) \cap J^-(q)$ are compact for all $p, q \in \mathcal{M}$.* [2]

The notion of global hyperbolicity is a crucial feature in Lorentzian geometry that ensures the existence of maximal causal geodesic segments. Physically, this condition is closely connected to the issue of classical determinism and the strong cosmic censorship conjecture [46]. Even though this is by no means a condition satisfied a priori by all spacetimes, the 3+1 formalism assumes that all physically reasonable spacetimes are of this type. This assumption is justified by the desire to have "nice" chronological/causal features in our spacetime (i.e., no *grandfather paradox* or any similar pathological behavior). Moreover, the use of global hyperbolicity allows us to foliate our full 4D spacetime $\mathcal{M}$ in such a way that we can stack 3D spacelike Cauchy slices along a universal time axis, by virtue of $\mathcal{M}$ having topology $\Sigma \times \mathbb{R}$. This is certainly not the only way to foliate $\mathcal{M}$, but it is the most suitable option for the 3+1 formalism.

3.2 Spacetime Slicing and 3+1 Adapted Coordinates

Keeping in mind the specific foliation described in the previous section, we can now determine the geometry of the region of spacetime contained between two adjacent hypersurfaces Σ_t and $\Sigma_{t+\mathrm{d}t}$ from just three basic ingredients (refer to figure 3.1):

I The ***3D metric*** γ_{ij} (metric induced on Σ: $\gamma_{ab} \equiv \imath^* g_{ab}$, where $\imath : \Sigma \hookrightarrow \mathcal{M}$ is the embedding of Σ into $\mathcal{M}$) that measures proper distances within the hypersurface itself:

$$dl^2 = \gamma_{ij}\, \mathrm{d}x^i \mathrm{d}x^j.$$

The hypersurface is then said to be

- ***spacelike*** $\iff$ $\underbrace{\gamma_{ab} \text{ is positive definite; i.e., it has signature } (+,+,+)}_{\text{our case}}$;
- ***timelike*** $\iff$ γ_{ab} is Lorentzian; i.e., it has signature $(-,+,+)$;
- ***null*** $\iff$ γ_{ab} is degenerate; i.e., it has signature $(0,+,+)$.

(We will shortly justify why we express the spatial metric both as 3D object (γ_{ij}) and a 4D object (γ_{ab}).)

II The *lapse of proper time* between the hypersurfaces, as measured by observers whose worldlines extend along the direction normal to the hypersurfaces (these observers are usually referred to as ***Eulerian observers***):

$$\mathrm{d}\tau = \alpha(t, x^i)\mathrm{d}t,$$

where α is known as the ***lapse function*** (this is denoted as N by some references, e.g., [27], [40]).

[2] Here we used standard notation, where $J^+(p) = \{q \in \mathcal{M} \mid p \leq q\}$ and $J^-(p) = \{q \in \mathcal{M} \mid q \leq p\}$ are the *causal future* and *causal past*, respectively, of $p \in \mathcal{M}$.

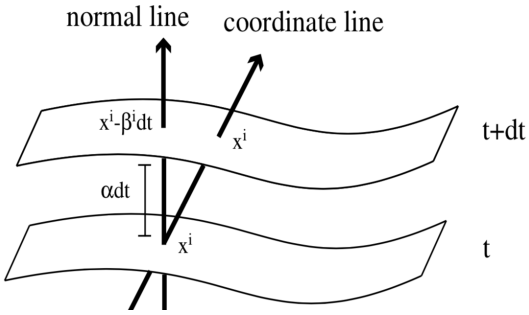

FIGURE 3.1: Two adjacent spacelike hypersurfaces. (Image from [2])

III The relative velocity β^i between the Eulerian observers:

$$x^i_{t+\mathrm{d}t} = x^i_t - \beta^i(t, x^i)\mathrm{d}t, \qquad \text{for Eulerian observers.}$$

This 3-vector β^i measures how much the coordinates are shifted as we move from one slice to the next, and it is therefore conventionally named as the ***shift vector***. (It is also denoted N^i in the literature.)

Note that, as we alluded to earlier, the foliation of $\mathcal{M}$ is not unique, and neither is the coordinates shift; α determines "how much slicing" is to be done, whilst β^i dictates how the spatial coordinates propagate from one hypersurface to the next. In fact, the latitude to choose a lapse function and shift vector demonstrates the gauge freedom that is inherent to the formulation of GR, a *covariant* theory.

From the *universal time function* t (given by the foliation), we have the vector field $\nabla^a t$ that is everywhere normal to the t = constant hypersurface Σ. In fact, $\nabla^a t$ is

- $\underbrace{\text{timelike} \iff \Sigma \text{ is spacelike}}_{\text{our case}}$;
- spacelike $\iff \Sigma$ is timelike;
- null $\iff \Sigma$ is null.

We use the 4-metric g_{ab} to normalise $\nabla^a t$:

$$\omega^a = \frac{\nabla^a t}{\|\nabla^a t\|} = \frac{\nabla^a t}{\sqrt{\pm \nabla^a t \nabla_a t}},$$

where the correct sign is

- $+$ for a timelike Σ (spacelike $\nabla^a t$);
- $-$ $\underbrace{\text{for a spacelike } \Sigma \text{ (timelike } \nabla^a t)}_{\text{our case}}$.

Thus, choosing the appropriate sign, we set the lapse function α to be

$$\alpha \equiv \left(-\nabla^a t \nabla_a t\right)^{-1/2} \qquad \text{so that} \qquad \omega^a = \alpha \nabla^a t.$$

Then we define the *future-pointing timelike* ***unit normal*** n^a to the slice Σ to be [3]

$$n^a \equiv -\omega^a = -\alpha \nabla^a t. \tag{3.4}$$

We think of n^a as the 4-velocity of an Eulerian observer, i.e., an observer whose worldline is always normal to the spatial slices (note that it is indeed unit timelike: $n^a n_a = (-\alpha \nabla^a t)(-\alpha \nabla_a t) = \alpha^2 \nabla^a t \nabla_a t = \alpha^2(-\alpha^{-2}) = -1$).

Now, having defined the unit normal, we can see that the three scalar quantities that yield the spatial components of the shift vector, β^i, are given by

$$\beta^i = -\alpha \left(\vec{n} \cdot \vec{\nabla} x^i \right). \tag{3.5}$$

These three scalar quantities can then be used to form a full 4-vector β^a (orthogonal to n^a, by construction) which, in the adapted 3+1 coordinates we are about to introduce, will have components $\beta^\mu = (0, \beta^i)$ (we will show this soon). [4] This shift vector β^a will measure the amount by which the spatial coordinates are shifted within a slice with respect to the normal vector (i.e., they determine how the coordinates evolve in time). A linear combination of β^a and the unit normal n^a define (see figure 3.2) the ***time vector*** t^a as

$$t^a \equiv \alpha n^a + \beta^a. \tag{3.6}$$

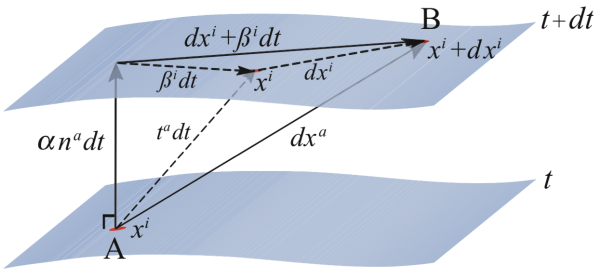

FIGURE 3.2: Simple Pythagorean triangulation that shows equation (3.6). Here we can see how the normal vector αn^a and the time vector t^a connect points on two neighbouring spatial slices, whilst β^a resides in a slice and measures their difference. (Image from[8])

This time vector is dual to $\nabla_a t$: for any spatial shift vector β^a,

$$t^a \nabla_a t = (\alpha n^a + \beta^a)\nabla_a t = \underbrace{\alpha n^a \nabla_a t}_{=1} + \underbrace{\beta^a \nabla_a t}_{=0} = 1. \tag{3.7}$$

The relevance of this *duality* will be evident from the following discussion. Note that t^a is nothing but the vector tangent to the *time lines*, i.e., the congruence of lines of constant spatial coordinates x^i. In the ***standard 3+1 coordinates***, which we now present, t^a is our timelike basis vector $e^a_{(0)} = t^a$ (t^a is a natural candidate to be the basis vector $e^a_{(0)}$ precisely because of the duality (3.7)). The remaining three

[3] The minus sign is chosen to ensure that n^a is always future-pointing.

[4] Recall *abstract index notation* (see "Conventions" page for reference).

spatial basis vectors $e^a_{(i)}$ are tangent to a particular slice Σ_t (i.e., they satisfy $e^a_{(i)}\nabla_a t = 0$). Moreover, they are *Lie dragged* along t^a,

$$\mathcal{L}_{\vec{t}}\, e^a_{(i)} = 0,$$

as illustrated in figure 3.3. (Note that some references (e.g., [27]) use a *normal evolution vector* $m^a \equiv \alpha n^a$ in place of t^a to Lie drag the hypersurfaces. This is justified by the fact that m^a is also dual to $\nabla_a t$ (note that in (3.7) the term $\beta^a \nabla_a t$ does not contribute).)

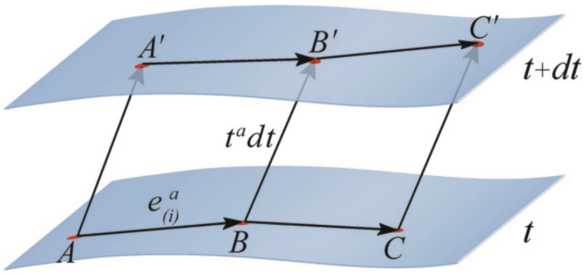

FIGURE 3.3: As a consequence of spatial basis vectors $e^a_{(i)}$ being Lie dragged from slice to slice along the coordinate congruence t^a, these basis vectors connect points with the same spatial coordinates on different slices (for instance, in this figure, they connect the unprimed labeled points on the bottom slice with their primed counterparts that lie on the top slice). (Image from[8])

We digress for a moment to introduce a crucial object: the *spatial projection operator*

$$P^a{}_b \equiv \delta^a{}_b + n^a n_b. \tag{3.8}$$

This operator projects a 4D tensor onto a spatial slice. For instance, if we take an arbitrary 4-vector v^a, and hit it with the projection operator,

$$\underbrace{v^a}_{\text{arbitrary, 4D}} \overset{P^a{}_b}{\longmapsto} \underbrace{P^a{}_b v^b}_{\text{purely spatial}}$$

we get a purely spatial object that lies entirely on a hypersurface. We can check that this is indeed the case: first expand $P^a{}_b v^b$,

$$P^a{}_b v^b = (\delta^a{}_b + n^a n_b)v^b = v^a + n^a n_b v^b,$$

and then contract with the normal,

$$\begin{aligned}
(P^a{}_b v^b)n_a &= (v^a + n^a n_b v^b)n_a \\
&= v^a n_a + n^a n_a n_b v^b \\
&= v^a n_a + (-1)v^b n_b && \text{(since } n_a \text{ is normalised and timelike)} \\
&= v^a n_a - v^a n_a = 0. && \text{(relabeling indices)}
\end{aligned}$$

Since there is no contribution whatsoever along n^a, we conclude that $P^a{}_b v^b$ is indeed purely spatial.

In a similar vein, to project higher rank tensors onto a spatial hypersurface, each free index of such tensors is to be contracted with a projection operator (e.g., for a rank-2 tensor T_{ab}, we hit it with two projections, one for each free index: $P_a{}^c P_b{}^d T_{cd}$). Now that this is clear, we see how we get the induced metric (expressed as a full 4D object, γ_{ab}) from the projection onto a slice of the spacetime metric g_{ab}:

$$\gamma_{ab} \equiv P_a{}^c P_b{}^d g_{cd} = \left(\delta^a{}_b + n^a n_b\right)\left(\delta^a{}_b + n^a n_b\right) g_{cd} = g_{ab} + n_a n_b.$$

So we have our ***spatial metric*** ,

$$\boxed{\gamma_{ab} = g_{ab} + n_a n_b.} \tag{3.9}$$

and, similarly, the ***inverse spatial metric***,

$$\gamma^{ab} = g^{ac} g^{bd} \gamma_{cd} = g^{ab} + n^a n^b. \tag{3.10}$$

Hence, γ_{ab} is a projection tensor that discards components of 4D geometric objects that lie along n^a; we use it to calculate distances between points that belong to the same spatial hypersurface. We can think of γ_{ab} as first computing four-dimensional distance (with g_{ab}), and then eliminating (with $n_a n_b$) the timelike contribution to the 4D distance calculation. We may check that γ_{ab} is purely spatial by contracting with the normal n^a:

$$n^a \gamma_{ab} = n^a g_{ab} + n^a n_a n_b = n_b - n_b = 0.$$

Now, from (3.9) we see that, if we raise only one index of the spatial metric γ_{ab},

$$\gamma^a{}_b = g^a{}_b + n^a n_b = \delta^a{}_b + n^a n_b,$$

we find out that our projection operator is merely the spatial metric with one raised index

$$P^a{}_b = \gamma^a{}_b.$$

Therefore, from now on we will exclusively use $\gamma^a{}_b$ to denote the ***spatial projection operator***; i.e., we rewrite (3.8) as

$$\boxed{\gamma^a{}_b = \delta^a{}_b + n^a n_b.} \tag{3.11}$$

We can now see that the shift vector β^a is nothing but the projection of t^a onto a hypersurface:

$$\gamma^a{}_b t^b = (\delta^a{}_b + n^a n_b)(\alpha n^b + \beta^b) = \alpha \delta^a{}_b n^b + \delta^a{}_b \beta^b + \alpha n^a \underbrace{n_b n^b}_{=-1} + n^a \underbrace{n_b \beta^b}_{=0} = \beta^a. \tag{3.12}$$

This provides us with a coordinate-free expression for the shift vector.

Thus far we have been writing objects in a coordinate-free matter for the most part. Now we use the standard 3+1 coordinates basis that we declared above to write out explicit components of these objects. First off, since t^a is aligned with the basis vector $e^a_{(0)}$ whilst all remaining (spatial) coordinates remain constant along t^a, we get

$$t^\mu = e^\mu_{(0)} = \delta^\mu{}_0 = (1, 0, 0, 0). \tag{3.13}$$

This means that any Lie derivative along t^a will reduce to a partial derivative with respect to t: $\mathcal{L}_{\vec{t}} = \partial_t$ (we will use this later!). Then, as discussed earlier, the remaining three spatial basis vectors $e^a_{(i)}$ reside on a particular slice Σ_t, so that

$$0 = \nabla_a t e^a_{(i)} \overset{\text{by (3.4)}}{=\!=\!=} -\alpha^{-1} n_a e^a_{(i)} \implies n_a e^a_{(i)} = 0.$$

But then, since the $e^a_{(i)}$ are the spatial basis vectors, they must span the hypersurface Σ_t. Hence the condition $n_a e^a_{(i)} = 0$ means that the covariant spatial components of the normal vector must vanish, i.e.,

$$n_i = 0. \tag{3.14}$$

Now, since objects that are purely spatial must vanish (by construction) when contracting with the normal, Eq. (3.14) implies that timelike contravariant components of spatial tensors must vanish. [5] For example, contract the shift vector with the normal,

$$0 \overset{\text{by construction}}{=\!=\!=\!=\!=\!=\!=\!=\!=\!=} n_a \beta^a = n_0 \beta^0 + \underbrace{n_i \beta^i}_{=0 \text{ by (3.14)}} = \underbrace{n_0}_{\neq 0} \beta^0 \implies \beta^0 = 0.$$

Combining this with (3.5), we can conclude that, in the adapted coordinates,

$$\beta^\mu = (0, \beta^i), \tag{3.15}$$

as we alluded to earlier. Also, note that from the definition of the time vector (3.6), we have

$$n^a = \frac{t^a}{\alpha} - \frac{\beta^a}{\alpha}.$$

Combining this with (3.13) and (3.15), we can get the contravariant components of n^a in the adapted coordinates:

$$n^0 = \alpha^{-1} \underbrace{t^0}_{=1} - \alpha^{-1} \underbrace{\beta^0}_{=0} = \alpha^{-1},$$

whilst

$$n^i = \alpha^{-1} \underbrace{t^i}_{0} - \alpha^{-1} \beta^i = -\alpha^{-1} \beta^i.$$

Thus we have found

$$n^\mu = (\alpha^{-1}, -\alpha^{-1} \beta^i), \tag{3.16}$$

and since n^a is unit timelike,

$$-1 = n^a n_a \overset{\text{by (3.14)}}{=\!=\!=} n^0 n_0 \implies n_0 = -\frac{1}{n^0} = -\alpha.$$

[5] Even though this rationale does not apply to covariant components of spatial tensors (as we can see from (3.16), the contravariant spatial components of the normal are generally nonzero), any contribution along the timelike direction is killed off when contracting with the normal by the condition that $n^{i_k} T_{i_1,\ldots,i_k,\ldots i_n} = 0$ for any purely spatial tensor $T_{i_1,\ldots i_n}$. Therefore *all the information about spatial tensors is effectively contained in their spatial components.* We will use this fact throughout.

Hence, combining this with (3.14), we have all covariant components of the normal in the adapted coordinates

$$n_\mu = (-\alpha, 0, 0, 0). \tag{3.17}$$

Now, from (3.9),

$$\gamma_{ij} = g_{ij} + \underbrace{n_i n_j}_{=0} = g_{ij}, \tag{3.18}$$

so that the spatial metric on Σ is just the spatial part of the spacetime 4-metric g_{ab}. Note also that, even though the covariant components do not necessarily vanish ($\gamma_{0\mu} = g_{0\mu} + n_0 n_\mu = g_{0\mu} + n_0 n_0 = g_{0\mu} + \alpha^2 \neq 0$, in general), any contribution to the timelike direction can be safely ignored since $n^a \gamma_{ab} = 0$ (see footnote 5). On the other hand, timelike components of spatial contravariant tensors do vanish (see discussion below equation (3.14)), so we must have $\gamma^{a0} = 0$. Therefore, from (3.10), we get the components of the inverse spacetime metric in these adapted coordinates:

$$\begin{aligned}
g^{ab} &= \gamma^{ab} - n^a n^b \\
g^{0a} &= -n^0 n^a \implies g^{00} = -\alpha^{-2} \quad \& \quad g^{0i} = \alpha^{-2}\beta^i \\
g^{ij} &= \gamma^{ij} - n^i n^j = \gamma^{ij} - (-\alpha^{-1}\beta^i)(-\alpha^{-1}\beta^j) = \gamma^{ij} - \alpha^{-2}\beta^i\beta^j.
\end{aligned}$$

In matrix form,

$$g^{\mu\nu} = \begin{pmatrix} -1/\alpha^2 & \beta^i/\alpha^2 \\ \beta^j/\alpha^2 & \gamma^{ij} - \beta^i\beta^j/\alpha^2 \end{pmatrix}. \tag{3.19}$$

Now, by the condition $g^{ab} g_{bc} = \delta^a{}_c$, we can invert (3.19) to write the spacetime metric in 3+1 coordinates:

$$g_{\mu\nu} = \begin{pmatrix} -\alpha^2 + \beta_k\beta^k & \beta_i \\ \beta_j & \gamma_{ij} \end{pmatrix}. \tag{3.20}$$

The covariant components β_i shown above come from lowering with the spatial metric, i.e., $\beta_i = \gamma_{ik}\beta^k$. We will always use the spatial metric to raise/lower indices of spatial objects, because γ_{ij} and γ^{ij} are inverses of each other in the adapted coordinates:

$$\begin{aligned}
\gamma^{ik}\gamma_{kj} &= (g^{ik} + n^i n^k)(g_{kj} + n_k n_j) \\
&= g^{ik} g_{kj} + g^{ik} n_k n_j + n^i n^k g_{kj} + n^i n^k n_k n_j \\
&= \delta^i{}_j + n^i \underbrace{n_j}_{=0} + n^i \underbrace{n_j}_{=0} - n^i \underbrace{n_j}_{=0} = \delta^i{}_j.
\end{aligned}$$

From (3.20) we see that the ***line element of the full spacetime metric in 3+1 coordinates*** is given by

$$\boxed{ds^2 = \left(-\alpha^2 + \beta_i\beta^i\right) \mathrm{d}t^2 + 2\beta_i \, \mathrm{d}t\mathrm{d}x^i + \gamma_{ij} \, \mathrm{d}x^i \mathrm{d}x^j.} \tag{3.21}$$

3.3 3D Curvature

The EFEs relate contractions of the 4D Riemann tensor (namely, the *Ricci tensor* and the *Ricci scalar*) to the energy-momentum tensor (these contractions are encoded in the Einstein tensor ${}^{(4)}G_{ab}$).

However, given our interest in the 3+1 formalism, we need to find a way to translate these four-dimensional (*spacetime*) quantities into three-dimensional (*spatial*) objects. As the reader may have wisely guessed, the projection operator (3.11) will play a key role in accomplishing this task. These projections will allow us to distinguish between properties that are *intrinsic* to the 3D geometry from those that are *extrinsic* (i.e., that depend on the embedding into the ambient 4D manifold). To elaborate further, we start with the following crucial definition:

Definition 2. *The* ***spatial connection*** D *intrinsic to a hypersurface* Σ *satisfies the following: Let* $X, Y_{(a)} \in \mathfrak{X}(\Sigma)$ *be vector fields on* Σ *(sections of the* tangent bundle $\Sigma \to T\Sigma$*) and let* $\omega^{(a)} \in \mathfrak{X}^*(\Sigma)$ *be* 1*-forms on* Σ *(sections of the* cotangent bundle $\Sigma \to T^*\Sigma$*). Then for any* $\binom{a}{b}$ *tensor field* $\boldsymbol{T} \in \mathcal{T}^a_b(\Sigma)$*, the map*

$$D\boldsymbol{T}\colon \underbrace{\mathfrak{X}^*(\Sigma) \times \ldots \times \mathfrak{X}^*(\Sigma)}_{a \text{ times}} \times \underbrace{\mathfrak{X}(\Sigma) \times \ldots \times \mathfrak{X}(\Sigma)}_{b+1 \text{ times}} \to C^\infty(\Sigma)$$

given by

$$D\boldsymbol{T}(\omega^1, \ldots, \omega^a, Y_1, \ldots, Y_b, X) = D_X\boldsymbol{T}(\omega^1, \ldots, \omega^a, Y_1, \ldots, Y_b)$$

defines an $\binom{a}{b+1}$ *tensor field, which we will call the* ***spatial covariant derivative****. It can be shown also that* D *is torsion-free and compatible with the 3D metric, i.e.,* $D_c\gamma_{ab} = 0$*.*

In a coordinate chart,

$$\begin{aligned}(D\boldsymbol{T})^{i_1\ldots i_a}{}_{j_1\ldots j_b c} &= D_c T^{i_1\ldots i_a}{}_{j_1\ldots j_b} \\ &= \partial_c T^{i_1\ldots i_a}{}_{j_1\ldots j_b} + \sum_{d=1}^{a} T^{i_1\ldots e\ldots i_a}{}_{j_1\ldots j_b}\Gamma^{i_d}_{ec} - \sum_{d=1}^{b} T^{i_1\ldots i_a}{}_{j_1\ldots e\ldots j_b}\Gamma^{e}_{j_d c},\end{aligned} \tag{3.22}$$

where

$$\Gamma^a_{bc} = \frac{1}{2}\gamma^{ad}(\partial_c\gamma_{db} + \partial_b\gamma_{dc} - \partial_d\gamma_{bc}). \tag{3.23}$$

For instance, take a $\binom{1}{1}$ tensor field $T^a{}_b$; then its covariant spatial derivative with respect to the $\vec{e}_{(c)}$ basis vector (i.e., the geometric object that shows how much $T^a{}_b$ varies as it is transported along congruence lines of $\vec{e}_{(c)}$) is the $\binom{1}{2}$ tensor field given by

$$(D\boldsymbol{T})^a{}_{bc} = T^a{}_{b;c} = D_c T^a{}_b = \partial_c T^a{}_b + T^e{}_b\Gamma^a_{ec} - T^a{}_e\Gamma^e_{bc}.$$

(The semicolon notation is commonly used in the GR literature to denote covariant differentiation. Instead, a comma is used for the standard partial derivative in flat space; e.g., $T^a{}_{b,c} \equiv \partial_c T^a{}_b$.) Having defined the above, it is not hard to show that the spatial covariant derivative is furnished by projecting *all* indices present in a 4D covariant derivative ∇ (connection of the ambient manifold $\mathcal{M}$) onto Σ; that is,

$$D_a T^{i_1\ldots i_b}{}_{j_1\ldots j_c} = \gamma_a{}^d\gamma^{i_1}{}_{k_1}\ldots\gamma^{i_b}{}_{k_b}\gamma_{j_1}{}^{\ell_1}\ldots\gamma_{j_c}{}^{\ell_c}\nabla_d T^{k_1\ldots k_b}{}_{\ell_1\ldots\ell_c}. \tag{3.24}$$

For a simple example, consider again a $\binom{1}{1}$ tensor field $T^a{}_b$. Then,

$$D_a T^b{}_c = \gamma_a{}^d\gamma^b{}_e\gamma_c{}^f\nabla_d T^e{}_f.$$

Now equipped with the spatial covariant derivative, we define the ***3D Riemann tensor*** associated with γ_{ij} by requiring that

⁂ (Ricci identity) for any spatial vector v^a,

$$2D_{[a}D_{b]}v^c = R^c{}_{dab}v^d; \tag{3.25}$$

⁂ (Purely spatial tensor) the contraction with the normal vanishes

$$R^d{}_{cba}n_d = 0. \tag{3.26}$$

The brackets used on the indices in Eq. (3.25) are common notation in GR; they are used to denote the *antisymmetric* part of a tensor $\boldsymbol{T}$:

$$T_{[\mu_1\ldots\mu_k]} = \frac{1}{k!}\hat{\epsilon}^{\mu_1\ldots\mu_k}T_{\mu_1\ldots\mu_k}, \tag{3.27}$$

where the *Levi-Civita symbol* $\hat{\boldsymbol{\epsilon}}$ is given by

$$\hat{\epsilon}^{\mu_1\ldots\mu_k} = \begin{cases} +1 & \text{if } (\mu_1\ldots\mu_k) \text{ is an even permutation of } 1,\ldots,k; \\ -1 & \text{if } (\mu_1\ldots\mu_k) \text{ is an odd permutation of } 1,\ldots,k; \\ 0 & \text{if there are any repeated indices in } 1,\ldots,k. \end{cases}$$

Similarly, to denote the *symmetric* part of a tensor $\boldsymbol{T}$ we use parentheses on the indices:

$$T_{(\mu_1\ldots\mu_k)} = \frac{1}{k!}\hat{\sigma}^{\mu_1\ldots\mu_k}T_{\mu_1\ldots\mu_k}, \tag{3.28}$$

where $\hat{\sigma}$ is given by

$$\hat{\sigma}^{\mu_1\ldots\mu_k} = \begin{cases} +1 & \text{for any permutation } (\mu_1\ldots\mu_k) \text{ of } 1,\ldots,k; \\ 0 & \text{if there are any repeated indices in } 1,\ldots,k. \end{cases}$$

For example,

$$\begin{aligned} T_{[ab]} &= \frac{1}{2}(T_{ab} - T_{ba}) \\ T_{(ab)} &= \frac{1}{2}(T_{ab} + T_{ba}) \\ T_{[abc]} &= \frac{1}{3!}(T_{abc} + T_{bca} + T_{cab} - T_{acb} - T_{cba} - T_{bac}) \\ T_{(abc)} &= \frac{1}{3!}(T_{abc} + T_{bca} + T_{cab} + T_{acb} + T_{cba} + T_{bac}). \end{aligned}$$

Now back to the topic at hand. It is not hard to show that, in a coordinate basis, the Riemann tensor takes the form

$$R^d{}_{abc} = \partial_b\Gamma^d_{ac} - \partial_c\Gamma^d_{ab} + \Gamma^e_{ac}\Gamma^d_{eb} - \Gamma^e_{ab}\Gamma^d_{ec}, \tag{3.29}$$

where the Christoffel symbols Γ^c_{ab} are the connection coefficients of the spatial metric (c.f., Eq. (3.23)). Moreover, a contraction of Eq. (3.29) yields the *3D Ricci tensor*

$$\begin{aligned} R_{ab} = R^d{}_{adb} &= \partial_d\Gamma^d_{ab} - \partial_b\Gamma^d_{ad} + \Gamma^e_{ab}\Gamma^d_{ed} - \Gamma^e_{ad}\Gamma^d_{eb} \\ &= 2\Gamma^d_{a[b,d]} + 2\Gamma^d_{e[d}\Gamma^e_{b]a}, \end{aligned} \tag{3.30}$$

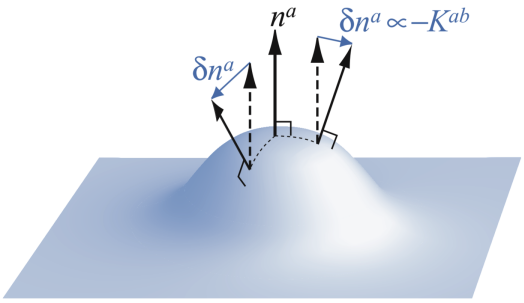

FIGURE 3.4: K_{ab} yields information about the bending of the slice in the ambient spacetime by measuring how much the normal varies from point to point on said slice; i.e., it measures the change of the normal vector under parallel transport within a slice. (Image from[8])

and yet a further contraction provides the *3D Ricci scalar*:

$$R = R^a{}_a = \gamma^{ab} R_{ab} = 2\gamma^{ab}\left(\Gamma^d_{a[b,d]} + \Gamma^d_{e[d}\Gamma^e_{b]a}\right). \tag{3.31}$$

The 3D Riemann tensor (3.29) is a quantity that measures the curvature *intrinsic* to a specific hypersurface by measuring how much a vector deviates from its initial position after being parallelly transported along a closed loop (equivalently, it measures curvature by calculating how much covariant (second) derivatives do or do not commute (see Ricci identity (3.25)). That is all fun and games, but we also want to know how our hypersurfaces are embedded in the ambient spacetime; therefore we must be able to compute geometric features that are *not intrinsic* to the slice. We start by defining a crucial object, the ***extrinsic curvature tensor***: [6]

$$\boxed{K_{ab} = -\gamma_a{}^c \gamma_b{}^d \nabla_c n_d.} \tag{3.32}$$

Note that K_{ab} is merely a projection of gradients of the normal vector onto a slice; it measures how much n^a varies as we move from point to point on a particular slice (see figure 3.4). Let us now expand:

$$\begin{aligned}
K_{ab} &= -\gamma_a{}^c \gamma_b{}^d \nabla_c n_d \\
&= -\left[(\delta_a{}^c + n_a n^c)(\delta_b{}^d + n_b n^d)\nabla_c n_d\right] \\
&= -\left[(\delta_a{}^c \delta_b{}^d + n_a n^c \delta_b{}^d + \delta_a{}^c n_b n^d + n_a n^c n_b n^d)\nabla_c n_d\right] \\
&= -[\nabla_a n_b + n_a n^c \nabla_c n_b + n_b \underbrace{n^d \nabla_a n_d}_{=0} + n_a n_b n^c \underbrace{n^d \nabla_c n_d}_{=0}] \\
&= -\nabla_a n_b - n_a n^c \nabla_c n_b.
\end{aligned}$$

On the fourth equality we claimed that $n^d \nabla_a n_d = 0$ from the the following fact:

$$\underbrace{\nabla_a(\overbrace{n_b n^b}^{=-1})}_{=0} = n^b \nabla_a n_b + n_b \nabla_a n^b$$

[6] The minus sign is merely a convention in the NR community. In the cosmology community the sign is usually positive!

$$\implies 0 = n^b \nabla_a n_b + \underbrace{n_b \nabla_a g^{bc} n_c}_{= n_b g^{bc} \nabla_a n_c = n^c \nabla_a n_c}$$

$$\implies n^b \nabla_a n_b = -n^b \nabla_a n_b$$

$$\implies n^b \nabla_a n_b = 0.$$

Hence, once we expand (3.32) we have

$$\boxed{K_{ab} = -\nabla_a n_b - n_a n^c \nabla_c n_b.} \tag{3.33}$$

This form is obviously more practical for computations, so it shall be the one we use hereafter (along with (3.37); see below). Note that since n^a is regarded as the 4-velocity of some Eulerian observer, we may consider the quantity $n^c \nabla_c n_b$ to be the ***4-acceleration*** a_b of such Eulerian observer:

$$\mathsf{a}_b \equiv n^c \nabla_c n_b. \tag{3.34}$$

Now expand (3.34):

$$\begin{aligned}
\mathsf{a}_a = n^b \nabla_b n_a &= n^b \nabla_b \underbrace{(-\alpha \nabla_a t)}_{\text{def of } n_a} = -n^b \nabla_b \alpha \underbrace{\nabla_a t}_{=-\frac{1}{\alpha} n_a} - \alpha n^b \underbrace{\nabla_b \nabla_a t}_{=\nabla_a \nabla_b t} \\
&= \frac{1}{\alpha} n_a n^b \nabla_b \alpha - \alpha n^b \nabla_a \left(-\frac{1}{\alpha} n_b \right) \\
&= \frac{1}{\alpha} n_a n^b \nabla_b \alpha + \alpha \frac{1}{\alpha} \underbrace{n^b \nabla_a n_b}_{=0} + \alpha \underbrace{n^b n_b}_{=-1} \underbrace{\nabla_a \frac{1}{\alpha}}_{=-\alpha^{-2} \nabla_a \alpha} \\
&= \frac{1}{\alpha} n_a n^b \nabla_b \alpha - \alpha \left(-\frac{1}{\alpha^2} \nabla_a \alpha \right) = \frac{1}{\alpha} \left(n_a n^b \nabla_b \alpha + \nabla_a \alpha \right) \\
&= \frac{1}{\alpha} \left((\delta_a{}^b + n_a n^b) \nabla_b \alpha \right) = \frac{1}{\alpha} \gamma_a{}^b \nabla_b \alpha = \frac{1}{\alpha} D_a \alpha \\
&= D_a \log \alpha.
\end{aligned}$$

This shows that a_b is actually the spatial gradient of the logarithm of the lapse function:

$$\boxed{\mathsf{a}_a = D_a \log \alpha.} \tag{3.35}$$

Now, since it will come in handy later, we take yet another spatial derivate of this quantity:

$$\begin{aligned}
D_a \mathsf{a}_b &= D_a D_b \log \alpha \\
&= D_a \left(\frac{1}{\alpha} D_b \alpha \right) = \frac{1}{\alpha} D_a D_b \alpha + D_a \left(\frac{1}{\alpha} \right) D_b \alpha \\
&= \frac{1}{\alpha} D_a D_b \alpha - \frac{1}{\alpha^2} D_a \alpha \, D_b \alpha = \frac{1}{\alpha} D_a D_b \alpha - \underbrace{\frac{1}{\alpha} D_a \alpha}_{= D_a \log \alpha} \underbrace{\frac{1}{\alpha} D_b \alpha}_{= D_b \log \alpha} \\
&= \frac{1}{\alpha} D_a D_b \alpha - \mathsf{a}_a \mathsf{a}_b.
\end{aligned} \tag{3.36}$$

We will use both(3.35) and (3.36) later when computing a certain projection of the 4D Riemann tensor. It is important to make sure that K_{ab} is indeed a purely spatial object:

$$\begin{aligned} n^a K_{ab} &= n^a(-\nabla_a n_b - n_a n^c \nabla_c n_b) \\ &= -n^a \nabla_a n_b - n^a n_a n^c \nabla_c n_b \\ &= -n^a \nabla_a n_b + n^a \nabla_a n_b = 0. \qquad \text{(after relabelling)} \end{aligned}$$

Thus, we are allowed to discard timelike components (we discussed this earlier) and focus exclusively on the spatial components K_{ij} (we will certainly use this fact later). Another key property of K_{ab} is its symmetry ($K_{ab} = K_{ba}$); we prove this by writing it as the *Lie derivative* of the spatial metric along the normal direction: [7]

$$\boxed{K_{ab} = -\frac{1}{2}\mathcal{L}_{\vec{n}}\gamma_{ab}.} \tag{3.37}$$

Proof. We expand using the definition of the Lie derivative:

$$\begin{aligned} \mathcal{L}_{\vec{n}}\gamma_{ab} &= n^c \nabla_c \gamma_{ab} + \gamma_{ac}\nabla_b n^c + \gamma_{cb}\nabla_a n^c \\ &= n^c \nabla_c (n_a n_b) + g_{ac}\nabla_b n^c + g_{cb}\nabla_a n^c \\ &= n^c n_a \nabla_c n_b + n^c n_b \nabla_c n_a + \nabla_b n_a + \nabla_a n_b \\ &= (\gamma_a{}^c - g_a{}^c)\nabla_c n_b + (\gamma_b{}^c - g_b{}^c)\nabla_c n_a + \nabla_b n_a + \nabla_a n_b \\ &= \gamma_a{}^c \nabla_c n_b + \gamma_b{}^c \nabla_c n_a = -2K_{ab}. \end{aligned}$$

□

Here we used the fact that $\nabla_c g_{ab} = 0$ and the identity $n^c \nabla_a n_c = 0$. Another (more compact) computation shows the same result:

$$\begin{aligned} \mathcal{L}_{\vec{n}}\gamma_{ab} &= \mathcal{L}_{\vec{n}}(g_{ab} + n_a n_b) = 2\nabla_{(a} n_{b)} + n_a \mathcal{L}_{\vec{n}} n_b + n_b \mathcal{L}_{\vec{n}} n_a \\ &= 2\left(\nabla_{(a} n_{b)} + n_{(a} \mathsf{a}_{b)}\right) = -2K_{ab}. \end{aligned}$$

Since n^a is a timelike vector, equation (3.37) illustrates the intuitive interpretation of the extrinsic curvature as a geometric generalisation of the "time derivative" of the spatial metric γ_{ab}, i.e., the "velocity" of the spatial metric as seen by the Eulerian observers. However, $\mathcal{L}_{\vec{n}}$ is not a natural time derivative, since n^a is not dual to the surface 1-form $\nabla_a t = \nabla_a t$, i.e., their dot product is not unity:

$$n^a \nabla_a t = -\alpha \underbrace{\nabla^a t \nabla_a t}_{=-\alpha^{-2}} = \alpha^{-1}.$$

Instead, recall that the time vector $t^a = \alpha n^a + \beta^a$ *is* in fact dual to $\nabla_a t$, as we showed via equation (3.7). Thus we can use t^a to rewrite (3.37) as a more natural time derivative of the metric:

$$\begin{aligned} K_{ab} = -\frac{1}{2}\mathcal{L}_{\vec{n}}\gamma_{ab} &= -\frac{1}{2}\mathcal{L}_{\frac{\vec{t}-\vec{\beta}}{\alpha}}\gamma_{ab} \\ &= -\frac{1}{2\alpha}\left(\mathcal{L}_{\vec{t}}\gamma_{ab} - \mathcal{L}_{\vec{\beta}}\gamma_{ab}\right) \\ &= -\frac{1}{2\alpha}\left(\partial_t \gamma_{ab} - \mathcal{L}_{\vec{\beta}}\gamma_{ab}\right), \end{aligned} \tag{3.38}$$

where on the last line we used the fact that, in the adapted coordinates, $\mathcal{L}_{\vec{t}}$ reduces to ∂_t.

[7] This is in fact taken as the definition of K_{ab} in many references!

3.4 ADM Evolution & Constraints

The twelve quantities $\{\gamma_{ij}, K_{ij}\}$ encode all the geometric data, both intrinsic and extrinsic, of the 3D hypersurfaces. Thus, in our efforts to pose the EFEs as a Cauchy problem we need to determine the evolution of this system (c.f., Eq. (3.3)), starting with some initial data $\{\gamma_{ij}^{(0)}, K_{ij}^{(0)}\}$ that is prescribed on an initial slice $\Sigma_{t=0}$. However, we recall that this data cannot be arbitrary, as constraints must be satisfied at the initial slice *and* throughout the entire time-evolution (c.f., Eq. (3.2)). In this section we derive both the evolution and constraint equations, in the ADM formalism. A conformal reformulation of these equations will be presented in the next chapter, when we discuss the so-called *BSSN* formalism.

Let us start by rewriting Eq. (3.38) as

$$\partial_t \gamma_{ab} = \mathcal{L}_{\vec{\beta}} \gamma_{ab} - 2\alpha K_{ab}. \tag{3.39}$$

Since –as we have previously discussed– the entire content of any spatial tensor is available from its spatial components alone, we can drop the timelike components and expand:

$$\begin{aligned}
\partial_t \gamma_{ij} &= \mathcal{L}_{\vec{\beta}} \gamma_{ij} - 2\alpha K_{ij} \\
&= \beta^k \underbrace{D_k \gamma_{ij}}_{=0} + D_i(\gamma_{kj}\beta^k) + D_j(\gamma_{ik}\beta^k) - 2\alpha K_{ij} \\
&= D_i\beta_j + D_j\beta_i - 2\alpha K_{ij}.
\end{aligned}$$

Hence, Eq. (3.39) boils down to

$$\boxed{\partial_t \gamma_{ij} = 2D_{(i}\beta_{j)} - 2\alpha K_{ij}.} \tag{3.40}$$

This is our sought-after ***evolution equation of the spatial metric***. While we are at it, let us also present a useful contraction of this equation that will come in handy later. Per usual convention, we denote the determinant of the spatial metric by $\gamma \equiv \det \gamma_{ij}$. Then,

$$\begin{aligned}
\partial_t \log\sqrt{\gamma} = \frac{1}{2}\partial_t \log\gamma &= \frac{1}{2}\frac{1}{\gamma}\partial_t \gamma \\
&= \frac{1}{2}\mathrm{Tr}\left(\gamma^{ij}\partial_t \gamma_{kl}\right) \\
&= \frac{1}{2}\gamma^{ij}\partial_t \gamma_{ij} \\
&= \frac{1}{2}\gamma^{ij}\left(-2\alpha K_{ij} + D_i\beta_j + D_j\beta_i\right) \qquad \text{(By (3.40))} \\
&= -\alpha K + D_i\beta^i.
\end{aligned} \tag{3.41}$$

Here we used *Jacobi's formula*: For an invertible matrix A,

$$\frac{\mathrm{d}}{\mathrm{d}t}\left[\det A(t)\right] = \det A(t) \cdot \mathrm{Tr}\left[A^{-1}(t) \cdot \frac{\mathrm{d}}{\mathrm{d}t}A(t)\right]. \tag{3.42}$$

We note that to derive the evolution of the spatial metric we did not use the EFEs at all. That all changes for the derivation of the evolution of the extrinsic curvature –as well as for the constraints.–

Our starting point is to cast the EFEs in 3+1 form, which can be achieved by contracting them with the projection operator $\gamma^a{}_b$ and with the normal vector n^a. There are only three unique types of contractions (all other projections vanish identically thanks to the symmetries of the Riemann tensor):

- Normal projection (1 equation):

$$n^a n^b ({}^{(4)}G_{ab} - 8\pi T_{ab}) = 0. \tag{3.43}$$

- Projection onto the hypersurface (6 equations):

$$\gamma_c{}^a \gamma_d{}^b ({}^{(4)}G_{ab} - 8\pi T_{ab}) = 0. \tag{3.44}$$

- Mixed projection (3 equations):

$$\gamma_c{}^b \left[n^a ({}^{(4)}G_{ab} - 8\pi T_{ab}) \right] = 0. \tag{3.45}$$

These expressions come about by using the celebrated ***Gauss-Codazzi***, ***Codazzi-Mainardi***, and ***Ricci*** equations, which are given, respectively, by the following:

$$\gamma_a{}^e \gamma_b{}^f \gamma_c{}^g \gamma_d{}^h {}^{(4)}R_{efgh} = R_{abcd} + K_{ac}K_{bd} - K_{ad}K_{cb} \tag{3.46a}$$

$$\gamma_a{}^e \gamma_b{}^f \gamma_c{}^g n^h {}^{(4)}R_{efgh} = D_b K_{ac} - D_a K_{bc} \tag{3.46b}$$

$$\gamma_a{}^q \gamma_b{}^r n^c n^d {}^{(4)}R_{qcrd} = \mathcal{L}_{\vec{n}} K_{ab} + \frac{1}{\alpha} D_a D_b \alpha + K_b{}^c K_{ac}. \tag{3.46c}$$

These three important equations are proven in gory detail in Appendix A. Note how Eqs. (3.46a) and (3.46b) depend exclusively on the spatial metric, the extrinsic curvature, and their spatial derivatives; they will give rise to the constraint equations. On the other hand, Eq. (3.46c) will yield the *evolution equation for the extrinsic curvature*, which we will show last.

Without further ado then, let us now derive the constraint equations from contractions of (3.46a) and (3.46b). Starting with (3.46a), first raise an index and then contract (all with the 3-metric γ_{ab}):

$$\begin{aligned}
\gamma^{pa}\gamma_a{}^e \gamma_b{}^f \gamma_c{}^g \gamma_d{}^h {}^{(4)}R_{efgh} &= \gamma^{pa} R_{abcd} + \gamma^{pa} K_{ac} K_{bd} - \gamma^{pa} K_{ad} K_{cb} \\
\gamma^{pe} \gamma_b{}^f \gamma_c{}^g \gamma_d{}^h {}^{(4)}R_{efgh} &= R^p{}_{bcd} + K^p{}_c K_{bd} - K^p{}_d K_{cb} \\
\gamma_b{}^f \gamma_d{}^h \gamma^{eg} {}^{(4)}R_{efgh} &= R_{bd} + K K_{bd} - K^c{}_d K_{cb},
\end{aligned} \tag{3.47}$$

where on the third line we contracted (again, with γ_{ab}) on indices p and c, and we introduced the ***trace of the extrinsic curvature*** $K \equiv K^a{}_a$. Now, a further contraction yields

$$\begin{aligned}
\gamma^{pb} \gamma_b{}^f \gamma_d{}^h \gamma^{eg} {}^{(4)}R_{efgh} &= \gamma^{pb} R_{bd} + \gamma^{pb} K K_{bd} - \gamma^{pb} K^c{}_d K_{cb} \\
\gamma^{pf} \gamma^{eg} \gamma_d{}^h {}^{(4)}R_{efgh} &= R^p{}_d + K K^p{}_d - K^c{}_d K_c{}^p \\
\gamma^{fh} \gamma^{eg} {}^{(4)}R_{efgh} &= R + K^2 - K^c{}_p K_c{}^p.
\end{aligned} \tag{3.48}$$

Here we again contracted on indices p and d on the last line. Now note that

$$K^c{}_p K_c{}^p = K^c{}_p \gamma^{pr} K_{cr} = K^{cr} K_{cr},$$

and we can also expand on the left hand side of (3.48) as

$$\begin{aligned}
\gamma^{fh}\gamma^{eg}\,{}^{(4)}R_{efgh} &= (g^{fh} + n^f n^h)(g^{eg} + n^e n^g)\,{}^{(4)}R_{efgh} \\
&= (g^{fh}g^{eg} + n^f n^h g^{eg} + n^e n^g g^{fh} + n^f n^h n^e n^g)\,{}^{(4)}R_{efgh} \\
&= g^{fh}g^{eg}\,{}^{(4)}R_{efgh} + n^f n^h g^{eg}\,{}^{(4)}R_{efgh} + n^e n^g g^{fh}\,{}^{(4)}R_{fehg} \\
&\quad + \underbrace{n^f n^h n^e n^g\,{}^{(4)}R_{efgh}}_{=0 \text{ by symmetries of } {}^{(4)}R_{efgh}} \\
&= g^{fh}\,{}^{(4)}R_{fh} + n^f n^h\,{}^{(4)}R_{fh} + n^e n^g\,{}^{(4)}R_{eg} \\
&= {}^{(4)}R + 2n^f n^h\,{}^{(4)}R_{fh}. \qquad \text{(by relabeling)}
\end{aligned}$$

Thus we can rewrite (3.48) as

$${}^{(4)}R + 2n^a n^b\,{}^{(4)}R_{ab} = R + K^2 - K^{ab}K_{ab}.$$

Yet we can do better…Close inspection of the left hand side tells us that the Einstein tensor is lurking somewhere:

$$\begin{aligned}
{}^{(4)}R + 2n^a n^b\,{}^{(4)}R_{ab} &= -\underbrace{n^a n_a}_{\text{since } n^a n_a = -1}\,{}^{(4)}R + 2n^a n^b\,{}^{(4)}R_{ab} \\
&= -g_{ab}n^a n^b\,{}^{(4)}R + 2n^a n^b\,{}^{(4)}R_{ab} \\
&= 2n^a n^b\left({}^{(4)}R_{ab} - \frac{1}{2}\,{}^{(4)}R g_{ab}\right) \\
&= 2n^a n^b\,{}^{(4)}G_{ab}.
\end{aligned}$$

Then, by means of the EFEs, ${}^{(4)}G_{ab} = 8\pi T_{ab}$, we get

$$\begin{aligned}
R + K^2 - K^{ab}K_{ab} &= 2n^a n^b\,{}^{(4)}G_{ab} \\
R + K^2 - K^{ab}K_{ab} &= 16\pi n^a n^b T_{ab}.
\end{aligned}$$

Defining the total ***energy density*** ρ (as measured by a normal observer n^a) as

$$\rho \equiv n^a n^b T_{ab}, \tag{3.49}$$

we end up with

$$R + K^2 - K^{ab}K_{ab} = 16\pi\rho. \tag{3.50}$$

This is the so-called ***Hamiltonian constraint*** which, after dropping timelike components, we write as

$$\boxed{R + K^2 - K^{ij}K_{ij} = 16\pi\rho.} \tag{3.51}$$

Now on to find the remaining constraint equation; we use (3.46b), raise an index and then contract (all with the 3-metric γ_{ab}):

$$\begin{aligned}
\gamma^{rc}\gamma_a{}^d\gamma_b{}^e\gamma_c{}^f n^p {}^{(4)}R_{defp} &= \gamma^{rc}D_bK_{ac} - \gamma^{rc}D_aK_{bc} \\
\gamma_a{}^d\gamma_b{}^e\gamma^{rf} n^p {}^{(4)}R_{defp} &= D_bK_a{}^r - D_aK_b{}^r \qquad \text{(Since } D_a \text{ is compatible with } \gamma_{ab}\text{)} \\
\gamma_a{}^d\gamma^{ef} n^p {}^{(4)}R_{defp} &= D_bK_a{}^b - D_aK, \qquad (3.52)
\end{aligned}$$

where on the last line we contracted on indices r and b. Then expanding the left hand side of (3.52)

$$\begin{aligned}
\gamma_a{}^d\gamma^{ef} n^p {}^{(4)}R_{defp} &= \gamma_a{}^d\left(g^{ef} + n^e n^f\right) n^p {}^{(4)}R_{defp} \\
&= \gamma_a{}^d n^p g^{ef} {}^{(4)}R_{defp} + \gamma_a{}^d \underbrace{n^e n^f n^p {}^{(4)}R_{defp}}_{=0 \text{ by symmetries of } {}^{(4)}R_{abcd}} \\
&= -\gamma_a{}^d n^p g^{ef} {}^{(4)}R_{edfp} = -\gamma_a{}^d n^p {}^{(4)}R_{dp}.
\end{aligned}$$

So, plugging back into (3.52), we get

$$D_bK_a{}^b - D_aK = -\gamma_a{}^d n^p {}^{(4)}R_{dp}. \qquad (3.53)$$

Yet we want to bring in the Einstein tensor to the scene, so we can push a bit further and expand the right hand side of (3.53):

$$-\gamma_a{}^d n^p {}^{(4)}R_{dp} = -(\gamma_a{}^d n^p {}^{(4)}R_{dp} - \frac{1}{2}\underbrace{\gamma_a{}^d n^p g_{dp}}_{=\gamma_{ap}n^p=0} {}^{(4)}R) = -\gamma_a{}^d n^p {}^{(4)}G_{dp}.$$

Then, once again invoking the EFEs, ${}^{(4)}G_{ab} = 8\pi T_{ab}$, we get

$$\begin{aligned}
D_bK_a{}^b - D_aK &= -\gamma_a{}^d n^p {}^{(4)}G_{dp} \\
D_bK_a{}^b - D_aK &= -\gamma_a{}^d n^p 8\pi T_{dp}.
\end{aligned}$$

Defining the ***momentum density*** S_a (as measured by a normal observer n^a) by

$$S_a \equiv -\gamma_a{}^b n^c T_{bc}, \qquad (3.54)$$

we end up with the ***momentum constraints***

$$D_bK_a{}^b - D_aK = 8\pi S_a. \qquad (3.55)$$

As usual we now drop the timelike components,

$$D_jK_i{}^j - D_iK = 8\pi S_i,$$

and then raise indices

$$\gamma^{ki}\left(D_j K_i^{\ j} - D_i K\right) = \gamma^{ki} 8\pi S_i$$
$$D_j\left(K^{jk} - \gamma^{jk}K\right) = 8\pi S^k,$$

where we used the compatibility of D with γ_{ab}. This leaves (3.55) in the final form

$$\boxed{D_j\left(K^{ij} - \gamma^{ij}K\right) = 8\pi S^i.} \tag{3.56}$$

Both (3.51) and (3.56) are constraints that need to be satisfied and respected on each time slice Σ. They are restrictions placed on γ_{ab} and K_{ab} so that the spatial slices "fit nicely" when embedded into the ambient spacetime $\mathcal{M}$. We will discuss further the *initial data problem* on § 5.1.

Now, with the evolution of the metric and the constraints taken care of, we move on to find the last key result from this chapter; the evolution equation of K_{ab}. We start by considering its Lie derivative along t^a,

$$\partial_t K_{ab} = \mathcal{L}_{\vec{t}} K_{ab} = \mathcal{L}_{\alpha\vec{n}+\vec{\beta}} K_{ab} = \alpha\mathcal{L}_{\vec{n}} K_{ab} + \mathcal{L}_{\vec{\beta}} K_{ab}.$$

In order to tackle the first term on the RHS, we use Ricci's equation (3.46c)

$$\gamma_a^{\ e}\gamma_b^{\ f} n^c n^d {}^{(4)}R_{ecfd} = \mathcal{L}_{\vec{n}} K_{ab} + \frac{1}{\alpha} D_a D_b \alpha + K_b^{\ c} K_{ac},$$

so that

$$\partial_t K_{ab} = \alpha\left(\gamma_a^{\ e}\gamma_b^{\ f} n^c n^d {}^{(4)}R_{ecfd} - \frac{1}{\alpha} D_a D_b \alpha - K_b^{\ c} K_{ac}\right) + \mathcal{L}_{\vec{\beta}} K_{ab}. \tag{3.57}$$

Now we should tidy up a bit... First recall that the EFEs ${}^{(4)}G_{ab} = 8\pi T_{ab}$ can be written in the following equivalent way, by contracting with g^{ab}:

$$g^{ab}\,{}^{(4)}G_{ab} = g^{ab}\,{}^{(4)}R_{ab} - \frac{1}{2}\,{}^{(4)}R\,\underbrace{g^{ab}g_{ab}}_{=4} = 8\pi\,\underbrace{g^{ab}T_{ab}}_{\equiv T}$$
$${}^{(4)}R - 2\,{}^{(4)}R = 8\pi T \implies {}^{(4)}R = -8\pi T$$
$${}^{(4)}R_{ab} = 8\pi\left(T_{ab} - \frac{1}{2}T g_{ab}\right), \tag{3.58}$$

where we defined the ***trace of the stress-energy tensor***

$$T \equiv g^{ab}T_{ab}. \tag{3.59}$$

Now note that

$$\begin{aligned}
\gamma_a{}^e\gamma_b{}^f n^c n^{d\,(4)}R_{ecfd} &= \gamma_a{}^e\gamma_b{}^f(\gamma^{cd}-g^{cd})^{(4)}R_{ecfd}\\
&= \gamma_a{}^e\gamma_b{}^f\gamma^{cd\,(4)}R_{ecfd} - \gamma_a{}^e\gamma_b{}^f g^{cd\,(4)}R_{cedf}\\
&= \gamma_a{}^e\gamma_b{}^f\gamma^{cd\,(4)}R_{ecfd} - \gamma_a{}^e\gamma_b{}^{f\,(4)}R_{ef}\\
&= \underbrace{R_{ab}+KK_{ab}-K_{ac}K^c{}_b}_{\text{By (3.47) (contraction of (3.46a))}} - \underbrace{8\pi\gamma_a{}^e\gamma_b{}^f\left(T_{ef}-\frac{1}{2}Tg_{ef}\right)}_{\text{By (3.58)}}\\
&= R_{ab}+KK_{ab}-K_{ac}K^c{}_b - 8\pi\underbrace{\gamma_a{}^e\gamma_b{}^f T_{ef}}_{\equiv S_{ab}\ (\textbf{spatial stress})} + 4\pi\underbrace{\gamma_a{}^e\gamma_b{}^f g_{ef}}_{=\gamma_{ab}}\underbrace{T}_{=g^{pr}T_{pr}}\\
&= R_{ab}+KK_{ab}-K_{ac}K^c{}_b - 8\pi S_{ab} + 4\pi\gamma_{ab}\,g^{pr}T_{pr}\\
&= R_{ab}+KK_{ab}-K_{ac}K^c{}_b - 8\pi S_{ab} + 4\pi\gamma_{ab}(\gamma^{pr}-n^p n^r)T_{pr}\\
&= R_{ab}+KK_{ab}-K_{ac}K^c{}_b - 8\pi S_{ab} + 4\pi\gamma_{ab}(\underbrace{\gamma^{pr}T_{pr}}_{=S^a{}_a\equiv S} - \underbrace{n^p n^r T_{pr}}_{=\rho})\\
&= R_{ab}+KK_{ab}-K_{ac}K^c{}_b - 8\pi S_{ab} + 4\pi\gamma_{ab}(S-\rho). \qquad (3.60)
\end{aligned}$$

Here we defined the ***spatial stress***

$$S_{ab} \equiv \gamma_a{}^c\gamma_b{}^d T_{cd}, \qquad (3.61)$$

as well as its trace

$$S \equiv \gamma^{ab}S_{ab} = S^a{}_a. \qquad (3.62)$$

Now, inserting the results obtained in (3.60) back into (3.57), we get

$$\begin{aligned}
\partial_t K_{ab} &= \alpha\left(\gamma_a{}^e\gamma_b{}^f n^c n^{d\,(4)}R_{ecfd} - \frac{1}{\alpha}D_aD_b\alpha - K_b{}^cK_{ac}\right) + \mathcal{L}_{\vec\beta}K_{ab}\\
&= \alpha(R_{ab}+KK_{ab}-K_{ac}K^c{}_b - 8\pi\left(S_{ab}-\frac{1}{2}\gamma_{ab}(S-\rho)\right) - \frac{1}{\alpha}D_aD_b\alpha\\
&\quad - K_b{}^cK_{ac}) + \mathcal{L}_{\vec\beta}K_{ab}\\
&= \alpha(R_{ab}+KK_{ab}-2K_{ac}K^c{}_b) - 8\pi\alpha\left(S_{ab}-\frac{1}{2}\gamma_{ab}(S-\rho)\right) - D_aD_b\alpha + \mathcal{L}_{\vec\beta}K_{ab}.
\end{aligned}$$

Lastly, since the entire content of spatial tensors is available from their spatial components, we can write our results as

$$\boxed{\begin{aligned}\partial_t K_{ij} &= \alpha(R_{ij}+KK_{ij}-2K_{ik}K^k{}_j) - 8\pi\alpha\left(S_{ij}-\frac{1}{2}\gamma_{ij}(S-\rho)\right) - D_iD_j\alpha\\ &\quad + \beta^k D_k K_{ij} + 2K_{k(i}D_{j)}\beta^k,\end{aligned}} \qquad (3.63)$$

where we used

$$\mathcal{L}_{\vec\beta}K_{ij} = \beta^k D_k K_{ij} + K_{kj}D_i\beta^k + K_{ik}D_j\beta^k.$$

Equation (3.63) is the ***evolution of the extrinsic curvature***, our last piece of the puzzle.

Now, in theory at least, once we have gravitational field data (γ_{ij}, K_{ij}) that satisfies the momentum and Hamiltonian constraints on on some initial spatial slice, we may then integrate forward the evolution equations to obtain a spacetime that satisfies the EFE's. [8] In practice, however, numerical stability is highly dependent on gauge choice and initial data prescribed. Moreover, the ADM equations presented above are, in fact, not very stable with respect to constraint violations (this has to do with the degree of *hyperbolicity* of the equations). We will touch on these issues again once we introduce the *BSSN formalism* in Chapter 4. For now, let us present a useful contraction of (3.63), namely

$$\partial_t K = \alpha\left(4\pi(\rho + S) + K_{ij}K^{ij}\right) - D^2\alpha + \beta^i\partial_i K, \tag{3.64}$$

where $D^2 = \gamma^{ij}D_iD_j$ is the ***spatial Laplace operator***. Let us prove this.

Proof of (3.64). In what follows we will use the Hamiltonian constraint (3.51). Moreover, since we want to expand $\partial_t K = \partial_t(\gamma^{ij}K_{ij}) = \gamma^{ij}\partial_t K_{ij} + K_{ij}\partial_t\gamma^{ij}$, we need the time evolution of the inverse spatial metric. Note that since $\gamma^{ij}\gamma_{jk} = \delta^i{}_k$, we have $\partial_t(\gamma^{ij}\gamma_{jk}) = 0$, which implies

$$\begin{aligned} \gamma_{jk}\partial_t\gamma^{ij} &= -\gamma^{ij}\,\partial_t\gamma_{jk} \\ \implies \underbrace{\gamma^{lk}\gamma_{jk}}_{=\delta^l{}_j}\partial_t\gamma^{ij} &= -\gamma^{lk}\gamma^{ij}\,\partial_t\gamma_{jk} \\ \implies \partial_t\gamma^{il} &= -\gamma^{lk}\gamma^{ij}\,\partial_t\gamma_{jk}. \end{aligned} \tag{3.65}$$

Now,

$$\begin{aligned} \partial_t K = \partial_t(\gamma^{ij}K_{ij}) &= \gamma^{ij}\partial_t K_{ij} + K_{ij}\partial_t\gamma^{ij} \\ &= \gamma^{ij}[\alpha(R_{ij} + KK_{ij} - 2K_{ik}K^k{}_j) - 8\pi\alpha\left(S_{ij} - \frac{1}{2}\gamma_{ij}(S-\rho)\right) - D_iD_j\alpha \\ &\quad + \beta^k D_k K_{ij} + K_{kj}D_i\beta^k + K_{ki}D_j\beta^k] + K_{ij}[-\gamma^{jk}\gamma^{im}\partial_t\gamma_{mk}] \\ &= \alpha(\underbrace{R + K^2 - K_{ij}K^{ij}}_{=\,16\pi\rho \text{ by (3.51)}} - K_{ij}K^{ij}) - 8\pi\alpha\left(S - \frac{3}{2}(S-\rho)\right) - D^2\alpha + \beta^i\underbrace{D_iK}_{=\partial_i K} + 2K_{ij}D^i\beta^j \\ &\quad - K^{mk}(-2\alpha K_{mk} + D_m\beta_k + D_k\beta_m) \\ &= \alpha(16\pi\rho - K_{ij}K^{ij}) - 8\pi\alpha S + 12\pi\alpha S - 12\pi\alpha\rho - D^2\alpha + \beta^i\partial_i K + 2K_{ij}D^i\beta^j \\ &\quad + 2\alpha K_{ij}K^{ij} - \underbrace{\gamma^{nm}\gamma^{lk}K_{nl}\left(D_m\beta_k + D_k\beta_m\right)}_{=2K_{ij}D^i\beta^j} \\ &= \alpha\left(4\pi(\rho + S) + K_{ij}K^{ij}\right) - D^2\alpha + \beta^i\partial_i K. \end{aligned}$$

□

[8] Of course, if matter is present, then we must also take into account the matter fields and specify them on the initial hypersurface as well. Then we must use the matter evolution equations, $\nabla_a T^{ab} = 0$, and integrate simultaneously with the field evolution equations to build a spacetime. More on this on § 5.3.

We will use this result later when we develop the BSSN formalism. In this formulation, instead of evolving K_{ij}, we first split it into its trace K and its traceless part. Then –after a suitable conformal rescaling, in the case of the traceless part of K_{ij}– we evolve these quantities instead of the full extrinsic curvature itself.

ADM (à la York) Equations

⁕ **Evolution Equations:**

$$\begin{aligned}
&\partial_t \gamma_{ij} = 2D_{(i}\beta_{j)} - 2\alpha K_{ij} \\
&\partial_t K_{ij} = \alpha(R_{ij} + KK_{ij} - 2K_{ik}K^k{}_j) - 8\pi\alpha\left(S_{ij} - \frac{1}{2}\gamma_{ij}(S-\rho)\right) - D_iD_j\alpha \\
&\qquad\quad + \beta^k D_k K_{ij} + 2K_{k(i}D_{j)}\beta^k
\end{aligned}$$

⁕ **Constraint Equations:**

$$\begin{aligned}
R + K^2 - K_{ij}K^{ij} &= 16\pi\rho \\
D_j\left(K^{ij} - \gamma^{ij}K\right) &= 8\pi S^i
\end{aligned}$$

Chapter 4

Conformal Reformulation

The 3+1 ADM (à la York) decomposition of the EFEs presented in the previous chapter poses a very straightforward, elegant formulation. Unfortunately, however, the EFEs as presented in this form are not quite suitable for numerical implementations. Alas, we need to put in more work before we take a crack at computing anything, since in practice one finds that this form of the 3+1 decomposition results in large instabilities that develop during a computer simulation (this issue is known to be mainly due to the fact that the EFEs in this ADM form are *weakly hyperbolic*; i.e., they are not *well-posed*. [1]) To get around this problem, in an effort to make the EFEs more *strongly hyperbolic* (i.e., more "wave-like"), many modern NR codes utilize the so-called *BSSN* (aka *BSSNOK*) *formalism* which –together with suitable gauge conditions for the lapse and shift– does admit a more robust computational formulation of the EFEs.

Refinements to the already very successful BSSN formalism do exist. For instance, by further modifying the BSSN equations through introducing a propagating Hamiltonian, we end up with a $Z4$-like formulation of GR. The original $Z4$ system was introduced by Bona and collaborators in 2013 (see [14] and, subsequently, [13]), and it has sprung a whole family of $Z4$-like systems ever since: consult [10] for the *conformal* $Z4$ *formalism* ($Z4c$); for the *conformal and covariant* $Z4$ *formalism* (CCZ4) the reader may refer to [5], and slight variations of the latter, such as the *fully conformal and covariant* $Z4$ *formalism* (fCCZ4), can be found in [47]. As was demonstrated by Bernuzzi and Hilditch ([10]), there are instances in which a conformal $Z4$ approach yields even more accurate results than BSSN, especially when we consider non-vacuum spacetimes. [2] Since we are ultimately interested in modelling scalar fields coupled to the EFEs, it seems highly likely that we will at some point implement a $Z4$-like formulation in our modelling. However, for the time being we will stick to the more traditional BSSN equations.

4.1 The BSSN Formalism

In place of the ADM data $\{\gamma_{ij}, K_{ij}\}$, the BSSN formalism splits γ_{ij} into a conformal factor χ and a conformally-related metric $\bar{\gamma}_{ij}$, and it also splits K_{ij} into its trace K and a traceless part A_{ij}. Moreover, three coefficients $\bar{\Gamma}^i$ of the conformal metric are introduced as well. Then, it is these variables that are evolved instead of the original ADM physical quantities… Long story short, the dynamical variables

[1] For more on the concept of hyperbolicity (in the numerical sense), see the detailed analysis on [48].

[2] In BSSN evolutions of matter spacetimes the Hamiltonian constraint, in particular, is largely violated. The constraint-damping capabilities allowed by $Z4$-like formulations offers a solution to this problem, although ultimately it is the propagation of constraints what seems to work best, as described by Bernuzzi and Hilditch. [10]

that we consider in the BSSN formalism are

$$\{\chi, \bar{\gamma}_{ij}, \bar{A}_{ij}, K, \bar{\Gamma}^i\}. \tag{4.1}$$

We will present each of these quantities and their evolution equations in this chapter. Let us start by considering a conformal rescaling of the spatial metric of the form

$$\gamma_{ij} = \psi^4 \bar{\gamma}_{ij}, \tag{4.2}$$

where ψ is some positive scaling factor called the ***conformal factor***, and the background auxiliary metric $\bar{\gamma}_{ij}$ is known as the ***conformally-related metric*** (or simply ***conformal metric***). It may seem unclear at the moment why we scaled the spatial metric in this way, but later on we will see that, indeed, this "trick" will actually yield a convenient and tractable system for the EFEs. May it suffice to say for now though, that besides the mathematical convenience that such a conformal rescaling brings about, there is also the fact that equivalence classes of conformally-related manifolds share some geometric properties. For example, it can be shown that two strongly causal Lorentzian metrics $g^{(1)}_{ab}$ and $g^{(2)}_{ab}$ for some manifold $\mathcal{M}$ determine the same future and past sets at all points (events) if and only if the two metrics are globally conformal, i.e., if $g^{(1)}_{ab} = \Psi g^{(2)}_{ab}$, for some smooth function $\Psi \in C^\infty(\mathcal{M})$ (see, e.g., [9]).. In this case, both spacetimes $(\mathcal{M}, g^{(1)}_{ab})$ and $(\mathcal{M}, g^{(2)}_{ab})$ belong to the same conformal class and share the same causal structure.

A somewhat natural choice for a representative object in a conformal equivalence class of spatial metric tensors would be a metric $\bar{\gamma}_{ij}$ whose determinant is the same as the determinant of a flat metric f_{ij}, in any general chart. Thus, if we adopt a Cartesian coordinate system ($f_{ij} = \delta_{ij}$), we can always enforce that our conformal representative must have unit determinant, i.e., $\bar{\gamma} = \delta = 1$. Plugging this back into (4.2), we get

$$1 = \det \bar{\gamma}_{ij} = \det(\psi^{-4}\gamma_{ij}) = (\psi^{-4})^3 \underbrace{\det \gamma_{ij}}_{\equiv \gamma} = \psi^{-12}\gamma.$$

This would correspond to the choice $\psi = \gamma^{1/12}$, so that $\gamma_{ij} = \gamma^{1/3}\bar{\gamma}_{ij}$. Any spatial metric γ_{ij} in this conformal class yields the same value of $\bar{\gamma}_{ij}$. However note that, since the determinant γ is coordinate-dependent, the conformal factor $\psi = \gamma^{1/12}$ *is not* a scalar field. In fact, $\bar{\gamma}_{ij}$ is not a tensor field, but rather a *tensor density* of *weight* $-2/3$; we show this now.

Definition 3. *A* $\binom{k}{\ell}$ ***tensor density of weight*** $\omega \in \mathbb{Q}$ *is a quantity* $\Xi^{i_1,\dots,i_k}{}_{j_1,\dots,j_\ell}$ *that transforms under a change of coordinates as*

$$\Xi^{i'_1,\dots,i'_k}{}_{j'_1,\dots,j'_\ell} = J^\omega \frac{\partial x^{i'_1}}{\partial x^{i_1}} \cdots \frac{\partial x^{i'_k}}{\partial x^{i_k}} \frac{\partial x^{j_1}}{\partial x^{j'_1}} \cdots \frac{\partial x^{j_\ell}}{\partial x^{j'_\ell}} \Xi^{i_1,\dots,i_k}{}_{j_1,\dots,j_\ell} \tag{4.3}$$

where J *is the Jacobian* $J = \det|\partial x^{i'_k}/\partial x^{i_k}|$.

According to this definition, then, a tensor field is nothing but a tensor density of weight zero. In our case, we are interested in *spatial* tensor densities; these are regular (zero weight) tensors that multiply a power of the determinant γ. In other words, a ***spatial tensor density*** $\boldsymbol{\tau}$ ***of weight*** $\omega \in \mathbb{Q}$ is an object

$$\boldsymbol{\tau} = \gamma^{\omega/2}\, \boldsymbol{T}, \tag{4.4}$$

where $\boldsymbol{T}$ is a tensor field. Since $\bar{\gamma}_{ij} = \gamma^{-1/3}\gamma_{ij}$, (4.4) shows that, indeed, $\bar{\gamma}_{ij}$ is a tensor density of weight $-2/3$, as we claimed earlier.

To get around this issue of tensor densities, we could introduce a *background flat metric* f_{ij} of Riemannian signature $(+,+,+)$ and set $\psi \equiv (\gamma/f)^{1/12}$, so that ψ becomes a scalar field in this manner, and we could then use non-Cartesian coordinates. However, for our purposes of implementing the standard BSSN formalism, it is convenient to stick to Cartesian coordinates; to see the implementation of this extended BSSN formalism (where non-Cartesian coordinates are used), the reader is referred to [27]. That being said, since we have chosen to deal with tensor densities in our treatment, we must discuss the ***Lie derivative of a tensor density***, which is given by

$$\mathcal{L}_{\vec{x}}\boldsymbol{\tau} = \left[\mathcal{L}_{\vec{x}}\boldsymbol{\tau}\right]_{\omega=0} + \omega\boldsymbol{\tau}\,\partial_i x^i, \tag{4.5}$$

where the first term is the usual Lie derivative we would compute if $\boldsymbol{\tau}$ had zero weight (i.e., if $\boldsymbol{\tau}$ was a tensor field rather than a tensor density). Likewise, the ***covariant derivative of a tensor density*** $\boldsymbol{\tau}$ is furnished by [3]

$$\nabla_c\boldsymbol{\tau} = \left[\nabla_c\boldsymbol{\tau}\right]_{\omega=0} - \omega\boldsymbol{\tau}\,\Gamma^d_{dc}, \tag{4.6}$$

where, again, the first term is the usual covariant derivative we would compute if $\boldsymbol{\tau}$ had zero weight. Using the expression (3.22) we see that, in coordinates, (4.6) expands as

$$\begin{aligned}(\nabla\boldsymbol{\tau})^{i_1\ldots i_a}{}_{j_1\ldots j_b c} &= \nabla_c\tau^{i_1\ldots i_a}{}_{j_1\ldots j_b} \\ &= \partial_c\tau^{i_1\ldots i_a}{}_{j_1\ldots j_b} + \sum_{d=1}^{a}\tau^{i_1\ldots e\ldots i_a}{}_{j_1\ldots j_b}\Gamma^{i_d}_{ec} - \sum_{d=1}^{b}\tau^{i_1\ldots i_a}{}_{j_1\ldots e\ldots j_b}\Gamma^{e}_{j_d c} - \omega\tau^{i_1\ldots i_a}{}_{j_1\ldots j_b}\Gamma^d_{dc}.\end{aligned} \tag{4.7}$$

We will frequently encounter Lie and covariant derivatives of a tensor density in our work.

Before proceeding any further, we should comment on the choice of scaling factor. The fourth power chosen for ψ turns out to be convenient for certain calculations, but otherwise it is arbitrary. In fact, this particular factor is just one of the three most popular conformal factors found in the NR literature, the other two being

$$\chi = \psi^{-4} = \gamma^{-1/3} \qquad \text{and} \qquad \phi = \log\psi = \frac{1}{12}\log\gamma,$$

turning (4.2) into

$$\gamma_{ij} = \frac{1}{\chi}\bar{\gamma}_{ij}, \tag{4.8}$$

and

$$\gamma_{ij} = e^{4\phi}\bar{\gamma}_{ij}, \tag{4.9}$$

[3] Note that the ∇ we are using for this discussion is not necessarily the connection of the $4D$ spacetime $\mathcal{M}$; this is a rather general discussion, so ∇ can be replaced by whatever affine connection.

respectively. The choice of scaling factor is a matter of *mathematical* and *computational* convenience (the *physical* interpretation must be the same regardless of which factor we choose). When dealing with the initial data problem (§ 5.1) the factor ψ is the one widely used in the community, since it puts the constraint equations in a nice elliptic form that we can solve. As for the evolution of the system, on the other hand, the very succesful *moving punctures* method (see the landmark paper [18]) proposes χ as the preferred scaling factor, since it goes to zero at the black hole singularity (it is C^4 at the puncture), [4] and in doing so avoids singularity excision altogether.

Following the moving punctures method, we choose χ as our conformal factor when deriving the evolution formulæ of the system. Henceforth, the ***conformal metric*** shall be given by

$$\boxed{\bar{\gamma}_{ij} = \chi \gamma_{ij}} \tag{4.10a}$$

$$\boxed{\bar{\gamma}^{ij} = \chi^{-1} \gamma^{ij},} \tag{4.10b}$$

where the factor for the inverse metric follows naturally from the fact that

$$\bar{\gamma}^{ij}\bar{\gamma}_{jk} = (\chi^{-1}\gamma^{ij})(\chi\gamma_{jk}) = \gamma^{ij}\gamma_{jk} = \delta^i{}_k,$$

so that $\bar{\gamma}^{ij}$ and $\bar{\gamma}_{jk}$ are, indeed, inverses of each other. Moreover, in the BSSN formulation, the conformal factor is one of the dynamical variables that we need to take into account; therefore, let us now derive its evolution equation. Recall the spatial metric evolution (c.f., Eq. (3.40)):

$$\partial_t \gamma_{ij} = -2\alpha K_{ij} + D_i\beta_j + D_j\beta_i.$$

Using this and Jacobi's formula (c.f., Eq. (3.42)), we get

$$\begin{aligned} \partial_t \gamma &= \gamma\gamma^{ij}\partial_t\gamma_{ij} \\ &= \gamma\left(-2\alpha K + 2D_i\beta^i\right). \end{aligned} \tag{4.11}$$

Now, since $D_i\beta^i = \partial_i\beta^i + \Gamma^i_{ij}\beta^j$, with

$$\begin{aligned} \Gamma^i_{ij} &= \frac{1}{2}\gamma^{ik}(\partial_i\gamma_{jk} + \partial_j\gamma_{ik} - \partial_k\gamma_{ij}) \\ &= \frac{1}{2}\gamma^{ik}\partial_j\gamma_{ik}, \qquad \text{(by relabeling)} \end{aligned}$$

we can insert this back into (4.11) to obtain

$$\begin{aligned} \partial_t\gamma &= \gamma\left(-2\alpha K + 2\partial_i\beta^i + \left(\gamma^{ik}\partial_j\gamma_{ik}\right)\beta^j\right) \\ &= \gamma\left(-2\alpha K + 2\partial_i\beta^i + \left(\frac{1}{\gamma}\partial_j\gamma\right)\beta^j\right) \\ &= 2\gamma\left(\partial_i\beta^i - \alpha K\right) + \beta^i\partial_i\gamma. \end{aligned} \tag{4.12}$$

[4] This is contrast to ψ, which yields a $\mathcal{O}(1/r)$ singularity, and ϕ, which is $\mathcal{O}(\log r)$.

Now this result, combined with our choice $\chi = \psi^{-4}$, yields

$$\begin{aligned}
\partial_t \chi &= \partial_t \psi^{-4} \\
&= -4\psi^{-5}\partial_t \psi \\
&= -4\psi^{-5}\left[\frac{1}{6}\psi(\partial_i \beta^i - \alpha K) + \beta^i \partial_i \psi\right] \\
&= -\frac{2}{3}\psi^{-4}(\partial_i \beta^i - \alpha K) - 4\psi^{-5}\beta^i \partial_i \chi^{-1/4} \\
&= \frac{2}{3}\chi(\alpha K - \partial_i \beta^i) - \beta^i 4\psi^{-4}\psi^{-1} \cdot \left(-\frac{1}{4}\right)\chi^{-5/4}\partial_i \chi \\
&= \frac{2}{3}\chi(\alpha K - \partial_i \beta^i) + \beta^i \cdot \chi \cdot \chi^{1/4} \cdot \chi^{-1/4} \cdot \chi^{-1}\partial_i \chi \\
&= \frac{2}{3}\chi(\alpha K - \partial_i \beta^i) + \beta^i \partial_i \chi. \qquad (4.13)
\end{aligned}$$

Thus we have the ***evolution of the conformal factor*** ,

$$\boxed{\partial_t \chi = \frac{2}{3}\chi(\alpha K - \partial_i \beta^i) + \beta^i \partial_i \chi.} \qquad (4.14)$$

Let us now introduce the ***traceless part of the extrinsic curvature***, which we denote by A_{ij}, and is given by

$$\boxed{A_{ij} = K_{ij} - \frac{1}{3}\gamma_{ij}K.} \qquad (4.15)$$

Note that A_{ij} is indeed traceless: $\gamma^{ij}A_{ij} = \gamma^{ij}\left(K_{ij} - 1/3\gamma_{ij}K\right) = K - 1/3 \cdot 3K = K - K = 0$. This way, the extrinsic curvature K_{ij} is naturally split into its trace K and its traceless part A_{ij}:

$$K_{ij} = A_{ij} + \frac{1}{3}\gamma_{ij}K. \qquad (4.16)$$

Just as we rescaled the spatial metric in (4.10), we shall also rescale the traceless curvature A_{ij} as

$$\boxed{\begin{aligned} \bar{A}_{ij} &= \chi A_{ij} \qquad (4.17a) \\ \bar{A}^{ij} &= \chi^{-1}A^{ij} \qquad (4.17b) \end{aligned}}$$

which, just as its conformally related A_{ij}, is also traceless:

$$\bar{\gamma}^{ij}\bar{A}_{ij} = \chi\bar{\gamma}^{ij}K_{ij} - \frac{1}{3}\bar{\gamma}^{ij}\bar{\gamma}_{ij}K = \chi\chi^{-1}\gamma^{ij}K_{ij} - \frac{1}{3}\cdot 3K = K - K = 0. \quad \surd$$

This rescaling of the conformal traceless curvature was first considered by Nakamura [42], therefore we will refer to it as the ***Nakamura scaling of*** A_{ij} (be aware that we shall use a different scaling for A_{ij} when we deal with the initial data problem (c.f., § 5.1)). This way the conformal version of Eq. (4.15) is

$$\boxed{\bar{A}_{ij} = \chi K_{ij} - \frac{1}{3}\bar{\gamma}_{ij}K.} \tag{4.18}$$

We will refer to $\bar{A}_{ij}$ as the ***conformal traceless curvature***. We shall shortly derive its evolution equation (spoiler alert: it is quite messy!), but first let us start with something simpler, such as rewriting the evolution of the trace K in terms of the newly introduced conformal factors. Recall Eq. (3.64):

$$\partial_t K = \alpha\left(4\pi(\rho + S) + K_{ij}K^{ij}\right) - D^2\alpha + \beta^i\partial_i K.$$

Now from (4.18) we write K_{ij} as

$$K_{ij} = \chi^{-1}\left(\bar{A}_{ij} + \frac{1}{3}\bar{\gamma}_{ij}K\right), \tag{4.19}$$

and similarly,

$$\begin{aligned} K^{ij} &= \gamma^{im}\gamma^{jn}K_{mn} \\ &= \gamma^{im}\gamma^{jn}\chi^{-1}\left(\bar{A}_{mn} + \frac{1}{3}\bar{\gamma}_{mn}K\right) \\ &= \chi^2\bar{\gamma}^{im}\bar{\gamma}^{jn}\chi^{-1}\left(\bar{A}_{mn} + \frac{1}{3}\bar{\gamma}_{mn}K\right) \\ &= \chi\left(\bar{A}^{ij} + \frac{1}{3}\bar{\gamma}^{ij}K\right). \end{aligned} \tag{4.20}$$

This last equation, by the way, yields the contravariant version of the conformal traceless curvature (4.18):

$$\boxed{\bar{A}^{ij} = \chi^{-1}K^{ij} - \frac{1}{3}\bar{\gamma}^{ij}K.} \tag{4.21}$$

Now, plugging Eqs. (4.19) and (4.20) back into (3.64), we get

$$\begin{aligned} \partial_t K &= \alpha\left(4\pi(\rho + S) + K_{ij}K^{ij}\right) - D^2\alpha + \beta^i\partial_i K \\ &= \alpha\left[4\pi(\rho + S) + \left(\chi^{-1}\left(\bar{A}_{ij} + \frac{1}{3}\bar{\gamma}_{ij}K\right)\right)\left(\chi\left(\bar{A}^{ij} + \frac{1}{3}\bar{\gamma}^{ij}K\right)\right)\right] - D^2\alpha + \beta^i\partial_i K \\ &= \alpha[4\pi(\rho + S) + \bar{A}_{ij}\bar{A}^{ij} + \underbrace{\frac{1}{3}\bar{A}_{ij}\bar{\gamma}^{ij}K}_{=0\text{ (tracelessness of }\bar{A}_{ij})} + \underbrace{\frac{1}{3}\bar{A}^{ij}\bar{\gamma}_{ij}K}_{=0\text{ (tracelessness of }\bar{A}_{ij})} + \frac{1}{9}\underbrace{\bar{\gamma}_{ij}\bar{\gamma}^{ij}}_{=3}K^2] - D^2\alpha + \beta^i\partial_i K \\ &= \alpha\left(4\pi(\rho + S) + \bar{A}_{ij}\bar{A}^{ij} + \frac{1}{3}K^2\right) - D^2\alpha + \beta^i\partial_i K. \end{aligned}$$

And thus we have the ***evolution of the trace of the extrinsic curvature***, which takes care of yet another variable presented in (4.1),

$$\boxed{\partial_t K = \alpha\left(\bar{A}_{ij}\bar{A}^{ij} + \frac{1}{3}K^2\right) + 4\pi\alpha(\rho + S) - D^2\alpha + \beta^i\partial_i K.} \tag{4.22}$$

Note, however, that in this equation we are using covariant derivatives D of the lapse with respect to the physical metric γ_{ij}, even though we would like to write everything in this expression in terms of the conformal metric $\bar{\gamma}_{ij}$. We will fix this issue later once we introduce the conformal connection $\bar{D}$ of $\bar{\gamma}_{ij}$ (c.f., Eq. (4.36)).

Now, before tackling the evolution of $\bar{A}_{ij}$, we need to clarify a few things. First note that

$$K^k{}_j = \gamma^{ki}K_{ij} = \chi\bar{\gamma}^{ki}K_{ij} = \chi\bar{\gamma}^{ki}\chi^{-1}\left(\bar{A}_{ij} + \frac{1}{3}\bar{\gamma}_{ij}K\right) = \bar{A}^k{}_j + \delta^k{}_j K.$$

We will use this in the calculations that follow, just as we will also use the notation $[\cdots]^{\mathrm{TF}}$ to denote the trace-free part of whatever object lies inside the brackets (e.g., $[K_{ij}]^{\mathrm{TF}} = A_{ij}$). In general, for a tensor $\boldsymbol{T}$ in a D-dimensional metric $\boldsymbol{g}$, we have $[\boldsymbol{T}]^{\mathrm{TF}} = \boldsymbol{T} - \boldsymbol{g}/D\,\mathrm{Tr}(\boldsymbol{T})$ (we have already used this when we defined A_{ij} in (4.15)). Naturally, it follows that if $\boldsymbol{T}$ is already trace-free, then $[\boldsymbol{T}]^{\mathrm{TF}} = \boldsymbol{T}$. Furthermore, we will also use the fact that the metric tensor does not contain any trace-free part (for instance, for $\bar{\gamma}_{ij}$, we have $[\bar{\gamma}_{ij}]^{\mathrm{TF}} = \bar{\gamma}_{ij} - \bar{\gamma}_{ij}/3\,\mathrm{Tr}(\bar{\gamma}_{ij}) = \bar{\gamma}_{ij} - \bar{\gamma}_{ij}/3\cdot 3 = 0$). Lastly, we also note that since $\bar{A}_{ij}$ and χ^{-1} are tensor densities of weights $-2/3$ and $2/3$, respectively (c.f., Eq. (4.4)), their Lie derivatives are given by

$$\mathcal{L}_{\vec{\beta}}\bar{A}_{ij} = \beta^k\partial_k\bar{A}_{ij} + \bar{A}_{ik}\partial_j\beta^k + \bar{A}_{kj}\partial_i\beta^k - \frac{2}{3}\bar{A}_{ij}\partial_k\beta^k, \tag{4.23}$$

and

$$\mathcal{L}_{\vec{\beta}}\chi^{-1} = \beta^k\partial_k\chi^{-1} + \frac{2}{3}\chi^{-1}\partial_k\beta^k = -\chi^{-2}\beta^k\partial_k\chi + \frac{2}{3}\chi^{-1}\partial_k\beta^k. \tag{4.24}$$

Now we are (at last!) ready to calculate the evolution of $\bar{A}_{ij}$:

$$\begin{aligned}
\partial_t\bar{A}_{ij} &= \partial_t(\chi A_{ij}) = \chi\partial_t A_{ij} + A_{ij}\partial_t\chi \\
&= \chi[\partial_t K_{ij}]^{\mathrm{TF}} + A_{ij}\partial_t\chi \\
&= \chi\left[\alpha(R_{ij} + KK_{ij} - 2K_{ik}K^k{}_j) - 8\pi\alpha(S_{ij} - \frac{1}{2}\underbrace{\gamma_{ij}}_{\text{no TF}}(S-\rho)) - D_iD_j\alpha + \mathcal{L}_{\vec{\beta}}K_{ij}\right]^{\mathrm{TF}} \\
&\quad + \chi^{-1}\bar{A}_{ij}\left[\frac{2}{3}\chi(\alpha K - \partial_i\beta^i) + \beta^i\partial_i\chi\right] \\
&= [\alpha\chi R_{ij} + \alpha\chi\chi^{-1}K\left(\bar{A}_{ij} + \frac{1}{3}\bar{\gamma}_{ij}K\right) - 2\alpha\chi\chi^{-1}\left(\bar{A}_{ik} + \frac{1}{3}\bar{\gamma}_{ik}K\right)\left(\bar{A}^k{}_j + \delta^k{}_j K\right)\ldots \\
&\quad \cdots - 8\pi\alpha\chi S_{ij} - \chi D_iD_j\alpha]^{\mathrm{TF}} + \chi\underbrace{[\mathcal{L}_{\vec{\beta}}K_{ij}]^{\mathrm{TF}}}_{=\mathcal{L}_{\vec{\beta}}A_{ij}} + \frac{2}{3}\bar{A}_{ij}\alpha K - \frac{2}{3}\bar{A}_{ij}\partial_k\beta^k + \bar{A}_{ij}\chi^{-1}\beta^k\partial_k\chi
\end{aligned}$$

$$
\begin{aligned}
&= [\alpha\chi R_{ij} + \alpha K\bar{A}_{ij} + \frac{1}{3}\alpha \underbrace{\bar{\gamma}_{ij}}_{\text{no TF}} K^2 - 2\alpha\bar{A}_{ik}\bar{A}^k{}_j - 2\alpha K\bar{A}_{ij} - \frac{2}{3}\alpha K\bar{A}_{ij} - \frac{2}{3}\alpha \underbrace{\bar{\gamma}_{ij}}_{\text{no TF}} K^2 \dots \\
&\quad \dots - 8\pi\alpha\chi S_{ij} - \chi D_i D_j\alpha]^{\text{TF}} + \chi \underbrace{\mathcal{L}_{\vec{\beta}}\bar{A}_{ij}}_{=\mathcal{L}_{\vec{\beta}}(\chi^{-1}\bar{A}_{ij})} + \frac{2}{3}\bar{A}_{ij}\alpha K - \frac{2}{3}\bar{A}_{ij}\partial_k\beta^k + \bar{A}_{ij}\chi^{-1}\beta^k\partial_k\chi \\
&= \left[\alpha\chi R_{ij} + \alpha K\bar{A}_{ij} - 2\alpha\bar{A}_{ik}\bar{A}^k{}_j - 2\alpha K\bar{A}_{ij} - \frac{2}{3}\alpha K\bar{A}_{ij} - 8\pi\alpha\chi S_{ij} - \chi D_i D_j\alpha\right]^{\text{TF}} \\
&\quad + \chi\mathcal{L}_{\vec{\beta}}(\chi^{-1}\bar{A}_{ij}) + \frac{2}{3}\bar{A}_{ij}\alpha K - \frac{2}{3}\bar{A}_{ij}\partial_k\beta^k + \bar{A}_{ij}\chi^{-1}\beta^k\partial_k\chi \\
&= \left[\alpha\chi R_{ij} - 8\pi\alpha\chi S_{ij} - \chi D_i D_j\alpha\right]^{\text{TF}} - 2\alpha\bar{A}_{ik}\bar{A}^k{}_j - \alpha K\bar{A}_{ij} - \frac{2}{3}\alpha K\bar{A}_{ij} + \frac{2}{3}\alpha K\bar{A}_{ij} \\
&\quad + \chi\chi^{-1}\mathcal{L}_{\vec{\beta}}\bar{A}_{ij} + \bar{A}_{ij}\chi\mathcal{L}_{\vec{\beta}}\chi^{-1} - \frac{2}{3}\bar{A}_{ij}\partial_k\beta^k + \bar{A}_{ij}\chi^{-1}\beta^k\partial_k\chi \\
&= \left[\chi(\alpha R_{ij} - 8\pi\alpha S_{ij} - D_i D_j\alpha)\right]^{\text{TF}} - \alpha(2\bar{A}_{ik}\bar{A}^k{}_j + \bar{A}_{ij}K) + \mathcal{L}_{\vec{\beta}}\bar{A}_{ij} \\
&\quad + \bar{A}_{ij}\chi\left(-\chi^{-2}\beta^k\partial_k\chi + \frac{2}{3}\chi^{-1}\partial_k\beta^k\right) - \frac{2}{3}\bar{A}_{ij}\partial_k\beta^k + \bar{A}_{ij}\chi^{-1}\beta^k\partial_k\chi \\
&= \left[\chi(\alpha R_{ij} - 8\pi\alpha S_{ij} - D_i D_j\alpha)\right]^{\text{TF}} - \alpha(2\bar{A}_{ik}\bar{A}^k{}_j + \bar{A}_{ij}K) + \mathcal{L}_{\vec{\beta}}\bar{A}_{ij}.
\end{aligned}
$$

After all this mess(!) and evaluating $\mathcal{L}_{\vec{\beta}}\bar{A}_{ij}$ by (4.23), we arrive at our sought-after ***evolution of the conformal traceless curvature***.

$$
\boxed{\begin{aligned}
\partial_t\bar{A}_{ij} = &\left[\chi(\alpha R_{ij} - 8\pi\alpha S_{ij} - D_i D_j\alpha)\right]^{\text{TF}} - \alpha(2\bar{A}_{ik}\bar{A}^k{}_j + \bar{A}_{ij}K) \\
&+ \beta^k\partial_k\bar{A}_{ij} + \bar{A}_{ik}\partial_j\beta^k + \bar{A}_{kj}\partial_i\beta^k - \frac{2}{3}\bar{A}_{ij}\partial_k\beta^k.
\end{aligned}} \tag{4.25}
$$

Without the $[\dots]^{\text{TF}}$ notation, we can write this as

$$
\begin{aligned}
\partial_t\bar{A}_{ij} = \chi&\left[(\alpha\left(R_{ij} - \frac{1}{3}\gamma_{ij}R\right) - 8\pi\alpha\left(S_{ij} - \frac{1}{3}\gamma_{ij}S\right) - (D_i D_j\alpha - \frac{1}{3}\gamma_{ij}D^2\alpha)\right] \\
&- \alpha(2\bar{A}_{ik}\bar{A}^k{}_j + \bar{A}_{ij}K) + \beta^k\partial_k\bar{A}_{ij} + \bar{A}_{ik}\partial_j\beta^k + \bar{A}_{kj}\partial_i\beta^k - \frac{2}{3}\bar{A}_{ij}\partial_k\beta^k.
\end{aligned}
$$

Once again, just as it was the case for the evolution equation of K (4.22), we have covariant derivatives D of the lapse with respect to the physical metric γ_{ij} (moreover, this time we also have the 3D Ricci tensor R_{ij} of γ_{ij} appearing in the expression). We will correct these problems soon by introducing the conformal connection $\bar{D}$ of $\bar{\gamma}_{ij}$ and rewriting everything in terms of the conformal metric.

The conformal traceless curvature $\bar{A}_{ij}$ shows up in the evolution of the conformal metric $\bar{\gamma}_{ij}$, which we shall now derive. To do so, we use Eq. (3.6) and the fact that $\mathcal{L}_{\vec{t}} = \partial_t$ in our adapted coordinates to

write

$$\partial_t \bar{\gamma}_{ij} = \mathcal{L}_{\vec{t}} \bar{\gamma}_{ij} = \alpha \mathcal{L}_{\vec{n}} \bar{\gamma}_{ij} + \mathcal{L}_{\vec{\beta}} \bar{\gamma}_{ij}. \tag{4.26}$$

To expand the second term on the RHS, we note that it is a Lie derivative of a tensor density of weight $-2/3$; thus we use (4.5) to get

$$\mathcal{L}_{\vec{\beta}} \bar{\gamma}_{ij} = \beta^k \partial_k \bar{\gamma}_{ij} + \bar{\gamma}_{ik} \partial_j \beta^k + \bar{\gamma}_{kj} \partial_i \beta^k - \frac{2}{3} \bar{\gamma}_{ij} \partial_k \beta^k. \tag{4.27}$$

Better yet, we can write this Lie derivative in terms of the conformal connection $\bar{D}$ (defined below; c.f., Eq. (4.32)). In this calculation we will need to expand the covariant derivative of $\bar{\gamma}_{ij}$ using the formula for the covariant derivative of a tensor density (c.f., Eq. (4.7)):

$$\bar{D}_k \bar{\gamma}_{ij} = \partial_k \bar{\gamma}_{ij} - \bar{\Gamma}^\ell_{ik} \bar{\gamma}_{\ell j} - \bar{\Gamma}^\ell_{jk} \bar{\gamma}_{i\ell} + \frac{2}{3} \bar{\gamma}_{ij} \bar{\Gamma}^\ell_{\ell k}.$$

Let us now expand Eq. (4.27):

$$\begin{aligned}
\mathcal{L}_{\vec{\beta}} \bar{\gamma}_{ij} &= \beta^k \partial_k \bar{\gamma}_{ij} + \bar{\gamma}_{ik} \partial_j \beta^k + \bar{\gamma}_{kj} \partial_i \beta^k - \frac{2}{3} \bar{\gamma}_{ij} \partial_k \beta^k \\
&= \beta^k \underbrace{\bar{D}_k \bar{\gamma}_{ij}}_{=0} + \beta^k \bar{\Gamma}^\ell_{ik} \bar{\gamma}_{\ell j} + \beta^k \bar{\Gamma}^\ell_{jk} \bar{\gamma}_{i\ell} - \frac{2}{3} \bar{\gamma}_{ij} \bar{\Gamma}^\ell_{\ell k} \beta^k + \underbrace{\bar{\gamma}_{ik} \bar{D}_j \beta^k}_{=\bar{D}_j \beta_i} - \bar{\gamma}_{ik} \bar{\Gamma}^k_{\ell j} \beta^\ell \\
&\quad + \underbrace{\bar{\gamma}_{kj} \bar{D}_i \beta^k}_{=\bar{D}_i \beta_j} - \bar{\gamma}_{kj} \bar{\Gamma}^k_{\ell i} \beta^\ell - \frac{2}{3} \bar{\gamma}_{ij} \bar{D}_k \beta^k + \frac{2}{3} \bar{\gamma}_{ij} \bar{\Gamma}^k_{\ell k} \beta^\ell \\
&= \underbrace{\beta^k \bar{\Gamma}^\ell_{ik} \bar{\gamma}_{\ell j} + \beta^k \bar{\Gamma}^\ell_{jk} \bar{\gamma}_{i\ell} - \frac{2}{3} \bar{\gamma}_{ij} \bar{\Gamma}^\ell_{\ell k} \beta^k - \bar{\gamma}_{ik} \bar{\Gamma}^k_{\ell j} \beta^\ell - \bar{\gamma}_{kj} \bar{\Gamma}^k_{\ell i} \beta^\ell + \frac{2}{3} \bar{\gamma}_{ij} \bar{\Gamma}^k_{\ell k} \beta^\ell}_{=\ 0 \text{ by relabeling}} + 2 \bar{D}_{(i} \beta_{j)} - \frac{2}{3} \bar{\gamma}_{ij} \bar{D}_k \beta^k \\
&= 2 \bar{D}_{(i} \beta_{j)} - \frac{2}{3} \bar{\gamma}_{ij} \bar{D}_k \beta^k.
\end{aligned} \tag{4.28}$$

And now we tackle the first term on the RHS of Eq. (4.26):

$$\begin{aligned}
\alpha \mathcal{L}_{\vec{n}} \bar{\gamma}_{ij} &= \alpha \mathcal{L}_{\vec{n}} (\chi \gamma_{ij}) \\
&= \alpha (\chi \underbrace{\mathcal{L}_{\vec{n}} \gamma_{ij}}_{=-2K_{ij}} + \gamma_{ij} \mathcal{L}_{\vec{n}} \chi) \\
&= -2\alpha \chi K_{ij} + \alpha \gamma_{ij} \frac{1}{\alpha} (\underbrace{\mathcal{L}_{\vec{t}}}_{\partial_t} \chi - \mathcal{L}_{\vec{\beta}} \chi) \\
&= -2\alpha \chi \left(\chi^{-1} \left(\bar{A}_{ij} + \frac{1}{3} \bar{\gamma}_{ij} K \right) \right) + \gamma_{ij} \left(\frac{2}{3} \chi (\alpha K - \partial_k \beta^k) + \beta^k \partial_k \chi - \left(\beta^k \partial_k \chi - \frac{2}{3} \chi \partial_k \beta^k \right) \right) \\
&= -2\alpha \bar{A}_{ij} - \frac{2}{3} \alpha \chi \gamma_{ij} K + \frac{2}{3} \alpha \chi \gamma_{ij} K - \frac{2}{3} \chi \gamma_{ij} \partial_k \beta^k + \frac{2}{3} \chi \gamma_{ij} \partial_k \beta^k + \gamma_{ij} \beta^k \partial_k \chi - \gamma_{ij} \beta^k \partial_k \chi \\
&= -2\alpha \bar{A}_{ij}.
\end{aligned} \tag{4.29}$$

Hence, combining Eqs. (4.29) and (4.28), equation (4.26) yields the ***evolution of the conformal metric***:

$$\boxed{\partial_t \bar{\gamma}_{ij} = -2\alpha \bar{A}_{ij} + 2\bar{D}_{(i}\beta_{j)} - \frac{2}{3}\bar{\gamma}_{ij}\bar{D}_k\beta^k.} \tag{4.30}$$

We are now down to the last item from (4.1), namely, the coefficients $\bar{\Gamma}^i \equiv \bar{\gamma}^{jk}\,\bar{\Gamma}^i_{jk}$ of the conformal metric $\bar{\gamma}_{ij}$, where

$$\bar{\Gamma}^i_{jk} = \frac{1}{2}\bar{\gamma}^{i\ell}\left(\partial_j\bar{\gamma}_{\ell k} + \partial_k\bar{\gamma}_{\ell j} - \partial_\ell\bar{\gamma}_{jk}\right). \tag{4.31}$$

These symbols are the connection coefficients of the ***conformal connection*** $\bar{D}$ of $\bar{\gamma}_{ij}$, from which (analogous to Eq. (3.22)) we define the ***conformal spatial derivative*** $\bar{D}_a$ of some $\binom{a}{b}$ tensor field $\boldsymbol{T}$ in a coordinate chart as [5]

$$\begin{aligned}(\bar{D}\boldsymbol{T})^{i_1\ldots i_a}{}_{j_1\ldots j_b c} &= \bar{D}_c T^{i_1\ldots i_a}{}_{j_1\ldots j_b} \\ &= \partial_c T^{i_1\ldots i_a}{}_{j_1\ldots j_b} + \sum_{d=1}^{a} T^{i_1\ldots e\ldots i_a}{}_{j_1\ldots j_b}\bar{\Gamma}^{i_d}_{ec} - \sum_{d=1}^{b} T^{i_1\ldots i_a}{}_{j_1\ldots e\ldots j_b}\bar{\Gamma}^{e}_{j_d c}.\end{aligned} \tag{4.32}$$

We first note that in Cartesian coordinates, where $\bar{\gamma} = 1$, we have

$$\begin{aligned}\bar{\Gamma}^i &= \bar{\gamma}^{jk}\bar{\Gamma}^i_{jk} \\ &= \bar{\gamma}^{jk}\left[\frac{1}{2}\bar{\gamma}^{i\ell}\left(\partial_j\bar{\gamma}_{\ell k} + \partial_k\bar{\gamma}_{\ell j} - \partial_\ell\bar{\gamma}_{jk}\right)\right] \\ &= -\frac{1}{2}\underbrace{\bar{\gamma}^{jk}\bar{\gamma}_{\ell k}}_{=\delta^j{}_\ell}\partial_j\bar{\gamma}^{i\ell} - \frac{1}{2}\underbrace{\bar{\gamma}^{jk}\bar{\gamma}_{\ell j}}_{=\delta^k{}_\ell}\partial_k\bar{\gamma}^{i\ell} - \frac{1}{2}\bar{\gamma}^{i\ell}\underbrace{\bar{\gamma}^{jk}\partial_\ell\bar{\gamma}_{jk}}_{=0 \text{ by (4.34)}} \\ &= -\frac{1}{2}\partial_\ell\bar{\gamma}^{i\ell} - \frac{1}{2}\partial_\ell\bar{\gamma}^{i\ell} \\ &= -\partial_j\bar{\gamma}^{ij},\end{aligned} \tag{4.33}$$

where we used

$$\partial_j(\bar{\gamma}^{i\ell}\bar{\gamma}_{\ell k}) = \partial_j\delta^i{}_k = 0 \implies \bar{\gamma}^{i\ell}\partial_j\bar{\gamma}_{\ell k} = -\bar{\gamma}_{\ell k}\partial_j\bar{\gamma}^{i\ell},$$

as well as Jacobi's formula (c.f., Eq. (3.42)):

$$\bar{\gamma}^{jk}\partial_\ell\bar{\gamma}_{jk} = \frac{1}{\bar{\gamma}}\partial_\ell\bar{\gamma} \overset{\text{since } \bar{\gamma}=1}{=\!=\!=} 0. \tag{4.34}$$

[5] Note, however, that due to the tensor density nature of $\bar{\gamma}_{ij}$, the connection $\bar{D}$ is not unique (i.e., it is not a Levi-Civita connection). Nevertheless, it *is* compatible with the conformal metric; i.e., $\bar{D}_k\bar{\gamma}_{ij} = 0$.

The conversion from the Christoffel symbols Γ^i_{jk} of the spatial metric γ_{ij} to the conformal symbols $\bar{\Gamma}^i_{jk}$ of the conformal metric $\bar{\gamma}_{ij}$ is given as follows:

$$
\begin{aligned}
\Gamma^i_{jk} &= \frac{1}{2}\gamma^{i\ell}\left(\partial_j\gamma_{\ell k} + \partial_k\gamma_{\ell j} - \partial_\ell\gamma_{jk}\right) \\
&= \frac{1}{2}\chi\bar{\gamma}^{i\ell}\left(\partial_j(\chi^{-1}\bar{\gamma}_{\ell k}) + \partial_k(\chi^{-1}\bar{\gamma}_{\ell j}) - \partial_\ell(\chi^{-1}\bar{\gamma}_{jk})\right) \\
&= \frac{1}{2}\chi\bar{\gamma}^{i\ell}\left(\chi^{-1}\,\partial_j\bar{\gamma}_{\ell k} + \bar{\gamma}_{\ell k}\,\partial_j\chi^{-1} + \chi^{-1}\,\partial_k\bar{\gamma}_{\ell j} + \bar{\gamma}_{\ell j}\,\partial_k\chi^{-1} - \chi^{-1}\,\partial_\ell\bar{\gamma}_{jk} - \bar{\gamma}_{jk}\,\partial_\ell\chi^{-1}\right) \\
&= \underbrace{\frac{1}{2}\bar{\gamma}^{i\ell}\left(\partial_j\bar{\gamma}_{\ell k} + \partial_k\bar{\gamma}_{\ell j} - \partial_\ell\bar{\gamma}_{jk}\right)}_{=\bar{\Gamma}^i_{jk}} + \frac{1}{2}\chi\bar{\gamma}^{i\ell}\left(-\chi^{-2}\bar{\gamma}_{\ell k}\,\partial_j\chi - \chi^{-2}\bar{\gamma}_{\ell j}\,\partial_k\chi + \chi^{-2}\bar{\gamma}_{jk}\,\partial_\ell\chi\right) \\
&= \bar{\Gamma}^i_{jk} - \frac{1}{2}\chi^{-1}\left(\delta^i{}_k\,\partial_j\chi + \delta^i{}_j\,\partial_k\chi - \bar{\gamma}_{jk}\bar{\gamma}^{i\ell}\,\partial_\ell\chi\right). \qquad (4.35)
\end{aligned}
$$

Now it is time to rectify the issues we alluded to earlier regarding the spatial covariant derivative of the lapse and the spatial Ricci tensor showing up in equations where every other term is written in terms of the conformal factors (see comments below Eqs. (4.22) and (4.25)):

- **[Spatial Derivative]** Using (4.35), we expand the term $D_iD_j\alpha$ that appears both in the evolution of K (4.22) and in the evolution of $\bar{A}_{ij}$ (4.25):

$$
\begin{aligned}
D_iD_j\alpha = D_i\partial_j\alpha &= \partial_i\partial_j\alpha - \Gamma^k_{ij}\partial_k\alpha \\
&= \partial_i\partial_j\alpha - \left[\bar{\Gamma}^k_{ij} - \frac{1}{2}\chi^{-1}\left(\delta^k{}_i\,\partial_j\chi + \delta^k{}_j\,\partial_i\chi - \bar{\gamma}_{ij}\bar{\gamma}^{k\ell}\,\partial_\ell\chi\right)\right]\partial_k\alpha \\
&= \partial_i\partial_j\alpha - \bar{\Gamma}^k_{ij}\,\partial_k\alpha + \frac{1}{2\chi}\left(2\partial_{(i}\chi\partial_{j)}\alpha - \bar{\gamma}_{ij}\bar{\gamma}^{k\ell}\,\partial_\ell\chi\,\partial_k\alpha\right).
\end{aligned}
$$

  Then, using the fact that both χ and α are treated as scalars when taking covariant derivates, we get the final expression

$$
\boxed{D_iD_j\alpha = \bar{D}_i\bar{D}_j\alpha + \frac{1}{2\chi}\left(2\bar{D}_{(i}\chi\bar{D}_{j)}\alpha - \bar{\gamma}_{ij}\,\bar{D}_k\chi\,\bar{D}^k\alpha\right).} \qquad (4.36)
$$

- **[Spatial Ricci Tensor]** The $3D$ (spatial) Ricci tensor can be split into the conformal Ricci tensor

$$
\bar{R}_{ij} = \partial_k\bar{\Gamma}^k_{ij} - \partial_j\bar{\Gamma}^k_{ik} + \bar{\Gamma}^k_{\ell k}\,\bar{\Gamma}^\ell_{ij} - \bar{\Gamma}^k_{\ell j}\,\bar{\Gamma}^\ell_{ik} \qquad (4.37)
$$

  and some extra terms that arise as a result of the rescaling of the metric. The whole derivation of this split of the Ricci tensor requires quite a bit of work, however, so instead of straying too far off here on a tangent, the reader may refer to Appendix B, where everything is derived in gory detail. Here we will simply quote the result obtained in the appendix: R_{ij} can be split as

$$
R_{ij} = \bar{R}_{ij} + R^\chi_{ij},
$$

where $\bar{R}_{ij}$ is given by (4.37), and R^{χ}_{ij} is given by

$$R^{\chi}_{ij} = \frac{1}{2}\left(\bar{D}_i\bar{D}_j(\log\chi) + \bar{\gamma}_{ij}\,\bar{D}_k\bar{D}^k(\log\chi)\right) + \frac{1}{4}\left(\bar{D}_i(\log\chi)\bar{D}_j(\log\chi) - \bar{\gamma}_{ij}\,\bar{D}_k(\log\chi)\bar{D}^k(\log\chi)\right).$$

Moreover, making use of the newly introduced coefficients $\bar{\Gamma}^i$, equation (4.37) may be rewritten as

$$\bar{R}_{ij} = -\frac{1}{2}\bar{\gamma}^{k\ell}\partial_k\partial_\ell\bar{\gamma}_{ij} + \bar{\gamma}_{k(i}\partial_{j)}\bar{\Gamma}^k + \bar{\Gamma}^k\,\bar{\Gamma}_{(ij)k} + \bar{\gamma}^{k\ell}\left(2\,\bar{\Gamma}^m_{k(i}\bar{\Gamma}_{j)m\ell} + \bar{\Gamma}^m_{ik}\,\bar{\Gamma}_{j\ell m}\right).$$

The reason why we want to write $\bar{R}_{ij}$ in this form is because, with the exception of the Laplacian term $\bar{\gamma}^{k\ell}\partial_k\partial_\ell\bar{\gamma}_{ij}$, every other second derivative of the metric $\bar{\gamma}_{ij}$ is being absorbed into first derivatives of $\bar{\Gamma}^i$. This in turns makes the BSSN equations more "wave-like" (i.e., *hyperbolic*; see, e.g., [48]). We sum up our discussion on this segment here:

$$R_{ij} = \bar{R}_{ij} + R^{\chi}_{ij} \tag{4.38a}$$

$$\bar{R}_{ij} = -\frac{1}{2}\bar{\gamma}^{k\ell}\partial_k\partial_\ell\bar{\gamma}_{ij} + \bar{\gamma}_{k(i}\partial_{j)}\bar{\Gamma}^k + \bar{\Gamma}^k\,\bar{\Gamma}_{(ij)k} + \bar{\gamma}^{k\ell}\left(2\,\bar{\Gamma}^m_{k(i}\bar{\Gamma}_{j)m\ell} + \bar{\Gamma}^m_{ik}\,\bar{\Gamma}_{j\ell m}\right) \tag{4.38b}$$

$$R^{\chi}_{ij} = \frac{1}{2}\left(\bar{D}_i\bar{D}_j(\log\chi) + \bar{\gamma}_{ij}\,\bar{D}_k\bar{D}^k(\log\chi)\right) + \frac{1}{4}\left(\bar{D}_i(\log\chi)\bar{D}_j(\log\chi) - \bar{\gamma}_{ij}\,\bar{D}_k(\log\chi)\bar{D}^k(\log\chi)\right). \tag{4.38c}$$

The expression for the lapse derivative (4.36) is to be inserted into both (4.22) and (4.25), in addition to the split of the Ricci tensor (4.38) being inserted into (4.25). This fixes the issues we brought up earlier.

Now, by writing $\bar{R}_{ij}$ in the form presented on Eq. (4.38b), we are making the $\bar{\Gamma}^i$ independent variables; therefore an evolution equation for these coefficients must be derived as well. To that end, using Eq. (4.33), we start by writing

$$\partial_t\bar{\Gamma}^i = \partial_t(-\partial_j\bar{\gamma}^{ij}) = -\partial_j\partial_t\bar{\gamma}^{ij},$$

where on the last line we used the fact that ordinary partial derivatives commute. Naturally, we now need an evolution equation for the inverse conformal metric; to that end we proceed as we did for (3.65): note that since $\bar{\gamma}^{ij}\bar{\gamma}_{jk} = \delta^i{}_k$, we have $\partial_t(\bar{\gamma}^{ij}\bar{\gamma}_{jk}) = 0$, which implies

$$\begin{aligned} \bar{\gamma}_{jk}\partial_t\bar{\gamma}^{ij} &= -\bar{\gamma}^{ij}\,\partial_t\bar{\gamma}_{jk} \\ \implies \underbrace{\bar{\gamma}^{lk}\bar{\gamma}_{jk}}_{=\delta^l{}_j}\partial_t\bar{\gamma}^{ij} &= -\bar{\gamma}^{lk}\bar{\gamma}^{ij}\,\partial_t\bar{\gamma}_{jk} \\ \implies \partial_t\bar{\gamma}^{il} &= -\bar{\gamma}^{lk}\bar{\gamma}^{ij}\,\partial_t\bar{\gamma}_{jk}. \end{aligned}$$

Hence we have

$$\partial_t\bar{\Gamma}^i = -\partial_j\partial_t\bar{\gamma}^{ij} = -\partial_j\left(-\bar{\gamma}^{ik}\bar{\gamma}^{j\ell}\,\partial_t\bar{\gamma}_{k\ell}\right). \tag{4.39}$$

Now recall the evolution of conformal metric,

$$\partial_t \bar{\gamma}_{k\ell} = -2\alpha \bar{A}_{k\ell} + \mathcal{L}_{\vec{\beta}} \bar{\gamma}_{k\ell} = -2\alpha \bar{A}_{k\ell} + \beta^m \partial_m \bar{\gamma}_{k\ell} + \bar{\gamma}_{km} \partial_\ell \beta^m + \bar{\gamma}_{\ell m} \partial_k \beta^m - \frac{2}{3} \bar{\gamma}_{k\ell} \partial_m \beta^m,$$

and note the following fact:

$$\begin{aligned}
\partial_m \bar{\gamma}^{ij} &= \partial_m \left(\bar{\gamma}^{ik} \bar{\gamma}^{j\ell} \bar{\gamma}_{k\ell} \right) \\
&= \bar{\gamma}^{ik} \bar{\gamma}^{j\ell} \partial_m \bar{\gamma}_{k\ell} + \underbrace{\bar{\gamma}^{ik} \bar{\gamma}_{k\ell}}_{=\delta^i{}_\ell} \partial_m \bar{\gamma}^{j\ell} + \underbrace{\bar{\gamma}^{j\ell} \bar{\gamma}_{k\ell}}_{=\delta^j{}_k} \partial_m \bar{\gamma}^{ik} \\
&= \bar{\gamma}^{ik} \bar{\gamma}^{j\ell} \partial_m \bar{\gamma}_{k\ell} + 2\partial_m \bar{\gamma}^{ij} \\
\implies \bar{\gamma}^{ik} \bar{\gamma}^{j\ell} \partial_m \bar{\gamma}_{k\ell} &= -\partial_m \bar{\gamma}^{ij}.
\end{aligned}$$

Now expand Eq. (4.39),

$$\begin{aligned}
\partial_t \bar{\Gamma}^i &= -\partial_j \left(-\bar{\gamma}^{ik} \bar{\gamma}^{j\ell} \partial_t \bar{\gamma}_{k\ell} \right) \\
&= \partial_j \left[\bar{\gamma}^{ik} \bar{\gamma}^{j\ell} \left(-2\alpha \bar{A}_{k\ell} + \beta^m \partial_m \bar{\gamma}_{k\ell} + \bar{\gamma}_{km} \partial_\ell \beta^m + \bar{\gamma}_{\ell m} \partial_k \beta^m - \frac{2}{3} \bar{\gamma}_{k\ell} \partial_m \beta^m \right) \right] \\
&= \partial_j \left(-2\alpha \bar{A}^{ij} - \beta^m \partial_m \bar{\gamma}^{ij} + \bar{\gamma}^{j\ell} \partial_\ell \beta^i + \bar{\gamma}^{ik} \partial_k \beta^j - \frac{2}{3} \bar{\gamma}^{ij} \partial_m \beta^m \right) \\
&= \partial_j \left(-2\alpha \bar{A}^{ij} - \beta^k \partial_k \bar{\gamma}^{ij} + 2\bar{\gamma}^{k(i} \partial_k \beta^{j)} - \frac{2}{3} \bar{\gamma}^{ij} \partial_k \beta^k \right).
\end{aligned} \tag{4.40}$$

We may also rewrite Eq. (4.40) in terms of the coefficients $\bar{\Gamma}^i$, by using $\bar{\Gamma}^i = -\partial_j \bar{\gamma}^{ij}$:

$$\begin{aligned}
\partial_t \bar{\Gamma}^i &= -2\partial_j (\alpha \bar{A}^{ij}) - \partial_j \left(\beta^k \partial_k \bar{\gamma}^{ij} \right) + \partial_j \left(\bar{\gamma}^{ki} \partial_k \beta^j \right) + \partial_j \left(\bar{\gamma}^{kj} \partial_k \beta^i \right) - \frac{2}{3} \partial_j \left(\bar{\gamma}^{ij} \partial_k \beta^k \right) \\
&= -2\alpha \partial_j \bar{A}^{ij} - 2\bar{A}^{ij} \partial_j \alpha - \beta^k \partial_k \underbrace{\partial_j \bar{\gamma}^{ij}}_{=-\bar{\Gamma}^i} - \underbrace{\partial_k \bar{\gamma}^{ij} \partial_j \beta^k}_{(\ddagger)} + \underbrace{\bar{\gamma}^{ki} \partial_k \partial_j \beta^j}_{(\dagger)} + \underbrace{\partial_j \bar{\gamma}^{ki} \partial_k \beta^j}_{=(\ddagger) \text{ by relabelling}} \\
&\quad + \bar{\gamma}^{kj} \partial_k \partial_j \beta^i + \underbrace{\partial_j \bar{\gamma}^{kj}}_{=-\bar{\Gamma}^k} \partial_k \beta^i - \frac{2}{3} \underbrace{\bar{\gamma}^{ij} \partial_j \partial_k \beta^k}_{=(\dagger) \text{ by relabelling}} - \frac{2}{3} \partial_k \beta^k \underbrace{\partial_j \bar{\gamma}^{ij}}_{=-\bar{\Gamma}^i} \\
&= -2\alpha \partial_j \bar{A}^{ij} - 2\bar{A}^{ij} \partial_j \alpha + \beta^j \partial_j \bar{\Gamma}^i + \bar{\gamma}^{jk} \partial_j \partial_k \beta^i - \bar{\Gamma}^j \partial_j \beta^i + \frac{1}{3} \bar{\gamma}^{ij} \partial_j \partial_k \beta^k + \frac{2}{3} \bar{\Gamma}^i \partial_j \beta^j.
\end{aligned} \tag{4.41}$$

It may seem like we are now finally done deriving the evolution equations for all the BSSN variables listed on (4.1); however, we are still missing one crucial step! As it turns out, if we use the evolution equation for $\bar{\Gamma}^i$ in the form presented on Eq. (4.41), the whole system is numerically unstable (even more unstable than the ADM system we presented in Chapter 3!). To fix this, we need to expand the divergence of $\bar{A}_{ij}$ (first term on the RHS of Eq. (4.41)), with the aid of the momentum constraints. First recall the momentum constraints written in ADM form (c.f., Eq. (3.56)),

$$D_j \left(K^{ij} - \gamma^{ij} K \right) = 8\pi S^i.$$

Now raising indices on (4.16) and inserting into this expression, we get

$$D_j\left(A^{ij}-\frac{2}{3}\gamma^{ij}K\right)=8\pi S^i. \tag{4.42}$$

In order to expand this further, we will need the following result: using (4.35),

$$\begin{aligned}
D_j\bar{A}^{ij} &= \partial_j\bar{A}^{ij}+\Gamma^i_{jk}\bar{A}^{jk}+\Gamma^j_{jk}\bar{A}^{ik}\\
&= \partial_j\bar{A}^{ij}+\left[\bar{\Gamma}^i_{jk}-\frac{1}{2}\chi^{-1}\left(\delta^i{}_k\,\partial_j\chi+\delta^i{}_j\,\partial_k\chi-\bar{\gamma}_{jk}\bar{\gamma}^{i\ell}\,\partial_\ell\chi\right)\right]\bar{A}^{jk}\\
&\qquad+\left[\bar{\Gamma}^j_{jk}-\frac{1}{2}\chi^{-1}\left(\delta^j{}_k\,\partial_j\chi+\delta^j{}_j\,\partial_k\chi-\bar{\gamma}_{jk}\bar{\gamma}^{j\ell}\,\partial_\ell\chi\right)\right]\bar{A}^{ik}\\
&= \underbrace{\partial_j\bar{A}^{ij}+\bar{\Gamma}^i_{jk}\bar{A}^{jk}+\bar{\Gamma}^j_{jk}\bar{A}^{ik}}_{=\bar{D}_j\bar{A}^{ij}}-\frac{1}{2}\chi^{-1}\left(\bar{A}^{ij}\,\partial_j\chi+\bar{A}^{ik}\,\partial_k\chi+\bar{A}^{ij}\,\partial_j\chi+3\,\bar{A}^{ik}\partial_k\chi-\bar{A}^{ik}\partial_k\chi\right)\\
&= \bar{D}_j\bar{A}^{ij}-\frac{5}{2}\chi^{-1}\,\bar{A}^{ij}\,\bar{D}_j\chi.
\end{aligned}$$

Now we plug this back into (4.42) and expand,

$$\begin{aligned}
D_jA^{ij}-\frac{2}{3}\gamma^{ij}D_jK &= 8\pi S^i\\
D_j(\chi\bar{A}^{ij})-\frac{2}{3}\chi\bar{\gamma}^{ij}\bar{D}_jK &= 8\pi S^i\\
\chi\,D_j\bar{A}^{ij}+\bar{A}^{ij}D_j\chi-\frac{2}{3}\chi\bar{D}^iK &= 8\pi S^i\\
\chi\left(\bar{D}_j\bar{A}^{ij}-\frac{5}{2}\chi^{-1}\,\bar{A}^{ij}\,\bar{D}_j\chi\right)+\bar{A}^{ij}D_j\chi-\frac{2}{3}\chi\bar{D}^iK &= 8\pi S^i.
\end{aligned}$$

Writing $\bar{S}^i\equiv\chi^{-1}S^i$ $(=\chi^{-1}\gamma^{ij}S_j=\bar{\gamma}^{ij}S_j)$, we have our final expression for the momentum constraints in BSSN form:

$$\boxed{\bar{D}_j\bar{A}^{ij}-\frac{3}{2\chi}\bar{A}^{ij}\,\bar{D}_j\chi-\frac{2}{3}\bar{D}^iK=8\pi\bar{S}^i.} \tag{4.43}$$

We will leave this expression as our standard equation for the momentum constraints. However note that writing the full conformal covariant divergence on the first term on the LHS of (4.43) is unnecessary, since

$$\bar{D}_j\bar{A}^{ij}=\partial_j\bar{A}^{ij}+\bar{\Gamma}^i_{jk}\bar{A}^{jk}+\bar{\Gamma}^j_{jk}\bar{A}^{ik},$$

but

$$\bar{\Gamma}^j_{jk}=\frac{1}{2}\bar{\gamma}^{j\ell}\partial_k\bar{\gamma}_{j\ell}=\partial_k\log\sqrt{\bar{\gamma}}=0,$$

where we used (yet again) Jacobi's formula, as well as the fact that we are working in Cartesian coordinates where $\bar{\gamma}=1$. Hence, the conformal covariant divergence of $\bar{A}^{ij}$ simplifies to

$$\bar{D}_j\bar{A}^{ij}=\partial_j\bar{A}^{ij}+\bar{\Gamma}^i_{jk}\bar{A}^{jk}.$$

Now we isolate $\partial_j \bar{A}^{ij}$ on Equation (4.43),

$$\partial_j \bar{A}^{ij} = \frac{3}{2\chi}\bar{A}^{ij}\,\bar{D}_j\chi + \frac{2}{3}\bar{D}^i K + 8\pi\bar{S}^i - \bar{\Gamma}^i_{jk}\bar{A}^{jk},$$

and insert back into (4.41) to arrive at our sought-after evolution equation for the coefficients $\bar{\Gamma}^i$:

$$\begin{aligned}\partial_t\bar{\Gamma}^i = &-2\alpha\left(\frac{3}{2\chi}\bar{A}^{ij}\,\bar{D}_j\chi + \frac{2}{3}\bar{D}^i K + 8\pi\bar{S}^i - \bar{\Gamma}^i_{jk}\bar{A}^{jk}\right) - 2\bar{A}^{ij}\bar{D}_j\alpha \\ &+ \beta^j\partial_j\bar{\Gamma}^i + \bar{\gamma}^{jk}\partial_j\partial_k\beta^i - \bar{\Gamma}^j\partial_j\beta^i + \frac{2}{3}\bar{\Gamma}^i\partial_j\beta^j + \frac{1}{3}\bar{\gamma}^{ij}\partial_j\partial_k\beta^k.\end{aligned} \tag{4.44}$$

The last matter to take care of before we complete our presentation of the BSSN formalism is to also rewrite the Hamiltonian constraint in BSSN form; recall from Eq. (3.51),

$$R + K^2 - K_{ij}K^{ij} = 16\pi\rho.$$

From Eqs. (4.19) and (4.20), we have

$$\begin{aligned}K_{ij}K^{ij} &= \left[\chi^{-1}\left(\bar{A}_{ij} + \frac{1}{3}\bar{\gamma}_{ij}K\right)\right]\left[\chi\left(\bar{A}^{ij} + \frac{1}{3}\bar{\gamma}^{ij}K\right)\right] \\ &= \bar{A}_{ij}\bar{A}^{ij} + \frac{1}{3}K^2,\end{aligned} \tag{4.45}$$

where we used the tracelessness of $\bar{A}_{ij}$. We now plug this as well as the transformation law for the spatial Ricci scalar R (which is derived in full detail on Appendix B (c.f., Equation B.13)) into the Hamiltonian constraint:

$$\begin{aligned}\chi\bar{R} + 2\,\chi\bar{D}^2(\log\chi) - \frac{1}{2}\,\chi\bar{D}_k(\log\chi)\bar{D}^k(\log\chi) + K^2 - \bar{A}_{ij}\bar{A}^{ij} + \frac{1}{3}K^2 &= 16\pi\rho \\ \chi\bar{R} + 2\,\chi\bar{D}^2(\log\chi) - \frac{1}{2}\,\chi\bar{D}_k(\log\chi)\bar{D}^k(\log\chi) + \frac{4}{3}K^2 - \bar{A}_{ij}\bar{A}^{ij} &= 16\pi\rho.\end{aligned}$$

Writing $\bar{\rho}^i \equiv \chi^{-1}\rho$, we have our final expression for the Hamiltonian constraint in BSSN form:

$$\bar{R} + 2\,\bar{D}^2(\log\chi) - \frac{1}{2}\bar{D}_k(\log\chi)\bar{D}^k(\log\chi) + \frac{4}{3\chi}K^2 - \frac{1}{\chi}\bar{A}_{ij}\bar{A}^{ij} = 16\pi\bar{\rho}. \tag{4.46}$$

Equations (4.46) and (4.43) are the Hamiltonian and momentum constraints, respectively, in BSSN variables. We shall not use them in this form, however, when solving the initial data problem in the next chapter, since more suitable conformal scalings will be used there.

This concludes our presentation of the BSSN formalism of numerical general relativity. Admittedly, this formalism is not nearly as intuitive and straightforward as the ADM alternative that we presented on the previous chapter, but it is nevertheless a much more robust formulation (from a numerical perspective). This is a running theme in physics (and science in general): analytical and numerical implementations rarely play fair ball with each other. The ADM formalism is important for historical (and pedagogical) reasons, but it is nearly useless for practical purposes. We remark, however, that BSSN is not by any means the only modern successful approach to numerical relativistic studies; other flourishing alternatives such as the *Generalized Harmonic Coordinates with Constraint Damping* (GHCD) ([29], [44], [45]) and $Z4$-like formalisms ([5], [10], [14], [13], [47]) are just as good as (and in some cases even superior to) BSSN.

BSSN Equations

⁕ **Evolution Equations:**

$$
\begin{aligned}
\partial_t \chi &= \frac{2}{3}\chi(\alpha K - \partial_i \beta^i) + \beta^i \bar{D}_i \chi \\
\partial_t \bar{\gamma}_{ij} &= -2\alpha \bar{A}_{ij} + 2\bar{D}_{(i}\beta_{j)} - \frac{2}{3}\bar{\gamma}_{ij}\bar{D}_k \beta^k \\
\partial_t K &= \alpha\left(\bar{A}_{ij}\bar{A}^{ij} + \frac{1}{3}K^2\right) + 4\pi\alpha(\rho + S) - D^2\alpha + \beta^i \bar{D}_i K \\
\partial_t \bar{A}_{ij} &= \left[\chi(\alpha R_{ij} - 8\pi\alpha S_{ij} - D_i D_j \alpha)\right]^{\mathrm{TF}} - \alpha(2\bar{A}_{ik}\bar{A}^k{}_j + \bar{A}_{ij}K) \\
&\quad + \beta^k \partial_k \bar{A}_{ij} + \bar{A}_{ik}\partial_j \beta^k + \bar{A}_{kj}\partial_i \beta^k - \frac{2}{3}\bar{A}_{ij}\partial_k \beta^k \\
\partial_t \bar{\Gamma}^i &= -2\alpha\left(\frac{3}{2\chi}\bar{A}^{ij}\,\bar{D}_j \chi + \frac{2}{3}\bar{D}^i K + 8\pi \bar{S}^i - \bar{\Gamma}^i_{jk}\bar{A}^{jk}\right) - 2\bar{A}^{ij}\bar{D}_j \alpha \\
&\quad + \beta^j \partial_j \bar{\Gamma}^i + \bar{\gamma}^{jk}\partial_j \partial_k \beta^i - \bar{\Gamma}^j \partial_j \beta^i + \frac{2}{3}\bar{\Gamma}^i \partial_j \beta^j + \frac{1}{3}\bar{\gamma}^{ij}\partial_j \partial_k \beta^k
\end{aligned}
$$

In these equations we need to rewrite the (second) spatial derivatives of the lapse as

$$
D_i D_j \alpha = \bar{D}_i \bar{D}_j \alpha + \frac{1}{2\chi}\left(2\bar{D}_{(i}\chi \bar{D}_{j)}\alpha - \bar{\gamma}_{ij}\,\bar{D}_k \chi\,\bar{D}^k \alpha\right)
$$

Also the Ricci tensor is split as

$$
\begin{aligned}
R_{ij} &= \bar{R}_{ij} + R^{\chi}_{ij} \\
\bar{R}_{ij} &= -\frac{1}{2}\bar{\gamma}^{k\ell}\partial_k \partial_\ell \bar{\gamma}_{ij} + \bar{\gamma}_{k(i}\partial_{j)}\,\bar{\Gamma}^k + \bar{\Gamma}^k\,\bar{\Gamma}_{(ij)k} + \bar{\gamma}^{k\ell}\left(2\,\bar{\Gamma}^m_{k(i}\bar{\Gamma}_{j)m\ell} + \bar{\Gamma}^m_{ik}\,\bar{\Gamma}_{j\ell m}\right) \\
R^{\chi}_{ij} &= \frac{1}{2}\left(\bar{D}_i \bar{D}_j(\log\chi) + \bar{\gamma}_{ij}\,\bar{D}_k \bar{D}^k(\log\chi)\right) \\
&\quad + \frac{1}{4}\left(\bar{D}_i(\log\chi)\bar{D}_j(\log\chi) - \bar{\gamma}_{ij}\,\bar{D}_k(\log\chi)\bar{D}^k(\log\chi)\right)
\end{aligned}
$$

⁕ **Constraint Equations:**

$$
\begin{aligned}
\bar{R} + 2\,\bar{D}^2(\log\chi) - \frac{1}{2}\bar{D}_k(\log\chi)\bar{D}^k(\log\chi) + \frac{4}{3\chi}K^2 - \frac{1}{\chi}\bar{A}_{ij}\bar{A}^{ij} &= 16\pi\bar{\rho} \\
\bar{D}_j \bar{A}^{ij} - \frac{3}{2\chi}\bar{A}^{ij}\,\bar{D}_j \chi - \frac{2}{3}\bar{D}^i K &= 8\pi\bar{S}^i
\end{aligned}
$$

Chapter 5

Further Considerations {Initial Data, Gauge Choice & Cosmology}

Having presented two of the main formalisms of numerical relativity, we now turn to a brief discussion of some further considerations that must be taken into account: the initial data problem (§5.1), gauge choice (§5.2), and some potential applications to cosmology (§5.3).

5.1 Choosing Initial Data

As we have alluded to earlier, we are not free to impose whatever data we like on our hypersurfaces; the initial data has to be chosen in such a way that the Hamiltonian (c.f., Eq. (3.51)) and momentum (c.f., Eq. (3.56)) constraints are satisfied from the onset and remain satisfied throught the entire time-evolution of the system. It can be shown (analytically, via the Bianchi identities) that if the constraints are satisfied on some initial time slice, they will remain fulfilled for the entirety of the simulation. This is, however, an *analytical* statement; in *numerical* simulations the constraints will be violated, and this is something that needs to be monitored. In practice, some sort of damping technique is applied to keep these violations in check. However, our concern here is exclusively on the *initial data*; the evolution of the EFEs, which are given by the BSSN equations presented in the previous chapter, will not be discussed any further in the remainder of this treatment.

Thus far we have exclusively used the conformal factor χ in our work since, as explained on Chapter 4, its use is helpful in avoiding singularity excision [18]. However, for the sake of solving the initial data problem it makes no difference which conformal factor we use, since in the end we are only after the *physical* data $\{\gamma_{ij}, K_{ij}\}$, which can be recovered from any conformally-related quantity. Both the CTT ([53], [54], [51]) and (X)CTS [52] decompositions use the factor ψ, so we will switch to using it for the purpose of solving initial data. Thus we start with the conformal rescaling

$$\boxed{\gamma_{ij} = \psi^4 \bar{\gamma}_{ij}} \tag{5.1a}$$

$$\boxed{\gamma^{ij} = \psi^{-4} \bar{\gamma}^{ij},} \tag{5.1b}$$

which is precisely the same one we used in the BSSN formulation (c.f., Eq. (4.10)), except we are now using ψ instead of χ. The quantity that will be scaled differently for the purpose of solving initial data will be A_{ij}; let us see why it is convenient to use a different factor for this quantity:

Start by putting

$$A^{ij} = \psi^{\eta} \widetilde{A}^{ij}, \tag{5.2}$$

where η is some user-defined constant. Note that we have now replaced the bar with a tilde (and we will do so throughout this chapter) to differentiate from the Nakamura rescaling of A_{ij} introduced in

the BSSN formalism (c.f., Eq. (4.17)) which, in terms of ψ, would equate to $\eta = -4$. Now consider the momentum constraints in the vacuum (c.f., Eq. (3.56))

$$D_j K^{ij} = D^i K. \tag{5.3}$$

From (4.16) we can rewrite this as

$$D_j \left(A^{ij} + \frac{1}{3}\gamma^{ij} K \right) = D^i K \quad \Longrightarrow \quad D_j A^{ij} = \frac{2}{3} D^i K. \tag{5.4}$$

We now expand the divergence of A_{ij} in terms of the conformal connection $\bar{D}$, using (B.11) and applying it on (B.1) (see Appendix B):

$$\begin{aligned}
D_j A^{ij} &= \bar{D}_j A^{ij} + A^{kj}\mathfrak{C}^i{}_{jk} + A^{ik}\mathfrak{C}^j{}_{jk} \\
&= \bar{D}_j A^{ij} + A^{kj}\left[4\delta_{(j}{}^i \bar{D}_{k)}(\log\psi) - 2\bar{\gamma}_{jk}\bar{D}^i(\log\psi)\right] \\
&\qquad + A^{ik}\left[4\delta_{(j}{}^j \bar{D}_{k)}(\log\psi) - 2\bar{\gamma}_{jk}\bar{D}^j(\log\psi)\right] \\
&= \bar{D}_j A^{ij} + 2A^{ik}\bar{D}_k(\log\psi) + 2A^{ij}\bar{D}_j(\log\psi) - 2A^{kj}\bar{\gamma}_{jk}\bar{D}^i(\log\psi) \\
&\qquad + 6A^{ik}\bar{D}_k(\log\psi) + 2A^{ij}\bar{D}_j(\log\psi) - 2A^{ik}\bar{D}_k(\log\psi) \\
&= \bar{D}_j A^{ij} + 10A^{ij}\bar{D}_j(\log\psi) - 2A^{jk}\bar{\gamma}_{jk}\bar{D}^i(\log\psi) \\
&= \bar{D}_j A^{ij} + 10A^{ij}\bar{D}_j(\log\psi) - 2\psi^{-4}\underbrace{A^{jk}\gamma_{jk}}_{=0}\bar{D}^i(\log\psi) \\
&= \bar{D}_j A^{ij} + 10A^{ij}\bar{D}_j(\log\psi).
\end{aligned}$$

This result can be rewritten as

$$D_j A^{ij} = \psi^{-10}\bar{D}_j\left(\psi^{10}A^{ij}\right), \tag{5.5}$$

which suggests that we define the quantity

$$\widetilde{A}^{ij} = \psi^{10}A^{ij}, \tag{5.6}$$

which corresponds to setting $\eta = -10$ on (5.2). This rescaling of A_{ij}, which was first introduced by Lichnerowicz [36], will be the one used when solving the constraints on the initial data; we shall call it the ***Lichnerowicz scaling of*** A_{ij} . Lowering indices on Eq. (5.6), we find [1]

$$\begin{aligned}
\gamma_{ik}\gamma_{j\ell}A^{ij} &= \psi^{-10}\widetilde{A}^{ij}\gamma_{ik}\gamma_{j\ell} \\
A_{k\ell} &= \psi^{-10}\widetilde{A}^{ij}\,\psi^4\bar{\gamma}_{ik}\,\psi^4\bar{\gamma}_{j\ell} \\
A_{k\ell} &= \psi^{-2}\widetilde{A}_{k\ell}.
\end{aligned}$$

In summary,

$$\boxed{\begin{aligned} A_{ij} &= \psi^{-2}\widetilde{A}_{ij} \qquad (5.7a) \\ A^{ij} &= \psi^{-10}\widetilde{A}^{ij}. \qquad (5.7b) \end{aligned}}$$

[1] Note that A_{ij} may have a different scaling factor, but it is still a quantity related to the conformal metric $\bar{\gamma}_{ij}$, so indices of $\widetilde{A}_{ij}$ shall be raised/lowered with $\bar{\gamma}_{ij}$.

Now, from (3.56) and (5.4)– (5.6),

$$D_j A^{ij} - \frac{2}{3}\gamma^{ij} D_j K = 8\pi S^i$$
$$\psi^{-10}\bar{D}_j \widetilde{A}^{ij} - \frac{2}{3}\psi^{-4}\bar{\gamma}^{ij}\bar{D}_j K = 8\pi S^i$$
$$\bar{D}_j \widetilde{A}^{ij} - \frac{2}{3}\psi^{6}\bar{D}^i K = 8\pi\psi^{10} S^i.$$

Rescaling the matter quantity

$$\widetilde{S}^i \equiv \psi^{10} S^i, \tag{5.8}$$

we have our momentum constraints using the Lichnerowicz scaling of A_{ij},

$$\boxed{\bar{D}_j \widetilde{A}^{ij} - \frac{2}{3}\psi^{6}\bar{D}^i K = 8\pi\widetilde{S}^i.} \tag{5.9}$$

Lastly, we need the Hamiltonian constraint; recall from (3.51),

$$R + K^2 - K_{ij}K^{ij} = 16\pi\rho.$$

From Eq. (4.45), we have

$$K_{ij}K^{ij} = \bar{A}_{ij}\bar{A}^{ij} + \frac{1}{3}K^2,$$

where $\bar{A}_{ij}$ is the Nakamura scaling of A_{ij}. Rewriting the first term on the RHS in terms of the Lichnerowicz scaling,

$$\bar{A}_{ij}\bar{A}^{ij} = \psi^4\psi^{-4}A_{ij}A^{ij} = A_{ij}A^{ij} = \psi^{-2}\psi^{-10}\widetilde{A}_{ij}\widetilde{A}^{ij} = \psi^{-12}\widetilde{A}_{ij}\widetilde{A}^{ij}, \tag{5.10}$$

and plugging in the transformation law for the spatial Ricci scalar R (which is derived in full detail on Appendix B (c.f., Eq. B.13)) in terms of ψ instead of χ,

$$R = \psi^{-4}\bar{R} - 8\psi^{-5}\bar{D}^2\psi,$$

we get

$$R + K^2 - K_{ij}K^{ij} - 16\pi\rho = 0$$
$$\psi^{-4}\bar{R} - 8\psi^{-5}\bar{D}^2\psi + \frac{2}{3}K^2 - \psi^{-12}\widetilde{A}_{ij}\widetilde{A}^{ij} - 16\pi\rho = 0$$
$$\bar{D}^2\psi + \frac{1}{8}\left(\psi^{-7}\widetilde{A}_{ij}\widetilde{A}^{ij} - \psi\bar{R}\right) + \psi^5\left(2\pi\rho - \frac{1}{12}K^2\right) = 0.$$

Rescaling the matter quantity

$$\widetilde{\rho} \equiv \psi^8\rho, \tag{5.11}$$

we have our Hamiltonian constraint in its final (Lichnerowicz) form,

$$\boxed{\bar{D}^2\psi + \frac{1}{8}\left(\psi^{-7}\widetilde{A}_{ij}\widetilde{A}^{ij} - \psi\bar{R}\right) - \frac{1}{12}\psi^5 K^2 + 2\pi\psi^{-3}\widetilde{\rho} = 0.} \tag{5.12}$$

Remark 1. *Whereas the motivation for the rescaling of the energy density in (5.11) is not as intuitively clear as the one for the momentum density in (5.8), it is a suitable one because the negative power of ψ on the $\widetilde{\rho}$ term guarantees some uniqueness of solutions (actually, any power > 5 would do the trick; 8 is chosen for later computational convenience).*

5.1.1 Conformal Transverse-Traceless (CTT) Decomposition

Most known decompositions of the initial data problem start with the conformal rescalings introduced above; from this point on the different approaches (such as the ones introduced in this subsection and the next) proceed to decompose the (rescaled) traceless extrinsic curvature $\widetilde{A}^{ij}$ in different ways. For the CTT decomposition, we start by splitting $\widetilde{A}^{ij}$ as [2]

$$\widetilde{A}^{ij} = \widetilde{A}^{ij}_{\mathrm{L}} + \widetilde{A}^{ij}_{\mathrm{TT}} = (\bar{\mathbb{L}}\boldsymbol{X})^{ij} + \widetilde{A}^{ij}_{\mathrm{TT}}, \tag{5.13}$$

where $\widetilde{A}^{ij}_{\mathrm{TT}}$ is the *transverse-traceless* (TT) part of $\widetilde{A}^{ij}$:

$$\bar{D}_j \widetilde{A}^{ij}_{\mathrm{TT}} = 0 \qquad \text{(Transverse)} \tag{5.14a}$$

$$\bar{\gamma}_{ij} \widetilde{A}^{ij}_{\mathrm{TT}} = 0. \qquad \text{(Traceless)} \tag{5.14b}$$

On the other hand, the *longitudinal* (L) part of $\widetilde{A}^{ij}$, namely $\widetilde{A}^{ij}_{\mathrm{L}}$, is expressed in terms of the ***conformal Killing operator*** $(\bar{\mathbb{L}}\boldsymbol{X})^{ij}$ associated with the conformal metric $\bar{\gamma}_{ij}$ and some vector field $\boldsymbol{X}$,

$$\boxed{(\bar{\mathbb{L}}\boldsymbol{X})^{ij} \equiv 2\bar{D}^{(i}X^{j)} - \frac{2}{3}\bar{\gamma}^{ij}\bar{D}_k X^k.} \tag{5.15}$$

The vector field $\boldsymbol{X}$ is determined from taking the divergence of (5.13)

$$\bar{D}_j(\bar{\mathbb{L}}\boldsymbol{X})^{ij} = \bar{D}_j \widetilde{A}^{ij}, \tag{5.16}$$

where we used the transverse property (5.14a). This second-order operator is crucial to our work, so we shall give it its own unique notation,

$$\bar{\Delta}_{\mathbb{L}} X^i \equiv \bar{D}_j(\bar{\mathbb{L}}\boldsymbol{X})^{ij}. \tag{5.17}$$

Expanding,

$$\begin{aligned}
\bar{\Delta}_{\mathbb{L}} X^i = \bar{D}_j(\bar{\mathbb{L}}\boldsymbol{X})^{ij} &= \bar{D}_j\left(\bar{D}^i X^j + \bar{D}^j X^i - \frac{2}{3}\bar{\gamma}^{ij}\bar{D}_k X^k\right) \\
&= \underbrace{\bar{D}_j\bar{D}^i X^j}_{=\bar{R}^i{}_j X^j + \bar{D}^i\bar{D}_j X^j} + \bar{D}^2 X^i - \frac{2}{3}\bar{D}^i\bar{D}_j X^j \\
&= \bar{D}^2 X^i + \bar{R}^i{}_j X^j + \frac{1}{3}\bar{D}^i\bar{D}_j X^j. \qquad \text{(by Ricci identity)}
\end{aligned}$$

Thus we have the ***conformal vector Laplacian***

$$\boxed{\bar{\Delta}_{\mathbb{L}} X^i = \bar{D}^2 X^i + \bar{R}^i{}_j X^j + \frac{1}{3}\bar{D}^i\bar{D}_j X^j.} \tag{5.18}$$

[2] In fact, it can be shown that *any* symmetric, trace-free tensor can be split into a sum of its transverse/orthogonal/divergence-free part and its longitudinal part, the latter being given by the Killing operator, as in (5.15).

From Eq. (5.16) we see that the existence and uniqueness of the L-TT decomposition (5.13) is guaranteed iff there exists a unique solution X^i to (5.18). We shall now rewrite the momentum constraints using this conformal Laplacian operator: from (5.16)–(5.17), we see that (5.9) becomes

$$\boxed{\bar{\Delta}_{\mathbb{L}} X^i - \frac{2}{3}\psi^6 \bar{D}^i K = 8\pi \widetilde{S}^i.} \tag{5.19}$$

Thus we have reduced the Hamiltonian and momentum constraints to equations that need to be solved for ψ and X^i, respectively. [3] Once we have the solutions, we then need to recover the *physical* data from it: from ψ we recover $\bar{\gamma}_{ij}$ and, accordingly, γ_{ij}; from X^i we recover $\widetilde{A}^{ij}$ via (5.16) (consequently A_{ij} and, ultimately, the physical data K_{ij}).

Let us briefly recap the situation. We start off with twelve degrees of freedom (DoF) in the physical system $\{\gamma_{ij}, K_{ij}\}$, four of which are removed due to the constraints (one is the conformal factor ψ from the Hamiltonian (5.12); three come from X^i or, equivalently, the longitudinal part of the extrinsic curvature $\widetilde{A}^{ij}_{\mathrm{L}} = (\bar{\mathbb{L}}\boldsymbol{X})^{ij}$ which is recovered from the momentum constraints (5.19)). A further four DoF account for the gauge freedom that is inherent to GR (three spatial coordinates associated with the physical 3-metric γ_{ij} and a time coordinate that is associated with K). Hence from the initial twelve DoF we are left with only four that are still undetermined:

- (Two undetermined DoF in the conformal metric, $\bar{\gamma}_{ij}$) From the possible six DoF of $\bar{\gamma}_{ij}$, one is lost once we fix the conformal factor ψ whilst other three are due to the spatial-coordinate freedom. In other words, there are actually five DoF encoded in $\bar{\gamma}_{ij}$, albeit only two of them are true dynamical degrees of freedom of the gravitational field;

- (Two undetermined DoF in the TT part of the extrinsic curvature, $\widetilde{A}^{ij}_{\mathrm{TT}}$) From the possible six DoF of $\widetilde{A}^{ij}_{\mathrm{TT}}$, one is lost due to the traceless property (5.14b) and three more due to the transverse property (5.14a).

These four are the true dynamical DoF of the gravitational field; the remaining eight are either fixed by constrains (four) or represent gauge freedom (four). All in all, the CTT approach puts as *constrained data* the quantities ψ and X^i whilst leaving as *free data* the quantities $\{\widetilde{A}^{ij}_{\mathrm{TT}}, \bar{\gamma}_{ij}, K\}$ [4] as well as any matter terms ρ, S^i, if present. The choice of this *free background data* has to be made according to the physical meaning of the scenario one would like to present (e.g., black holes, neutron stars, exotic compacts).

[3] Note that the second term on the LHS of (5.19) couples the constraints; under the assumption that K = constant (e.g., the maximal slicing condition $K = 0$) they decouple. In such situations we can first solve (5.19) for X^i, from which we determine $\widetilde{A}^{ij}$, which we then plug into (5.12) and solve the Hamiltonian constraint for ψ.

[4] The last two listed quantities include of course the two free DoF of $\bar{\gamma}_{ij}$, plus the free coordinates (which includes a time coordinate associated with K).

CTT Decomposition

In the CTT approach, initial data is split as follows

- `Constrained Data:` ψ, X^i;
- `Free Data:` $\widetilde{A}^{ij}_{\mathrm{TT}}, \bar{\gamma}_{ij}, K,$ (matter terms (ρ, S^i), if present).

The Hamiltonian constraint is

$$\boxed{\bar{D}^2\psi + \frac{1}{8}\left(\psi^{-7}\widetilde{A}_{ij}\widetilde{A}^{ij} - \psi\bar{R}\right) - \frac{1}{12}\psi^5 K^2 + 2\pi\psi^{-3}\widetilde{\rho} = 0}$$

where $\widetilde{A}^{ij}$ is given by

$$\widetilde{A}^{ij} = \widetilde{A}^{ij}_{\mathrm{L}} + \widetilde{A}^{ij}_{\mathrm{TT}} = (\bar{\mathbb{L}}\boldsymbol{X})^{ij} + \widetilde{A}^{ij}_{\mathrm{TT}}.$$

It needs to be solved for ψ. On the other hand, the momentum constraints are

$$\boxed{\bar{\Delta}_{\mathbb{L}} X^i - \frac{2}{3}\psi^6 \bar{D}^i K = 8\pi\widetilde{S}^i}$$

which need to be solved for X^i.

The physical solution is then constructed from

$$\gamma_{ij} = \psi^4 \bar{\gamma}_{ij}$$
$$K_{ij} = \psi^{-2}\widetilde{A}_{ij} + \frac{1}{3}\gamma_{ij}K.$$

5.1.2 Conformal Thin-Sandwich (CTS) Decomposition

Unlike the CTT decomposition, where the initial data problem is dealt with on a single hypersurface, the alternative CTS approach considers the vicinity of the slice as well (consequently, it is no wonder that in this formalism the foliation variables α and β^i will make an appearance, which was not the case for CTT). Instead of starting with the single-slice data $\{\gamma_{ij}, K_{ij}\}$, our starting point will be the metric γ_{ij} of our initial slice Σ and its value in a neighbourhood of Σ (i.e., its time derivative $\dot{\gamma}_{ij} \equiv \partial_t \gamma_{ij}$). We then consider the traceless part of $\dot{\gamma}_{ij}$,

$$v_{ij} \equiv \gamma^{1/3} \partial_t (\gamma^{-1/3} \gamma_{ij}). \tag{5.20}$$

Note that v_{ij} is indeed traceless:

$$\begin{aligned}
\gamma^{ij} v_{ij} &= \gamma^{ij} \left(\gamma^{1/3} \partial_t (\gamma^{-1/3} \gamma_{ij}) \right) \\
&= \gamma^{ij} (\gamma^{1/3} \gamma^{-1/3} \partial_t \gamma_{ij} + \gamma^{1/3} \gamma_{ij} \underbrace{\partial_t \gamma^{-1/3}}_{= -\frac{1}{3} \gamma^{-4/3} \partial_t \gamma}) \\
&= \underbrace{\gamma^{ij} \partial_t \gamma_{ij}}_{= 2 \partial_t \log \sqrt{\gamma}} - \frac{1}{3} \underbrace{\gamma^{ij} \gamma_{ij}}_{=3} \underbrace{\overbrace{\gamma^{1/3} \gamma^{-4/3}}^{=\gamma} \partial_t \gamma}_{= 2 \partial_t \log \sqrt{\gamma}} \\
&= 2 \partial_t \log \sqrt{\gamma} - 2 \partial_t \log \sqrt{\gamma} = 0, \qquad \surd
\end{aligned}$$

where on the last line we used Jacobi's formula (c.f., Eq. (3.42)). Now recall from Eq. (3.40) the evolution equation of the spatial metric

$$\partial_t \gamma_{ij} = 2 D_{(i} \beta_{j)} - 2 \alpha K_{ij},$$

and from Eq. (3.41)

$$\partial_t \log \sqrt{\gamma} = -\alpha K + D_i \beta^i.$$

Now putting all this together we rewrite Eq. (5.20):

$$\begin{aligned}
v_{ij} &= \gamma^{1/3} \partial_t (\gamma^{-1/3} \gamma_{ij}) \\
&= \partial_t \gamma_{ij} - \frac{1}{3} \gamma_{ij} \underbrace{\gamma^{-1} \partial_t \gamma}_{= 2 \partial_t \log \sqrt{\gamma}} \\
&= 2 D_{(i} \beta_{j)} - 2 \alpha K_{ij} - \frac{2}{3} \gamma_{ij} \partial_t \log \sqrt{\gamma} \\
&= 2 D_{(i} \beta_{j)} - 2 \alpha \left(A_{ij} - \frac{1}{3} \gamma_{ij} K \right) - \frac{2}{3} \gamma_{ij} \left(-\alpha K + D_k \beta^k \right) \\
&= 2 D_{(i} \beta_{j)} - 2 \alpha A_{ij} - \frac{2}{3} \gamma_{ij} D_k \beta^k \\
&= (\mathbb{L} \boldsymbol{\beta})_{ij} - 2 \alpha A_{ij},
\end{aligned} \tag{5.21}$$

where on the last line we used the Killing operator $(\mathbb{L}\boldsymbol{\beta})_{ij} \equiv 2 D_{(i} \beta_{j)} - 2/3 \, \gamma_{ij} D_k \beta^k$, defined just as its conformal counterpart (5.15), but associated with the physical metric instead of the conformal one (hence the lack of a "bar" on top of the $\mathbb{L}$ symbol).

On the other hand, Eq. (5.21) looks awfully similar to the evolution of the conformal metric (c.f., Eq. (4.30))

$$\partial_t \bar{\gamma}_{ij} = 2\bar{D}_{(i}\beta_{j)} - \frac{2}{3}\bar{\gamma}_{ij}\bar{D}_k\beta^k - 2\alpha\bar{A}_{ij} = (\bar{\mathbb{L}}\boldsymbol{\beta})_{ij} - 2\alpha\bar{A}_{ij}, \tag{5.22}$$

where $\bar{A}_{ij} = \psi^{-4}A_{ij}$ is the Nakamura scaling of A_{ij} (c.f., (4.17)). This suggests that we rescale v_{ij} as $\bar{v}_{ij} \equiv \psi^{-4}v_{ij}$ and put

$$\bar{v}_{ij} \equiv \partial_t \bar{\gamma}_{ij}. \tag{5.23}$$

Indeed,

$$\bar{v}_{ij} \equiv \psi^{-4}v_{ij} = \psi^{-4}\overbrace{\gamma^{1/3}}^{=\psi^4}\partial_t(\underbrace{\overbrace{\gamma^{-1/3}}^{=\psi^{-4}}\gamma_{ij}}_{=\bar{\gamma}_{ij}}) = \partial_t\bar{\gamma}_{ij}. \qquad \surd$$

Note that, just like v_{ij}, the rescaled $\bar{v}_{ij}$ is also traceless:

$$\bar{\gamma}^{ij}\bar{v}_{ij} = \bar{\gamma}^{ij}\partial_t\bar{\gamma}_{ij} \overset{\text{Jacobi's identity}}{=\!=\!=} \underbrace{\bar{\gamma}^{-1}}_{=1}\underbrace{\partial_t\bar{\gamma}}_{=0} = 0. \qquad \surd$$

Now, from Eqs. (5.22) and (5.23), we have

$$\bar{A}_{ij} = \frac{1}{2\alpha}\left((\bar{\mathbb{L}}\boldsymbol{\beta})_{ij} - \bar{v}_{ij}\right).$$

However, we are using now the Nakamura scaling of A_{ij} and, as discussed earlier in the chapter, when dealing with the initial data problem it is more mathematically convenient to work instead with the Lichnerowicz scaling displayed on Eq. (5.7). Converting from Nakamura to Lichnerowicz,

$$\begin{aligned}\bar{A}_{ij} &= \psi^{-4}A_{ij} = \psi^{-4}\psi^{-2}\widetilde{A}_{ij} = \psi^{-6}\widetilde{A}_{ij}\\ \bar{A}^{ij} &= \psi^{4}A^{ij} = \psi^{4}\psi^{-10}\widetilde{A}^{ij} = \psi^{-6}\widetilde{A}^{ij},\end{aligned}$$

we have

$$\widetilde{A}_{ij} = \frac{\psi^6}{2\alpha}\left((\bar{\mathbb{L}}\boldsymbol{\beta})_{ij} - \bar{v}_{ij}\right) \tag{5.24a}$$

$$\widetilde{A}^{ij} = \frac{\psi^6}{2\alpha}\left((\bar{\mathbb{L}}\boldsymbol{\beta})^{ij} - \bar{v}^{ij}\right). \tag{5.24b}$$

It turns out to be convenient (not a simple matter of aesthetics; this is relevant for numerical implementations!) to use the ***densitised lapse*** (also referred to as the ***conformal lapse***)

$$\bar{\alpha} \equiv \psi^{-6}\alpha, \tag{5.25}$$

in terms of which (5.24) is rewritten as

$$\boxed{\widetilde{A}_{ij} = \frac{1}{2\bar{\alpha}}\left((\bar{\mathbb{L}}\boldsymbol{\beta})_{ij} - \bar{v}_{ij}\right)} \tag{5.26a}$$

$$\boxed{\widetilde{A}^{ij} = \frac{1}{2\bar{\alpha}}\left((\bar{\mathbb{L}}\boldsymbol{\beta})^{ij} - \bar{v}^{ij}\right).} \tag{5.26b}$$

In the CTS decomposition the Hamiltonian constraint is still the same equation (5.12) that needs to be solved for ψ, except this time $\widetilde{A}_{ij}$ and $\widetilde{A}^{ij}$ are understood to be replaced by the values derived on (5.26). As for the momentum constraints, let us first expand the divergence $\bar{D}_j\widetilde{A}^{ij}$ in terms of (5.26b):

$$\begin{aligned}\bar{D}_j\widetilde{A}^{ij} &= \bar{D}_j\left[\frac{1}{2\bar{\alpha}}\left((\mathbb{L}\boldsymbol{\beta})^{ij}-\bar{v}^{ij}\right)\right]\\ &= \frac{1}{2\bar{\alpha}}\bar{\Delta}_{\mathbb{L}}\beta^i-\frac{1}{2\bar{\alpha}^2}(\mathbb{L}\boldsymbol{\beta})^{ij}\bar{D}_j\bar{\alpha}-\frac{1}{2\bar{\alpha}}\bar{D}_j\bar{v}^{ij}+\frac{1}{2\bar{\alpha}^2}\bar{v}^{ij}\bar{D}_j\bar{\alpha}\\ &= \frac{1}{2\bar{\alpha}}\left(\bar{\Delta}_{\mathbb{L}}\beta^i-(\mathbb{L}\boldsymbol{\beta})^{ij}\bar{D}_j(\log\bar{\alpha})-\bar{D}_j\bar{v}^{ij}+\bar{v}^{ij}\bar{D}_j(\log\bar{\alpha})\right).\end{aligned}$$

Inserting this into the momentum constraints (5.9),

$$\begin{aligned}\bar{D}_j\widetilde{A}^{ij}-\frac{2}{3}\psi^6\bar{D}^iK &= 8\pi\widetilde{S}^i\\ \frac{1}{2\bar{\alpha}}[\bar{\Delta}_{\mathbb{L}}\beta^i-(\mathbb{L}\boldsymbol{\beta})^{ij}\bar{D}_j(\log\bar{\alpha})\underbrace{-\bar{D}_j\bar{v}^{ij}+\bar{v}^{ij}\bar{D}_j(\log\bar{\alpha})}_{=-\bar{\alpha}\bar{D}_j(\bar{\alpha}^{-1}\bar{v}^{ij})}]-\frac{2}{3}\psi^6\bar{D}^iK &= 8\pi\widetilde{S}^i\\ \bar{\Delta}_{\mathbb{L}}\beta^i-(\mathbb{L}\boldsymbol{\beta})^{ij}\bar{D}_j(\log\bar{\alpha})-\bar{\alpha}\bar{D}_j(\bar{\alpha}^{-1}\bar{v}^{ij})-\frac{4}{3}\bar{\alpha}\psi^6\bar{D}^iK &= 16\pi\bar{\alpha}\widetilde{S}^i.\end{aligned}$$

Thus the momentum constraints in the CTS decomposition are given by

$$\boxed{\bar{\Delta}_{\mathbb{L}}\beta^i-(\mathbb{L}\boldsymbol{\beta})^{ij}\bar{D}_j(\log\bar{\alpha})=\bar{\alpha}\bar{D}_j(\bar{\alpha}^{-1}\bar{v}^{ij})+\frac{4}{3}\bar{\alpha}\psi^6\bar{D}^iK+16\pi\bar{\alpha}\widetilde{S}^i.} \tag{5.27}$$

(Note that, as was the case for the CTT decomposition, in a constant-mean-curvature (i.e., $K = constant$) slice, the Hamiltonian and momentum constraints decouple.) Having made a choice for the background metric $\bar{\gamma}_{ij}$ and its time derivative $\bar{v}_{ij}$, as well as the densitised lapse and the trace of the extrinsic curvature K (as well as any matter terms, if applicable), we then proceed to solve the coupled system (5.12) & (5.27) for ψ and β^i, respectively. Note that, unlike the CTT decomposition where we started with twelve DoF (four of which were constrained and eight free), in CTS we find ourselves with a total of sixteen DoF: $\bar{\gamma}_{ij}$ (5), $\bar{v}_{ij}$ (5), K (1), $\bar{\alpha}$ (1), β^i (3), and ψ (1). Of these sixteen, the latter four $\{\beta^i, \psi\}$ are constrained; moreover, by constraining the conformal factor ψ we are removing one DoF from $\bar{\gamma}_{ij}$ (and consequently, also one DoF is removed from $\bar{v}_{ij}$). The four extra DoF in CTS are due to the appearance of the foliation variables (shift and lapse), since in this approach we are not working on a single hypersurface (as was the case for CTT).

CTS Decomposition

In the CTS approach, initial data is split as follows

- `Constrained Data:` ψ, β^i;
- `Free Data:` $\bar{\gamma}_{ij}, \bar{v}_{ij}, \bar{\alpha}, K$, (matter terms (ρ, S^i), if present).

The Hamiltonian constraint is

$$\boxed{\bar{D}^2\psi + \frac{1}{8}\left(\psi^{-7}\widetilde{A}_{ij}\widetilde{A}^{ij} - \psi\bar{R}\right) - \frac{1}{12}\psi^5 K^2 + 2\pi\psi^{-3}\widetilde{\rho} = 0}$$

where $\widetilde{A}^{ij}$ is given by

$$\widetilde{A}^{ij} = \frac{1}{2\bar{\alpha}}\left((\bar{\mathbb{L}}\boldsymbol{\beta})^{ij} - \bar{v}^{ij}\right).$$

It needs to be solved for ψ. On the other hand, the momentum constraints are

$$\boxed{\bar{\Delta}_{\bar{\mathbb{L}}}\beta^i - (\bar{\mathbb{L}}\boldsymbol{\beta})^{ij}\bar{D}_j(\log\bar{\alpha}) = \bar{\alpha}\bar{D}_j(\bar{\alpha}^{-1}\bar{v}^{ij}) + \frac{4}{3}\bar{\alpha}\psi^6\bar{D}^i K + 16\pi\bar{\alpha}\widetilde{S}^i}$$

which need to be solved for β^i.

The physical solution is then constructed from

$$\begin{aligned}\alpha &= \psi^6\bar{\alpha}\\ \gamma_{ij} &= \psi^4\bar{\gamma}_{ij}\\ K_{ij} &= \psi^{-2}\widetilde{A}_{ij} + \frac{1}{3}\gamma_{ij}K.\end{aligned}$$

Extended Conformal Thin-Sandwich (XCTS) Decomposition

The above CTS prescription is commonly referred to as the "original" conformal thin-sandwich decomposition; it was introduced by York in 1999 [52]. CTS is quite efficient in its own right and, moreover, it can be helpful when used in tandem with other conformal decompositions; for instance, when comparing with CTT, the presence of the time derivative of the conformal metric $\bar{v}_{ij}$ brings some intuition with regards to the prescription of the free CTT data $\widetilde{A}^{ij}_{\mathrm{TT}}$. That beings said, CTS has in particular one major drawback: there are situations in which there is no natural way of prescribing the densitised lapse $\bar{\alpha}$, as the latter has a more difficult physical interpretation. In an effort to solve this issue, Pfeiffer and York found a way to extend this CTS approach by giving the time derivative of the mean curvature (time derivative of the trace K) in order to determine the lapse [43]. This "extension" is referred to as, …well, …the *extended conformal thin-sandwich* (XCTS) decomposition; we shall present it now.

Since XCTS replaces CTS's free datum $\bar{\alpha}$ with $\partial_t K$, we start by recalling equation (4.22),

$$\partial_t K = \alpha\left(\bar{A}_{ij}\bar{A}^{ij} + \frac{1}{3}K^2\right) + 4\pi\alpha(\rho + S) - D^2\alpha + \beta^i\bar{D}_i K,$$

where S is trace of the spatial stress (c.f., Eq. (3.62)). Our first order of business then is to replace the Laplace operator D^2 with the conformal one $\bar{D}^2$. In order to accomplish this we need to convert from the Christoffel symbols Γ^i_{jk} of the spatial metric γ_{ij} to the conformal symbols $\bar{\Gamma}^i_{jk}$ of the conformal metric $\bar{\gamma}_{ij}$ (this was derived earlier on (4.35), but for the conformal factor χ; we now derive it for ψ):

$$\begin{aligned}
\Gamma^i_{jk} &= \frac{1}{2}\gamma^{i\ell}\left(\partial_j\gamma_{\ell k} + \partial_k\gamma_{\ell j} - \partial_\ell\gamma_{jk}\right)\\
&= \frac{1}{2}\psi^{-4}\bar{\gamma}^{i\ell}\left(\partial_j(\psi^4\bar{\gamma}_{\ell k}) + \partial_k(\psi^4\bar{\gamma}_{\ell j}) - \partial_\ell(\psi^4\bar{\gamma}_{jk})\right)\\
&= \frac{1}{2}\psi^{-4}\bar{\gamma}^{i\ell}\left(\psi^4\,\partial_j\bar{\gamma}_{\ell k} + 4\psi^3\bar{\gamma}_{\ell k}\,\partial_j\psi + \psi^4\,\partial_k\bar{\gamma}_{\ell j} + 4\psi^3\bar{\gamma}_{\ell j}\,\partial_k\psi - \psi^4\,\partial_\ell\bar{\gamma}_{jk} - 4\psi^3\bar{\gamma}_{jk}\,\partial_\ell\psi\right)\\
&= \underbrace{\frac{1}{2}\bar{\gamma}^{i\ell}\left(\partial_j\bar{\gamma}_{\ell k} + \partial_k\bar{\gamma}_{\ell j} - \partial_\ell\bar{\gamma}_{jk}\right)}_{=\bar{\Gamma}^i_{jk}} + 2\bar{\gamma}^{i\ell}\left(\bar{\gamma}_{\ell k}\,\partial_j(\log\psi) + \bar{\gamma}_{\ell j}\,\partial_k(\log\psi) - \bar{\gamma}_{jk}\,\partial_\ell(\log\psi)\right)\\
&= \bar{\Gamma}^i_{jk} + 4\delta^i{}_{(k}\,\partial_{j)}(\log\psi) - 2\bar{\gamma}_{jk}\bar{\gamma}^{i\ell}\,\partial_\ell(\log\psi)\\
&= \bar{\Gamma}^i_{jk} + 4\delta^i{}_{(k}\,\bar{D}_{j)}(\log\psi) - 2\bar{\gamma}_{jk}\bar{\gamma}^{i\ell}\,\bar{D}_\ell(\log\psi),
\end{aligned} \tag{5.28}$$

where on the last line we used the fact that ψ (and therefore $\log\psi$) is treated as a scalar (as opposed to a scalar tensor density) in covariant derivatives (we will also use this for the lapse below). Equipped with (5.28), we can rewrite $D^2\alpha$ in terms of the conformal connection $\bar{D}$ (again, we also did this on (4.36), but that was using χ; we now derive it for ψ):

$$\begin{aligned}
D_iD_j\alpha = D_i\partial_j\alpha &= \partial_i\partial_j\alpha - \Gamma^k_{ij}\partial_k\alpha\\
&= \partial_i\partial_j\alpha - \left[\bar{\Gamma}^k_{ij} + 4\delta^k{}_{(i}\,\bar{D}_{j)}(\log\psi) - 2\bar{\gamma}_{ij}\bar{\gamma}^{k\ell}\,\bar{D}_\ell(\log\psi)\right]\partial_k\alpha\\
&= \underbrace{\partial_i\partial_j\alpha - \bar{\Gamma}^k_{ij}\,\partial_k\alpha}_{=\bar{D}_i\bar{D}_j\alpha} - 4\bar{D}_{(i}\alpha\,\bar{D}_{j)}(\log\psi) + 2\bar{\gamma}_{ij}\bar{D}^k\alpha\,\bar{D}_k(\log\psi)\\
&= \bar{D}_i\bar{D}_j\alpha - 4\bar{D}_{(i}\alpha\,\bar{D}_{j)}(\log\psi) + 2\bar{\gamma}_{ij}\bar{D}^k\alpha\,\bar{D}_k(\log\psi).
\end{aligned} \tag{5.29}$$

Contracting, we get an expression for $D^2\alpha$ in terms of the conformal connection $\bar{D}$:

$$\begin{aligned} D^2\alpha = \gamma^{ij} D_i D_j \alpha &= \gamma^{ij} \left[\bar{D}_i \bar{D}_j \alpha - 4\bar{D}_{(i}\alpha\, \bar{D}_{j)}(\log\psi) + 2\bar{\gamma}_{ij}\bar{D}^k\alpha\, \bar{D}_k(\log\psi) \right] \\ &= \psi^{-4}\bar{\gamma}^{ij} \left[\bar{D}_i \bar{D}_j \alpha - 4\bar{D}_{(i}\alpha\, \bar{D}_{j)}(\log\psi) + 2\bar{\gamma}_{ij}\bar{D}^k\alpha\, \bar{D}_k(\log\psi) \right] \\ &= \psi^{-4} \left[\bar{D}^2\alpha - 4\bar{D}^i\alpha\, \bar{D}_i(\log\psi) + 6\bar{D}^i\alpha\, \bar{D}_i(\log\psi) \right] \\ &= \psi^{-4} \left[\bar{D}^2\alpha + 2\bar{D}^i\alpha\, \bar{D}_i(\log\psi) \right]. \end{aligned} \tag{5.30}$$

Thus, equation (4.22) becomes

$$\psi^{-4} \left[\bar{D}^2\alpha + 2\bar{D}^i\alpha\, \bar{D}_i(\log\psi) \right] = \alpha \left(\bar{A}_{ij}\bar{A}^{ij} + \frac{1}{3}K^2 \right) + 4\pi\alpha(\rho + S) + \beta^i \bar{D}_i K - \partial_t K. \tag{5.31}$$

Pfeiffer and York took it a step further and suggested that we combine this equation with the Hamiltonian constraint (5.12) to get an equation involving the quantity $\alpha\psi = \bar{\alpha}\psi^7$ that effectively eliminates the scalar product of gradients found in term $2\bar{D}^i\alpha\, \bar{D}_i(\log\psi)$:

$$\begin{aligned} \bar{D}^2(\alpha\psi) &= \bar{D}^i \left(\bar{D}_i(\alpha\psi) \right) \\ &= \bar{D}^i \left(\alpha\bar{D}_i\psi + \psi\bar{D}_i\alpha \right) \\ &= 2\bar{D}^i\alpha\, \bar{D}_i\psi + \alpha\bar{D}^2\psi + \psi\bar{D}^2\alpha. \end{aligned} \tag{5.32}$$

Multiplying this result by ψ^{-1},

$$\psi^{-1} \left[2\bar{D}^i\alpha\, \bar{D}_i\psi + \alpha\bar{D}^2\psi + \psi\bar{D}^2\alpha \right] = 2\bar{D}^i\alpha\, \bar{D}_i(\log\psi) + \psi^{-1}\alpha\bar{D}^2\psi + \bar{D}^2\alpha.$$

Combing this with (5.32), the LHS of (5.31) is rewritten as

$$\psi^{-4} \left[\bar{D}^2\alpha + 2\bar{D}^i\alpha\, \bar{D}_i(\log\psi) \right] = \psi^{-4} \left[\psi^{-1} \left(\bar{D}^2(\alpha\psi) - \alpha\bar{D}^2\psi \right) \right] = \psi^{-5} \left(\bar{D}^2(\alpha\psi) - \alpha\bar{D}^2\psi \right). \tag{5.33}$$

Now, recall from (5.10) that $\bar{A}_{ij}\bar{A}^{ij} = \psi^{-12}\widetilde{A}_{ij}\widetilde{A}^{ij}$, and from (5.11) the rescaled energy density $\widetilde{\rho} = \psi^8\rho$; moreover, we also rescale the trace of the spatial stress,

$$\widetilde{S} \equiv \psi^8 S. \tag{5.34}$$

Then we substitute these quantities and (5.33) into (5.31):

$$\psi^{-5} \left(\bar{D}^2(\alpha\psi) - \alpha\bar{D}^2\psi \right) = \alpha \left(\psi^{-12}\widetilde{A}_{ij}\widetilde{A}^{ij} + \frac{1}{3}K^2 \right) + 4\pi\alpha\psi^{-8}(\widetilde{\rho} + \widetilde{S}) + \beta^i \bar{D}_i K - \partial_t K. \tag{5.35}$$

To take this further we now replace the term $\bar{D}^2\psi$ with the Hamiltonian constraint (5.12)

$$\bar{D}^2\psi = \frac{1}{12}\psi^5 K^2 - \frac{1}{8} \left(\psi^{-7}\widetilde{A}_{ij}\widetilde{A}^{ij} - \psi\bar{R} \right) - 2\pi\psi^{-3}\widetilde{\rho},$$

so that (here comes the mess!)

$$\begin{aligned}
\psi^{-5}\bar{D}^2(\alpha\psi) &= \alpha\left[\frac{1}{12}K^2 - \frac{1}{8}\left(\psi^{-12}\widetilde{A}_{ij}\widetilde{A}^{ij} - \psi^{-4}\bar{R}\right) - 2\pi\psi^{-8}\widetilde{\rho}\right] + \alpha\left(\psi^{-12}\widetilde{A}_{ij}\widetilde{A}^{ij} + \frac{1}{3}K^2\right) \\
&\quad + 4\pi\alpha\psi^{-8}(\widetilde{\rho} + \widetilde{S}) + \beta^i\bar{D}_iK - \partial_tK \\
\psi^{-5}\bar{D}^2(\alpha\psi) &= \alpha\left(\frac{7}{8}\psi^{-12}\widetilde{A}_{ij}\widetilde{A}^{ij} + \frac{5}{12}K^2 + \frac{1}{8}\psi^{-4}\bar{R} + \pi\psi^{-8}2(2\widetilde{S} + \widetilde{\rho})\right) + \beta^i\bar{D}_iK - \partial_tK \\
\bar{D}^2(\alpha\psi) &= \alpha\psi\left(\frac{7}{8}\psi^{-8}\widetilde{A}_{ij}\widetilde{A}^{ij} + \frac{5}{12}\psi^4K^2 + \frac{1}{8}\bar{R} + 2\pi\psi^{-4}(2\widetilde{S} + \widetilde{\rho})\right) + \psi^5\left(\beta^i\bar{D}_iK - \partial_tK\right).
\end{aligned}$$

Hence, the XCTS decomposition contains an additional constraint equation

$$\boxed{\bar{D}^2(\alpha\psi) = \alpha\psi\left(\frac{7}{8}\psi^{-8}\widetilde{A}_{ij}\widetilde{A}^{ij} + \frac{5}{12}\psi^4K^2 + \frac{1}{8}\bar{R} + 2\pi\psi^{-4}(2\widetilde{S} + \widetilde{\rho})\right) + \psi^5\left(\beta^i\bar{D}_iK - \partial_tK\right).} \tag{5.36}$$

which needs to be solved for the quantity $\alpha\psi$ (or, equivalently, $\bar{\alpha}\psi^7$), thus adding an extra constraint datum α (or, equivalently, $\bar{\alpha}$) to the original CTS decomposition. Note that one major disadvantage of XCTS over CTS or CTT is that assuming constant mean curvature (i.e., setting $K = constant$) does not decouple the Hamiltonian and momentum constraints, which was a convenient feature in the other two decompositions. On the other hand, however, by having as free data the time derivatives of both the (conformal) metric and of the mean curvature K, the XCTS decomposition gives us a good measure of control over the initial data; for instance, since $\bar{v}_{ij}$ and ∂_tK are not constrained, we may choose to set both equal to zero, which is particularly useful in situations where we would like to prescribe equilibrium/quasi-equilibrium data (since $\partial_t\bar{\gamma}_{ij} = 0$ and $\partial_tK = 0$ are both necessary conditions for $\vec{\partial}_t$ to be a Killing vector).

XCTS Decomposition

In the XCTS approach, initial data is split as follows

- `Constrained Data:` ψ, β^i, α (or, equivalently, $\bar{\alpha}$ (if we use $\bar{\alpha}\psi^7$ in place of $\alpha\psi$ on (5.36)));
- `Free Data:` $\bar{\gamma}_{ij}, \bar{v}_{ij}, K, \partial_t K,$ (matter terms (ρ, S^i), if present).

The Hamiltonian constraint is

$$\boxed{\bar{D}^2\psi + \frac{1}{8}\left(\psi^{-7}\widetilde{A}_{ij}\widetilde{A}^{ij} - \psi\bar{R}\right) - \frac{1}{12}\psi^5 K^2 + 2\pi\psi^{-3}\widetilde{\rho} = 0}$$

where $\widetilde{A}^{ij}$ is given by

$$\widetilde{A}^{ij} = \frac{1}{2\bar{\alpha}}\left((\bar{\mathbb{L}}\boldsymbol{\beta})^{ij} - \bar{v}^{ij}\right).$$

It needs to be solved for ψ. On the other hand, the momentum constraints are

$$\boxed{\bar{\Delta}_{\mathbb{L}}\beta^i - (\bar{\mathbb{L}}\boldsymbol{\beta})^{ij}\bar{D}_j(\log\bar{\alpha}) = \bar{\alpha}\bar{D}_j(\bar{\alpha}^{-1}\bar{v}^{ij}) + \frac{4}{3}\bar{\alpha}\psi^6\bar{D}^i K + 16\pi\bar{\alpha}\widetilde{S}^i}$$

which need to be solved for β^i. Furthermore, an additional constraint equation

$$\boxed{\bar{D}^2(\alpha\psi) = \alpha\psi\left(\frac{7}{8}\psi^{-8}\widetilde{A}_{ij}\widetilde{A}^{ij} + \frac{5}{12}\psi^4 K^2 + \frac{1}{8}\bar{R} + 2\pi\psi^{-4}(2\widetilde{S} + \widetilde{\rho})\right) + \psi^5\left(\beta^i\bar{D}_i K - \partial_t K\right)}$$

needs to be solved for the quantity $\alpha\psi$ (or, equivalently, $\bar{\alpha}\psi^7$).

The physical solution is then constructed from

$$\begin{aligned}\alpha &= \psi^6\bar{\alpha}\\ \gamma_{ij} &= \psi^4\bar{\gamma}_{ij}\\ K_{ij} &= \psi^{-2}\widetilde{A}_{ij} + \frac{1}{3}\gamma_{ij}K.\end{aligned}$$

5.2 Gauge Choice

Even though, in theory (i.e., analytically) all gauge choices should yield the same physical result, at the numerical level this is an issue that merits some consideration. In order to achieve a long-term stable simulation we need to specify the right gauge (choice for α and β^i) and determine how these quantities will evolve in coordinate time. Choosing static gauges is not a very good idea, since we have no *a priori* knowledge of which functions will serve us better; the best approach is to choose the lapse and shift dynamically as functions of the evolving geometry.

One may naively think, for instance, that setting $\alpha = 1$ would be an ideal choice (certainly, our calculations would simplify quite a bit!). [5] Unfortunately, however, this turns out to be a terrible pick: recall from Eq. (3.35) that the acceleration of a normal observer is given in terms of the lapse function as $n^b \nabla_b n_a = D_a \log \alpha$; thus setting $\alpha = 1$ yields a vanishing acceleration of normal observers (hence the choice $\alpha = 1$ is usually referred to as *geodesic slicing*, since Eulerian observers are in free fall). A detailed examination then shows that this almost always leads to a singularity, since geodesics tend to focus in the presence of gravitating sources. Hence singularity-avoiding techniques such as *maximal slicing* (computationally expensive) or $1 + \log$ *slicing* (lower computational cost) must be employed. The former is the condition that sets the mean curvature K to be constant; if we enforce this not only on the initial slice but also during the evolution, we can write this condition WLOG as

$$K = 0 = \partial_t K. \tag{5.37}$$

The name "maximal slicing" comes from the fact that choosing $K = 0$ extremises the volume of spatial slices. With a Riemannian metric such extremal surfaces with vanishing mean curvature are minimal, whilst in the presence of a Lorentzian metric (our case) they are maximal. With the choice (5.37), the equation for the time evolution of K (c.f,. Eq. (3.64)) reduces to

$$D^2\alpha = \alpha \left(4\pi(\rho + S) + K_{ij}K^{ij}\right), \tag{5.38}$$

which decouples the lapse from the shift. We can then rewrite Eq. (5.38) in several different ways; for instance, combining with the Hamiltonian (3.51),

$$\begin{aligned} D^2\alpha &= \alpha \left(4\pi(\rho + S) + R - 16\pi\rho\right) \\ &= \alpha \left(4\pi(S - 3\rho) + R\right), \end{aligned} \tag{5.39}$$

or alternatively, in the additional constraint equation of the XCTS decomposition (c.f., Eq. (5.36)),

$$\bar{D}^2(\alpha\psi) = \alpha\psi \left(\frac{7}{8}\psi^{-8}\widetilde{A}_{ij}\widetilde{A}^{ij} + \frac{1}{8}\bar{R} + 2\pi\psi^{-4}(2\widetilde{S} + \widetilde{\rho})\right). \tag{5.40}$$

This maximal slicing condition (5.37) is a major improvement over geodisic slicing, since it avoids the focusing of normal observers that we mentioned takes place in the latter. This can be asserted from

$$\nabla_a n^a = \nabla_a g^{ab} n_b = g^{ab}\nabla_a n_b \underbrace{= (g^{ab} + n^a n^b)\nabla_a n_b}_{\text{since } n^b\nabla_a n_b = 0} = \gamma^{ab}\nabla_a n_b = -K;$$

[5] This corresponds to an evenly spaced slicing, so that coordinate time coincides with proper time of Eulerian observers (recall that $\mathrm{d}\tau = \alpha \mathrm{d}t$).

thus setting $K = 0$ we see that the expansion (negative or positive) of normal observers vanishes. This is equivalent to saying that maximal slices are volume-preserving along the normal congruence n^a, a fact that can also be verified from

$$0 = K = \gamma^{ab} K_{ab} = -\frac{1}{2}\gamma^{ab}\mathcal{L}_{\vec{n}}\gamma_{ab} = -\frac{1}{2\gamma}\mathcal{L}_{\vec{n}}\gamma = -\frac{1}{\gamma^{1/2}}\mathcal{L}_{\vec{n}}\gamma^{1/2} = -\mathcal{L}_{\vec{n}}\log\gamma^{1/2}, \tag{5.41}$$

where on the fourth equality we used Jacobi's formula yet again. Since $\gamma^{1/2}\mathrm{d}^3x$ is the proper volume element of a spatial hypersurface Σ, Eq. (5.41) shows that the negative of the mean curvature (zero in the maximal slicing assumption) measures the fractional change in the proper 3-volume along the normal congruence n^a.

The one major drawback of the maximal slicing condition is that it is prohibitively expensive to implement for most relevant applications. The $1 + \log$ slicing condition, on the other hand, has proven to be quite robust, and it has become adopted by most modern NR codes. It is a generalised hyperbolic slicing condition of Bona-Massó type [15], whose basic idea is to reduce the lapse in regions where the curvature is particularly strong. In general, the so-called ***alpha-driver*** condition is given by

$$\partial_t\alpha = -\zeta_1\,\alpha^{\zeta_2}K + \zeta_3\beta^i\partial_i\alpha, \tag{5.42}$$

with ζ_i being some positive scalar functions. From this equation we get the $1 + \log$ slicing by fixing $\zeta_1 = 2$ and $\zeta_2 = \zeta_3 = 1$.

Similarly, we may also choose a vanishing shift vector ($\beta^i = 0$), so that the coordinates are not shifted as we move from slice to slice. This would also certainly simplify matters, and it is in fact a common gauge choice that works well in certain applications. However, in black-hole spacetime simulations if we use a vanishing β^i the event horizon grows rapidly in coordinate space, due to the normal observers falling in, which causes the computational domain to end up eventually trapped inside the black hole [2]. Moreover, in oder to counter the large field gradients (or "slice-stretching") [6] incurred in the presence of a black hole, a nonvanishing β^i is required [3]. To deal with this slice-stretching issue, gauge conditions were designed so that second-time derivatives of the shift are proportional to first-time derivatives of the coefficients $\bar{\Gamma}^i$ (i.e., $\partial_t^2\beta^i \sim \partial_t\bar{\Gamma}^i$). In particular, a hyperbolic shift condition

$$\partial_t^2\beta^i = \eta\partial_t\bar{\Gamma}^i - \xi\partial_t\beta^i, \tag{5.43}$$

where η and ξ are positive scalar fields, was introduced. This is the so-called ***Gamma driver*** shift condition. We may then use an auxiliary vector field $\mathcal{B}^i$ to perform the usual trick of rewriting a second order derivative in first order,

$$\partial_t\mathcal{B}^i = \vartheta_1\,\alpha^{\vartheta_2}\,\partial_t\bar{\Gamma}^i - \varrho_1\,\mathcal{B}^i \tag{5.44a}$$

$$\partial_t\beta^i = \varrho_2\,\mathcal{B}^i, \tag{5.44b}$$

[6] 3+1 simulations of black hole spacetimes without singularity excision and with singularity-avoiding lapse and vanishing shift fail after an evolution time of around $t = 30-40M$ (M being the total ADM mass of the system) due to the so-called "slice stretching" [4].

where we also rewrote the scalar fields η and ξ in terms of four damping parameters $\vartheta_{1,2}$ and $\varrho_{1,2}$ that fine-tune the growth of the shift. A usual choice is $\vartheta_1 = \varrho_1 = 1, \vartheta_2 = 0$, and $\varrho_2 = 3/4$.

The very successful moving punctures method that we mentioned in Chapter 4 is a combination of the $1 + \log$ slicing for α and Gamma-driver for β [18]. It is very efficient at avoiding singularities, which in turns spares us from having to excise black holes from the spacetime (which is computationally expensive). Whence it has become *the* standard choice for simulation of black hole spacetimes. Evolving a black hole in this particular gauge combination results in the "trumpet" solution, where the central points asymptote to a finite distance from the singularity [30]. In this way we never resolve the singularity itself, and are thus able to achieve long term stable evolutions of the spacetime around it.

5.3 Scalar Fields in the Presence of Gravity

Thus far we have only discussed purely geometric aspects of the 3+1 formulation of GR, without discussing constraints or evolution of any potential matter field that might be coupled to the EFE's; we now turn to this topic (for a thorough treatment the reader may consult, e.g., Chapter 6 of [27]). Let us focus our succinct discussion in a scalar matter field ϕ minimally coupled to the EFE's. For such scalar field, the *Lagrangian* is given by

$$L_M = \frac{1}{2}\nabla_a\phi\nabla^a\phi + V(\phi), \tag{5.45}$$

where $V(\phi)$ is the *scalar potential*, which may be decomposed as

$$V(\phi) = \frac{1}{2}m^2\phi^2 + V_{\text{int}}(\phi), \tag{5.46}$$

m being the *mass* of the field and V_{int} the *interaction potential* (since we are interested in the minimally-coupled case, the field is noninteracting; i.e., $V_{\text{int}} = 0$). If we then add the associated *scalar matter Lagrangian density* $\mathcal{L}_M = \sqrt{-g}L_M$ to the *gravitational Lagrangian density*, namely $\mathcal{L}_G = \sqrt{-g}R$, then minimisation of the (modified) *Einstein-Hilbert action*

$$S = \frac{1}{16\pi}\int (\mathcal{L}_G + \mathcal{L}_M)\,\mathrm{d}^4x \tag{5.47}$$

leads to the EFE's with stress-energy tensor defined by

$$T_{ab} = \nabla_a\phi\nabla_b\phi - \frac{1}{2}g_{ab}\left(\nabla_c\phi\nabla^c\phi + 2V(\phi)\right). \tag{5.48}$$

Moreover, from (5.45) the *Euler-Lagrange* equations yield our *equation of motion*, which coincides with the *Klein-Gordon* equation in curved spacetime:

$$\nabla^2\phi = \frac{\mathrm{d}V(\phi)}{\mathrm{d}\phi} = m^2\phi, \tag{5.49}$$

where $\nabla^2 = g^{ab}\nabla_a\nabla_b$. Since this equation of motion is of second order, it would be useful to cast it into first order for integration purposes; we accomplish this with the aid of new auxiliary variables Π

and $\varkappa_i$ given by [7]

$$\Pi \equiv \frac{1}{\alpha}\left(\partial_t \phi - \beta^i \partial_i \phi\right) \tag{5.50}$$

$$\varkappa_i \equiv \partial_i \phi. \tag{5.51}$$

Using these variables, (5.49) splits as

$$\partial_t \phi = \alpha \Pi + \beta^i \varkappa_i \tag{5.52a}$$

$$\partial_t \varkappa_i = \beta^j \partial_j \varkappa_i + \varkappa_j \partial_i \beta^j + \alpha \partial_i \Pi + \Pi \partial_i \alpha \tag{5.52b}$$

$$\partial_t \Pi = \beta^i \partial_i \Pi + g^{ij}\left(\alpha \partial_j \varkappa_i + \varkappa_j \partial_i \alpha - \Gamma^k_{ij} \varkappa_k\right) + \alpha\left(K\Pi + \frac{\mathrm{d}V(\phi)}{\mathrm{d}\phi}\right). \tag{5.52c}$$

These equations must be solved in conjunction with the gravitational field's 3+1 equations in order to determine the complete evolution of a spacetime containing a scalar matter field. Note that (5.52a) is just the definition of Π (i.e., it is simply a rewriting of (5.50)), and (5.52b) follows directly from (5.51) and (5.52a) by commuting partial derivatives; the true equation of motion is in fact determined by (5.52c). The constraint given by (5.51), namely,

$$\mathcal{R}_i \equiv \varkappa_i - \partial_i \phi = 0, \tag{5.53}$$

must be preserved by the system (5.52). Of course, if (5.52) is solved *exactly*, the preservation of (5.53) is guaranteed throughout the evolution. The problem is at the *numerical* level, where truncation errors can give the residual $\mathcal{R}_i$ nonzero values; therefore it is important to keep a close eye out on $\mathcal{R}_i$ (in addition to the Hamiltonian and momentum constraints!) during the evolution to make sure that we are working with an accurate simulation.

Had we instead assumed homogeneity of the scalar field (i.e., $\nabla_i \phi = \partial_i \phi = 0$), then the equation of motion (5.49) for an FLRW metric would yield a relatively simple second-order ODE for the evolution of the "inflaton" scalar field $\phi(t)$,

$$\ddot{\phi} + 3H\dot{\phi} + m^2 \phi = 0, \tag{5.54}$$

where, per usual notation, $H(t) = \dot{a}(t)/a(t)$ represents *Hubble's constant*, and $a(t)$ is the *expansion parameter* that appears in the FLRW metric. The much more complicated problem of dealing with an inhomogeneous inflaton requires the full power of numerical relativity, and it is currently a very active research area. In fact, the addition of such scalar field to our 3+1 formulation of GR opens the doors to a plethora of interesting areas of study; for instance, *inhomogeneous cosmological inflation* ([21], [22], [34]) and *critical gravitational collapse* ([20], [21], [28]).

The study of critical collapse and the role of scalar fields in the very early universe are the ultimate direction of our future projects, for which this thesis presents the foundations. The interest on scalar fields, from a cosmological perspective, lies in the likelihood that (pseudo)scalar fields known as *axions* and *axion-like particles* (ALPs) are suitable dark matter candidates [7]. Indeed, inflation suggests that axions were created abundantly during the Big Bang. If axions have low mass, thus preventing other decay modes (since there is no lighter particles to decay into), theories predict that the universe would be filled with a very cold Bose-Einstein condensate of primordial axions [49]. Hence, axions

[7] Some references (e.g., [8]) define Π as the negative of ours; here we follow the convention on [21].

could plausibly explain the dark matter problem of cosmology. We are interested in axions because, even though they are (as of now) hypothetical elementary particles, if they do indeed exist and have low mass within a specific range, then they are likely to be a component of *cold dark matter* (CDM), since they satisfy the two necessary CDM criteria: (1) a non-relativistic population of axions could be present in our universe in sufficient quantities to provide the required dark matter energy density, and (2) they are effectively collisionless, i.e., the only significant long-range interactions are gravitational [33]. We intend to use both analytical techniques and numerical modelling based on general relativity and scalar boson models to investigate the central role that scalar fields play in solving the dark matter problem of cosmology.

On the other hand, gravitational collapse with nothing more than gravity and a scalar field is a remarkably rich subject. The null coordinate approach is fast, accurate, and reliable, but it is limited to spherically symmetric collapse [39]. In spherical symmetry, the system of the Einstein equations coupled to matter can be reduced to a 1+1D system, and hence it is widely studied. However, progress beyond spherical symmetry assumptions has been stifled due to the extremely high refinements required to study the stages of the collapse, which are magnified three-fold in full 3+1 codes. Thus, whilst the case presented in [39] has an important check on the results obtained from more sophisticated 3+1 integration schemes, it is ultimately the full 3+1 approach the one that is required for handling general collapse situations. It is in this configuration that we intend to study the axisymmetric and fully asymmetric settings, which are much less understood.

Appendix A

Proof of Gauss-Codazzi, Codazzi-Mainardi, & Ricci Equations

In this appendix we will write out detailed calculations that prove the Gauss-Codazzi, Codazzi-Mainardi, and Ricci Equations, all three of which we use in the main text to derive projections of the ambient (4D) spacetime curvature onto the (3D) spacelike hypersurfaces.

A.1 Proof of Gauss-Codazzi

Recall that he Riemann tensor is defined in terms of second covariant derivatives of a vector (Ricci identity),

$$2\nabla_{[c}\nabla_{d]}V^a = {}^{(4)}R^a{}_{bcd}V^b. \tag{A.1}$$

Thus, to relate ${}^{(4)}R^a{}_{bcd}$ to $R^a{}_{bcd}$, it is natural to consider the Ricci identity for the projected spatial derivative. We start there:

$$\begin{aligned} D_aD_bV^c = D_a\left(D_bV^c\right) &= \gamma_a{}^d\gamma_b{}^e\gamma^c{}_f\,\nabla_d(D_eV^f) \\ &= \gamma_a{}^d\gamma_b{}^e\gamma^c{}_f\,\nabla_d\left(\gamma_e{}^g\gamma^f{}_h\nabla_gV^h\right). \end{aligned} \tag{A.2}$$

In order to expand this further, we will make use of these facts:

$$\begin{aligned} &\nabla_d\gamma_e{}^g = \nabla_d\left(\delta_e{}^g + n_en^g\right) = \nabla_d(n_en^g) = n_e\nabla_dn^g + n^g\nabla_dn_e; \\ &\gamma_b{}^en_e = 0; \\ &n_aV^a = 0 \implies n_a\nabla_bV^a = -V^a\nabla_bn_a; \\ &\gamma^a{}_b\gamma^b{}_c = \gamma^a{}_c; \\ &\qquad 0 = \nabla_d\left(\gamma^c{}_fn^f\right) = \gamma^c{}_f\nabla_dn^f + n^f\nabla_d(n^cn_f) = \gamma^c{}_f\nabla_dn^f - \nabla_dn^c \\ &\qquad\quad \implies \gamma^c{}_f\nabla_dn^f = \nabla_dn^c. \end{aligned}$$

Now we may expand Eq. (A.2):

$$
\begin{aligned}
D_a D_b V^c &= \gamma_a{}^d \gamma_b{}^e \gamma^c{}_f \, \nabla_d \left(\gamma_e{}^g \gamma^f{}_h \nabla_g V^h \right) \\
&= \gamma_a{}^d \gamma_b{}^e \gamma^c{}_f \left\{ \gamma^f{}_h \nabla_g V^h \nabla_d \gamma_e{}^g + \gamma_e{}^g \nabla_g V^h \nabla_d \gamma^f{}_h + \gamma_e{}^g \gamma^f{}_h \nabla_d \nabla_g V^h \right\} \\
&= \gamma_a{}^d \gamma_b{}^e \gamma^c{}_f \{ \gamma^f{}_h \nabla_g V^h \left(n_e \nabla_d n^g + n^g \nabla_d n_e \right) \\
&\quad + \gamma_e{}^g \nabla_g V^h (n_h \nabla_d n^f + n^f \nabla_d n_h) + \gamma_e{}^g \gamma^f{}_h \nabla_d \nabla_g V^h \} \\
&= \gamma_a{}^d \gamma_b{}^e \gamma^c{}_f \{ \gamma^f{}_h \nabla_g V^h n^g \nabla_d n_e + \gamma_e{}^g \nabla_g V^h n_h \nabla_d n^f \\
&\quad + \gamma_e{}^g \gamma^f{}_h \nabla_d \nabla_g V^h \} \qquad \text{(Since } \gamma_b{}^a n_a = 0\text{)} \\
&= \gamma_a{}^d \gamma_b{}^e \underbrace{\gamma^c{}_f \gamma^f{}_h}_{=\gamma^c{}_h} n^g \nabla_g V^h \nabla_d n_e + \gamma_a{}^d \underbrace{\gamma_b{}^e \gamma_e{}^g}_{=\gamma_b{}^g} \gamma^c{}_f \nabla_d n^f \underbrace{n_h \nabla_g V^h}_{=-V^h \nabla_g n_h} \\
&\quad + \gamma_a{}^d \underbrace{\gamma_b{}^e \gamma_e{}^g}_{=\gamma_b{}^g} \underbrace{\gamma^c{}_f \gamma^f{}_h}_{=\gamma^c{}_h} \nabla_d \nabla_g V^h \\
&= \underbrace{\gamma_a{}^d \gamma_b{}^e \nabla_d n_e}_{=-K_{ab}} \gamma^c{}_h n^g \nabla_g V^h - \gamma_a{}^d \gamma_b{}^g \gamma^c{}_f \nabla_d n^f \underbrace{\nabla_g n_h}_{=\gamma_h{}^p \nabla_g n_p} V^h + \gamma_a{}^d \gamma_b{}^g \gamma^c{}_h \nabla_d \nabla_g V^h \\
&= -K_{ab} \gamma^c{}_h n^g \nabla_g V^h - \underbrace{\gamma_a{}^d \gamma^c{}_f \nabla_d n^f}_{=-K_a{}^c} \underbrace{\gamma_b{}^g \gamma_h{}^p \nabla_g n_p}_{=-K_{bh}} V^h + \gamma_a{}^d \gamma_b{}^g \gamma^c{}_h \nabla_d \nabla_g V^h \\
&= -K_{ab} \gamma^c{}_h n^g \nabla_g V^h - K_a{}^c K_{bh} V^h + \gamma_a{}^d \gamma_b{}^g \gamma^c{}_h \nabla_d \nabla_g V^h .
\end{aligned}
$$

Permuting the indices a and b and substracting from the above result to form $D_a D_b V^c - D_b D_a V^c$, the first term vanishes since K_{ab} is symmetric, and so we are left with

$$
D_a D_b V^c - D_b D_a V^c = \left(K_b{}^c K_{ah} - K_a{}^c K_{bh} \right) V^h + \gamma_a{}^d \gamma_b{}^g \gamma^c{}_h \left(\nabla_d \nabla_g V^h - \nabla_g \nabla_d V^h \right) . \tag{A.3}
$$

Now, applying both the 3D and 4D Ricci identities to Eq. (A.3), we get

$$
R^c{}_{fab} V^f = \left(K_b{}^c K_{af} - K_a{}^c K_{bf} \right) V^f + \gamma_a{}^d \gamma_b{}^g \gamma^c{}_h \, {}^{(4)}R^h_{fdg} V^f ,
$$

or equivalently, since $V^f = \gamma^f{}_p V^p$,

$$
\gamma_a{}^d \gamma_b{}^g \gamma^c{}_h \gamma_p{}^f \, {}^{(4)}R^h_{fdg} V^p = R^c{}_{pab} V^p + \left(K_a{}^c K_{bp} - K_b{}^c K_{ap} \right) V^p .
$$

But this relation must hold for any spatial vector V^p, so we have proven (3.46a):

$$
\boxed{\gamma_a{}^e \gamma_b{}^f \gamma^g{}_c \gamma_d{}^h \, {}^{(4)}R^c_{hef} = R^g{}_{dab} + K_a{}^g K_{bd} - K_b{}^g K_{ad} .} \tag{A.4}
$$

Equivalently, hitting (A.4) with g_{cg} on both sides,

$$
\begin{aligned}
\gamma_a{}^e \gamma_b{}^f \gamma^g{}_c \gamma_d{}^h \, {}^{(4)}R^c_{hef} \, g_{cg} &= g_{cg} R^g{}_{dab} + g_{cg} K_a{}^g K_{bd} - g_{cg} K_b{}^g K_{ad} \\
\gamma_a{}^e \gamma_b{}^f \gamma^g{}_c \gamma_d{}^h \, {}^{(4)}R_{ghef} &= \gamma_{cg} R^g{}_{dab} + \gamma_{cg} K_a{}^g K_{bd} - \gamma_{cg} K_b{}^g K_{ad}
\end{aligned}
$$

$$
\boxed{\gamma_a{}^e \gamma_b{}^f \gamma_c{}^g \gamma_d{}^h \, {}^{(4)}R_{efgh} = R_{abcd} + K_{ac} K_{bd} - K_{ad} K_{cb} .} \tag{A.5}
$$

A.2 Proof of Codazzi-Mainardi

First consider the spatial derivative of the extrinsic curvature:

$$\begin{aligned} D_a K_{bc} &= \gamma_a{}^d \gamma_b{}^e \gamma_c{}^f \nabla_d K_{ef} = \gamma_a{}^d \gamma_b{}^e \gamma_c{}^f \nabla_d \left(-\gamma_e{}^g \gamma_f{}^h \nabla_g n_h \right) \\ &= -\gamma_a{}^d \gamma_b{}^e \gamma_c{}^f \left(\nabla_d \nabla_e n_f + \nabla_d (n_e \mathsf{a}_f) \right) \\ &= -\gamma_a{}^d \gamma_b{}^e \gamma_c{}^f \nabla_d \nabla_e n_f - \gamma_a{}^d \gamma_c{}^f \underbrace{\gamma_b{}^e n_e}_{=0} \nabla_d \mathsf{a}_f - \underbrace{\gamma_c{}^f \mathsf{a}_f}_{=\mathsf{a}_c} \underbrace{\gamma_a{}^d \gamma_b{}^e \nabla_d n_e}_{=-K_{ab}} \\ &= -\gamma_a{}^d \gamma_b{}^e \gamma_c{}^f \nabla_d \nabla_e n_f + \mathsf{a}_c K_{ab}. \end{aligned}$$

Now, since K_{ab} is symmetric, the last term disappears when antisymmetrising, and we are left with

$$D_{[a} K_{b]c} = -\gamma_a{}^d \gamma_b{}^e \gamma_c{}^f \nabla_{[d} \nabla_{e]} n_f. \tag{A.6}$$

Using the Ricci identity, we get

$$\begin{aligned} 2\nabla_{[d} \nabla_{e]} n_f &= (\nabla_d \nabla_e - \nabla_e \nabla_d) n_f \\ &= -{}^{(4)}R^h{}_{fde} n_h = -n^p g_{hp} {}^{(4)}R^h{}_{fde} \\ &= -n^p {}^{(4)}R_{pfde}. \end{aligned}$$

Applying this to the RHS of (A.6), we get

$$D_{[a} K_{b]c} = \gamma_a{}^d \gamma_b{}^e \gamma_c{}^f n^p {}^{(4)}R_{pfde},$$

or similarly, applying the symmetries

$${}^{(4)}R_{pfde} = {}^{(4)}R_{depf} \quad \text{and} \quad {}^{(4)}R_{depf} = -{}^{(4)}R_{defp}$$

we arrive at (3.46b):

$$\boxed{D_b K_{ac} - D_a K_{bc} = \gamma_a{}^d \gamma_b{}^e \gamma_c{}^f n^p {}^{(4)}R_{defp}.} \tag{A.7}$$

Thanks to the symmetries of the Riemann tensor, changing the index contracted with n^p would not give an independent relation; it would at most result in a change of sign of the right-hand side.

A.3 Proof of Ricci Equation

In the proof we will use the previous results ((3.35) and (3.36)):

$$\mathsf{a}_a = D_a \log \alpha \qquad \text{and} \qquad D_a \mathsf{a}_b = \frac{1}{\alpha} D_a D_b \alpha - \mathsf{a}_a \mathsf{a}_b,$$

as well as the facts

$$K_{ab} = -\nabla_a n_b - n_a \mathsf{a}_b \implies \nabla_a n_b = -K_{ab} - n_a \mathsf{a}_b;$$
$$^{(4)}R^{e}{}_{bac} n_e = 2\nabla_{[c}\nabla_{a]} n_b \quad \& \quad {}^{(4)}R^{e}{}_{bac} = g^{de}\,{}^{(4)}R_{dbac}$$
$$\implies {}^{(4)}R_{dbac} n^d = 2\nabla_{[c}\nabla_{a]} n_b.$$

Let us compute the Lie derivative of K_{ab} in the direction of the normal n^a:

$$\begin{aligned}
\mathcal{L}_{\vec{n}} K_{ab} &= n^c \nabla_c K_{ab} + K_{cb}\nabla_a n^c + K_{ac}\nabla_b n^c \\
&= n^c \nabla_c(-\nabla_a n_b - n_a \mathsf{a}_b) + K_{cb}(-K_a{}^c - n_a \mathsf{a}^c) + \underbrace{K_{ac}}_{=K_{ca}}(-K_b{}^c - n_b \mathsf{a}^c) \\
&= -n^c \nabla_c \nabla_a n_b - n^c \nabla_c(n_a \mathsf{a}_b) - K_{cb}K_a{}^c - K_{ca}K_b{}^c - K_{cb} n_a \mathsf{a}^c - K_{ca} n_b \mathsf{a}^c \\
&= \underbrace{-n^c \nabla_c \nabla_a n_b}_{=-{}^{(4)}R_{dbac} n^d n^c - n^c \nabla_a \nabla_c n_b} - n_a n^c \nabla_c \mathsf{a}_b - \mathsf{a}_b \underbrace{n^c \nabla_c n_a}_{=\mathsf{a}_a} - K_{cb}K_a{}^c - K_{ca}K_b{}^c \\
&\quad - K_{cb} n_a \mathsf{a}^c - K_{ca} n_b \mathsf{a}^c \\
&= -n^c n^d\, {}^{(4)}R_{dbac} - n^c \nabla_a \nabla_c n_b - n_a n^c \nabla_c \mathsf{a}_b - \mathsf{a}_b \mathsf{a}_a - 2K_{c(b}K_{a)}{}^c - 2K_{c(b} n_{a)} \mathsf{a}^c.
\end{aligned}$$

Expanding upon the second term above,

$$\begin{aligned}
\nabla_a \underbrace{(n^c \nabla_c n_b)}_{=\mathsf{a}_b} &= n^c \nabla_a \nabla_c n_b + \nabla_c n_b \nabla_a n^c \\
\implies n^c \nabla_a \nabla_c n_b &= \nabla_a \mathsf{a}_b - \nabla_c n_b \nabla_a n^c \\
&= \nabla_a \mathsf{a}_b - (-K_{cb} - n_c \mathsf{a}_b)(-K_a{}^c - n_a \mathsf{a}^c) \\
&= \nabla_a \mathsf{a}_b - (K_{cb}K_a{}^c + K_{cb} n_a \mathsf{a}^c + \mathsf{a}_b \underbrace{n_c K_a{}^c}_{=0} + \mathsf{a}_b n_a \underbrace{n_c \mathsf{a}^c}_{=0}) \\
&= \nabla_a \mathsf{a}_b - K_{cb}K_a{}^c - K_{cb} n_a \mathsf{a}^c.
\end{aligned}$$

Thus, we have

$$\begin{aligned}
\mathcal{L}_{\vec{n}} K_{ab} &= -n^c n^d\, {}^{(4)}R_{dbac} - n^c \nabla_a \nabla_c n_b - n_a n^c \nabla_c \mathsf{a}_b - \mathsf{a}_b \mathsf{a}_a - 2K_{c(b}K_{a)}{}^c - 2K_{c(b} n_{a)} \mathsf{a}^c \\
&= -n^c n^d\, {}^{(4)}R_{dbac} - (\nabla_a \mathsf{a}_b - K_{cb}K_a{}^c - K_{cb} n_a \mathsf{a}^c) - n_a n^c \nabla_c \mathsf{a}_b - \mathsf{a}_b \mathsf{a}_a \\
&\quad - K_{cb}K_a{}^c - K_{ca}K_b{}^c - K_{cb} n_a \mathsf{a}^c - K_{ca} n_b \mathsf{a}^c \\
&= -n^c n^d\, {}^{(4)}R_{dbac} - \nabla_a \mathsf{a}_b - n_a n^c \nabla_c \mathsf{a}_b - \mathsf{a}_b \mathsf{a}_a - K_{ca}K_b{}^c - K_{ca} n_b \mathsf{a}^c.
\end{aligned}$$

Now, using

$$\begin{aligned}
n^a \nabla_a \underbrace{(K_{cb} n^c)}_{=0} &= n^a n^c \nabla_a K_{cb} + K_{cb} n^a \nabla_a n^c \\
\implies K_{cb} n^a \nabla_a n^c &= -n^a n^c \nabla_a K_{cb} \\
&= -n^c n^a \nabla_c K_{ab}, \qquad \text{(relabeling } a \leftrightarrow c\text{)}
\end{aligned}$$

we can show that $\mathcal{L}_{\vec{n}} K_{ab}$ is purely spatial, i.e.,

$$\begin{aligned} n^a \mathcal{L}_{\vec{n}} K_{ab} &= n^a n^c \nabla_c K_{ab} + K_{cb} n^a \nabla_a n^c + \underbrace{n^a K_{ac}}_{=0} \nabla_b n^c \\ &= n^a n^c \nabla_c K_{ab} - n^c n^a \nabla_c K_{ab} \\ &= 0. \end{aligned}$$

Thus, projecting onto the hypersurface the result

$$\mathcal{L}_{\vec{n}} K_{ab} = -n^c n^d \, {}^{(4)}R_{dbac} - \nabla_a \mathsf{a}_b - n_a n^c \nabla_c \mathsf{a}_b - \mathsf{a}_b \mathsf{a}_a - K_{ca} K_b{}^c - K_{ca} n_b \mathsf{a}^c \tag{A.8}$$

does not affect the left hand side, given that $\mathcal{L}_{\vec{n}} K_{ab}$ is purely spatial. Hence, since we have two free indices (a, b) on (A.8), we apply the projection operator twice:

$$\begin{aligned} \mathcal{L}_{\vec{n}} K_{ab} &= \gamma_a{}^e \gamma_b{}^f \mathcal{L}_{\vec{n}} K_{ef} \\ &= -n^c n^d \gamma_a{}^e \gamma_b{}^f \underbrace{{}^{(4)}R_{dfec}}_{=-{}^{(4)}R_{dfce}} - \underbrace{\gamma_a{}^e \gamma_b{}^f \nabla_e \mathsf{a}_f}_{=D_a \mathsf{a}_b} - \gamma_b{}^f \underbrace{\gamma_a{}^e n_e}_{=0} n^c \nabla_c \mathsf{a}_f \\ &\quad - \gamma_a{}^e \gamma_b{}^f \underbrace{\mathsf{a}_e \mathsf{a}_f}_{\text{purely spatial}} - \gamma_a{}^e \gamma_b{}^f \underbrace{K_{ce} K_f{}^c}_{\text{purely spatial}} - \gamma_a{}^e \underbrace{\gamma_b{}^f n_f}_{=0} K_{ce} \mathsf{a}^c \\ &= n^c n^d \gamma_a{}^e \gamma_b{}^f \, {}^{(4)}R_{dfce} - \underbrace{D_a \mathsf{a}_b}_{=\frac{1}{\alpha} D_a D_b \alpha - \mathsf{a}_a \mathsf{a}_b} - \mathsf{a}_a \mathsf{a}_b - K_{ca} K_b{}^c \\ &= n^c n^d \gamma_a{}^e \gamma_b{}^f \, {}^{(4)}R_{dfce} - \frac{1}{\alpha} D_a D_b \alpha - K_{ac} K_b{}^c. \end{aligned}$$

This concludes our proof of (3.46c),

$$\boxed{\gamma_a{}^e \gamma_b{}^f n^c n^d \, {}^{(4)}R_{ecfd} = \mathcal{L}_{\vec{n}} K_{ab} + \frac{1}{\alpha} D_a D_b \alpha + K_b{}^c K_{ac}.} \tag{A.9}$$

Appendix B

Weyl Transformations

One of the key steps in the BSSN formulation of 3+1 numerical relativity is the decomposition of the spatial Ricci tensor and Ricci scalar into their conformal relatives and additional terms that follow due to the rescaling of the metric. We show these derivations in gory detail here in the appendix, since its inclusion in the main text would have been an unwanted tangent.

First off we want to know how D and $\bar{D}$ are related; therefore a good starting point for our discussion would be to examine the relation between different connections on a manifold. [1] We start by considering the relation between the covariant derivative ∇_a of a connection ∇ and the covariant derivative $\widehat{\nabla}_a$ of a connection $\widehat{\nabla}$. Applying these covariant derivatives to some $\binom{a}{b}$ tensor field $\boldsymbol{T}$, we have

$$\nabla_c T^{i_1\ldots i_a}{}_{j_1\ldots j_b} = \widehat{\nabla}_c T^{i_1\ldots i_a}{}_{j_1\ldots j_b} + \sum_{d=1}^{a} T^{i_1\ldots e\ldots i_a}{}_{j_1\ldots j_b} \mathfrak{C}^{i_d}{}_{ec} - \sum_{d=1}^{b} T^{i_1\ldots i_a}{}_{j_1\ldots e\ldots j_b} \mathfrak{C}^{e}{}_{j_d c}, \tag{B.1}$$

where $\mathfrak{C}^c{}_{ab}$ is a symmetric ($\mathfrak{C}^c{}_{ab} = \mathfrak{C}^c{}_{ba}$) $\binom{1}{2}$ tensor field that encodes information regarding possible disagreements between the two connections ∇ and $\widehat{\nabla}$. We shall derive an expression for $\mathfrak{C}^c{}_{ab}$ straight away.

Applying (B.1) to the metric g_{ab} that is compatible with the connection ∇, we get

$$\begin{aligned} \underbrace{\nabla_c g_{ab}}_{=0} &= \widehat{\nabla}_c g_{ab} - \mathfrak{C}^d{}_{ac}\, g_{bd} - \mathfrak{C}^d{}_{bc}\, g_{ad}, \\ \implies \widehat{\nabla}_c g_{ab} &= \mathfrak{C}^d{}_{ac}\, g_{bd} + \mathfrak{C}^d{}_{bc}\, g_{ad} = \mathfrak{C}_{bac} + \mathfrak{C}_{abc}. \end{aligned} \tag{B.2}$$

Similarly, cyclic permutations yield

$$\widehat{\nabla}_a g_{cb} = \mathfrak{C}_{bca} + \mathfrak{C}_{cba} \tag{B.3}$$

$$\widehat{\nabla}_b g_{ac} = \mathfrak{C}_{acb} + \mathfrak{C}_{cab}. \tag{B.4}$$

Now we add (B.2) and (B.3) and subtract (B.4),

$$\begin{aligned} \widehat{\nabla}_c g_{ab} + \widehat{\nabla}_a g_{cb} - \widehat{\nabla}_b g_{ac} &= \mathfrak{C}_{bac} + \mathfrak{C}_{abc} + \underbrace{\mathfrak{C}_{bca}}_{=\mathfrak{C}_{bac}} + \mathfrak{C}_{cba} - \underbrace{\mathfrak{C}_{acb}}_{=\mathfrak{C}_{abc}} - \underbrace{\mathfrak{C}_{cab}}_{=\mathfrak{C}_{cba}} \\ &= 2\,\mathfrak{C}_{bac} \end{aligned}$$

[1] For more detail, the reader may consult, e.g., [50].

$$\implies \mathfrak{C}_{bac} = \frac{1}{2}\left(\widehat{\nabla}_c g_{ab} + \widehat{\nabla}_a g_{cb} - \widehat{\nabla}_b g_{ac}\right)$$
$$\implies \mathfrak{C}^d{}_{ac} = \frac{1}{2} g^{db}\left(\widehat{\nabla}_c g_{ab} + \widehat{\nabla}_a g_{cb} - \widehat{\nabla}_b g_{ac}\right).$$

Thus we have found an expression for $\mathfrak{C}^c{}_{ab}$, relating a metric g_{ab} to the connection $\widehat{\nabla}$ of another metric $\widehat{g}_{ab}$,

$$\boxed{\mathfrak{C}^c{}_{ab} = \frac{1}{2} g^{cd}\left(\widehat{\nabla}_a g_{bd} + \widehat{\nabla}_b g_{ad} - \widehat{\nabla}_d g_{ab}\right).} \tag{B.5}$$

This choice of $\mathfrak{C}^c{}_{ab}$ is manifestly unique; note that in the special case when $\widehat{\nabla}_a$ is the ordinary partial derivative ∂_a, then $\mathfrak{C}^c{}_{ab}$ is simply the Christoffel symbol Γ^c_{ab}.

Having now a well defined relation between connections, we may compare their curvature. Recall the Ricci identity of the Riemann tensor: for any one-form ω_d, [2]

$$2\nabla_{[a}\nabla_{b]}\omega_c = R_{abc}{}^d \omega_d. \tag{B.6}$$

We then apply (B.1) to this expression; consider the first term on the LHS of (B.6):

$$\begin{aligned}
\nabla_a\nabla_b\omega_c &= \nabla_a(\nabla_b\omega_c) \\
&= \nabla_a\left(\widehat{\nabla}_b\omega_c - \mathfrak{C}^d{}_{bc}\omega_d\right) \\
&= \nabla_a\left(\widehat{\nabla}_b\omega_c\right) - \nabla_a\left(\mathfrak{C}^d{}_{bc}\omega_d\right) \\
&= \widehat{\nabla}_a\widehat{\nabla}_b\omega_c - \mathfrak{C}^d{}_{ab}\widehat{\nabla}_d\omega_c - \mathfrak{C}^d{}_{ac}\widehat{\nabla}_b\omega_d \\
&\quad - \widehat{\nabla}_a\left(\mathfrak{C}^d{}_{bc}\omega_d\right) + \mathfrak{C}^d{}_{ec}\,\mathfrak{C}^e{}_{ab}\,\omega_d + \mathfrak{C}^d{}_{eb}\,\mathfrak{C}^e{}_{ac}\,\omega_d \\
&= \widehat{\nabla}_a\widehat{\nabla}_b\omega_c - \mathfrak{C}^d{}_{ab}\widehat{\nabla}_d\omega_c - \mathfrak{C}^d{}_{ac}\widehat{\nabla}_b\omega_d \\
&\quad - \mathfrak{C}^d{}_{bc}\,\widehat{\nabla}_a\omega_d - \omega_d\,\widehat{\nabla}_a\mathfrak{C}^d{}_{bc} + \mathfrak{C}^d{}_{ec}\,\mathfrak{C}^e{}_{ab}\,\omega_d + \mathfrak{C}^d{}_{eb}\,\mathfrak{C}^e{}_{ac}\,\omega_d.
\end{aligned}$$

Then permuting $a \leftrightarrow b$ and subtracting,

$$\begin{aligned}
2\nabla_{[a}\nabla_{b]}\omega_c &= \widehat{\nabla}_a\widehat{\nabla}_b\omega_c - \mathfrak{C}^d{}_{ab}\widehat{\nabla}_d\omega_c - \mathfrak{C}^d{}_{ac}\widehat{\nabla}_b\omega_d \\
&\quad - \mathfrak{C}^d{}_{bc}\,\widehat{\nabla}_a\omega_d - \omega_d\,\widehat{\nabla}_a\mathfrak{C}^d{}_{bc} + \mathfrak{C}^d{}_{ec}\,\mathfrak{C}^e{}_{ab}\,\omega_d + \mathfrak{C}^d{}_{eb}\,\mathfrak{C}^e{}_{ac}\,\omega_d \\
&\quad - \widehat{\nabla}_b\widehat{\nabla}_a\omega_c + \mathfrak{C}^d{}_{ab}\widehat{\nabla}_d\omega_c + \mathfrak{C}^d{}_{bc}\widehat{\nabla}_a\omega_d \\
&\quad + \mathfrak{C}^d{}_{ac}\,\widehat{\nabla}_b\omega_d + \omega_d\,\widehat{\nabla}_b\mathfrak{C}^d{}_{ac} - \mathfrak{C}^d{}_{ec}\,\mathfrak{C}^e{}_{ab}\,\omega_d - \mathfrak{C}^d{}_{ea}\,\mathfrak{C}^e{}_{bc}\,\omega_d. \\
&= \underbrace{2\,\widehat{\nabla}_{[a}\widehat{\nabla}_{b]}\omega_c}_{=\widehat{R}_{abc}{}^d\omega_d} - 2\,\widehat{\nabla}_{[a}\mathfrak{C}^d{}_{b]c}\omega_d + 2\,\mathfrak{C}^e{}_{c[a}\,\mathfrak{C}^d{}_{b]e}\omega_d \\
&= \widehat{R}_{abc}{}^d\omega_d - 2\,\widehat{\nabla}_{[a}\mathfrak{C}^d{}_{b]c}\omega_d + 2\,\mathfrak{C}^e{}_{c[a}\,\mathfrak{C}^d{}_{b]e}\omega_d.
\end{aligned}$$

[2] You may check that this expression for the Ricci identity is entirely equivalent to Eq. (3.25). Here $R_{abc}{}^d$ is obtained from the usual coordinate expression of the Riemann tensor $R^d{}_{abc}$ by performing some straightforward index gymnastics and using the known symmetries of the Riemann tensor ($R_{abc}{}^d = g^{de}R_{abce} = g^{de}R_{ceab} = -g^{de}R_{ecab} = -R^d{}_{cab} = R^d{}_{cba}$).

This relation holds for any one-form ω_d; thus we have found a transformation law for the Riemann tensor from a connection ∇ to a connection $\widehat{\nabla}$:

$$R_{abc}{}^{d} = \widehat{R}_{abc}{}^{d} - 2\,\widehat{\nabla}_{[a}\mathfrak{C}^{d}{}_{b]c} + 2\,\mathfrak{C}^{e}{}_{c[a}\,\mathfrak{C}^{d}{}_{b]e}. \tag{B.7}$$

Similarly, contracting $b = d$, we get a relation for the Ricci tensor:

$$R_{ac} = \widehat{R}_{ac} - 2\,\widehat{\nabla}_{[a}\mathfrak{C}^{b}{}_{b]c} + 2\,\mathfrak{C}^{e}{}_{c[a}\,\mathfrak{C}^{b}{}_{b]e}. \tag{B.8}$$

Then, if the conformal scaling of the metric is such that

$$\begin{aligned}\widehat{g}_{ab} &= \chi g_{ab}\\ \widehat{g}^{ab} &= \chi^{-1} g^{ab},\end{aligned}$$

(as it shall be in our case), then we can get a transformation law for the Ricci scalar as well by raising an index on (B.8) and contracting:

$$\begin{aligned} g^{ac}R_{ac} &= g^{ac}\left(\widehat{R}_{ac} - 2\,\widehat{\nabla}_{[a}\mathfrak{C}^{b}{}_{b]c} + 2\,\mathfrak{C}^{e}{}_{c[a}\,\mathfrak{C}^{b}{}_{b]e}\right)\\ R &= \chi\widehat{g}^{ac}\left(\widehat{R}_{ac} - 2\,\widehat{\nabla}_{[a}\mathfrak{C}^{b}{}_{b]c} + 2\,\mathfrak{C}^{e}{}_{c[a}\,\mathfrak{C}^{b}{}_{b]e}\right)\\ &= \chi\left(\widehat{R} - 2\,\widehat{g}^{ac}\widehat{\nabla}_{[a}\mathfrak{C}^{b}{}_{b]c} + 2\,\widehat{g}^{ac}\mathfrak{C}^{e}{}_{c[a}\,\mathfrak{C}^{b}{}_{b]e}\right). \end{aligned}$$

We summarise these three key curvature transformations here,

$$\boxed{\begin{aligned} R_{abc}{}^{d} &= \widehat{R}_{abc}{}^{d} - 2\,\widehat{\nabla}_{[a}\mathfrak{C}^{d}{}_{b]c} + 2\,\mathfrak{C}^{e}{}_{c[a}\,\mathfrak{C}^{d}{}_{b]e} && \text{(B.9a)}\\ R_{ab} &= \widehat{R}_{ab} - 2\,\widehat{\nabla}_{[a}\mathfrak{C}^{c}{}_{c]b} + 2\,\mathfrak{C}^{e}{}_{b[a}\,\mathfrak{C}^{c}{}_{c]e} && \text{(B.9b)}\\ R &= \chi\left(\widehat{R} - 2\,\widehat{g}^{ab}\widehat{\nabla}_{[a}\mathfrak{C}^{c}{}_{c]b} + 2\,\widehat{g}^{ab}\mathfrak{C}^{e}{}_{b[a}\,\mathfrak{C}^{c}{}_{c]e}\right). && \text{(B.9c)}\end{aligned}}$$

These are very important transformation laws that we will use quite often in the main text… In fact, let us use them now to write the conformal decomposition of both the $3D$ (spatial) Ricci tensor R_{ij} and Ricci scalar R that we are using in our treatment: We start by calculating the $\mathfrak{C}^{c}{}_{ab}$ relation between our two connections D and $\bar{D}$, using (B.5):

$$\begin{aligned}\mathfrak{C}^{k}{}_{ij} &= \frac{1}{2}\gamma^{k\ell}\left(\bar{D}_i\gamma_{j\ell} + \bar{D}_j\gamma_{i\ell} - \bar{D}_k\gamma_{ij}\right)\\ &= \frac{1}{2}\chi\bar{\gamma}^{k\ell}\left(\bar{D}_i(\chi^{-1}\bar{\gamma}_{j\ell}) + \bar{D}_j(\chi^{-1}\bar{\gamma}_{i\ell}) - \bar{D}_\ell(\chi^{-1}\bar{\gamma}_{ij})\right)\\ &= \frac{1}{2}\chi\bar{\gamma}^{k\ell}(\chi^{-1}\underbrace{\bar{D}_i\bar{\gamma}_{j\ell}}_{=0} + \bar{\gamma}_{j\ell}\,\bar{D}_i\chi^{-1} + \chi^{-1}\underbrace{\bar{D}_j\bar{\gamma}_{i\ell}}_{=0} + \bar{\gamma}_{i\ell}\,\bar{D}_j\chi^{-1} - \chi^{-1}\underbrace{\bar{D}_\ell\bar{\gamma}_{ij}}_{=0} - \bar{\gamma}_{ij}\,\bar{D}_\ell\chi^{-1})\\ &= \frac{1}{2}\chi\bar{\gamma}^{k\ell}\left(-\chi^{-2}\bar{\gamma}_{j\ell}\,\bar{D}_i\chi - \chi^{-2}\bar{\gamma}_{i\ell}\,\bar{D}_j\chi + \chi^{-2}\bar{\gamma}_{ij}\,\bar{D}_\ell\chi\right)\\ &= \frac{1}{2}\chi^{-1}\left(\bar{\gamma}_{ij}\,\bar{D}^k\chi - 2\,\delta_{(i}{}^{k}\,\bar{D}_{j)}\chi\right)\\ &= \frac{1}{2}\bar{\gamma}_{ij}\,\bar{D}^k(\log\chi) - \delta_{(i}{}^{k}\,\bar{D}_{j)}(\log\chi). \end{aligned} \tag{B.10}$$

Also, in terms of ψ (we will use this when dealing with the initial data problem (see Chapter 5)),

$$\begin{aligned}
\mathfrak{C}^k{}_{ij} &= \frac{1}{2}\gamma^{k\ell}\left(\bar{D}_i\gamma_{j\ell} + \bar{D}_j\gamma_{i\ell} - \bar{D}_k\gamma_{ij}\right)\\
&= \frac{1}{2}\psi^{-4}\bar{\gamma}^{k\ell}\left(\bar{D}_i(\psi^4\bar{\gamma}_{j\ell}) + \bar{D}_j(\psi^4\bar{\gamma}_{i\ell}) - \bar{D}_\ell(\psi^4\bar{\gamma}_{ij})\right)\\
&= \frac{1}{2}\psi^{-4}\bar{\gamma}^{k\ell}\left(4\psi^3\bar{\gamma}_{j\ell}\,\bar{D}_i\psi + 4\psi^3\bar{\gamma}_{i\ell}\,\bar{D}_j\psi - 4\psi^3\bar{\gamma}_{ij}\,\bar{D}_\ell\psi\right)\\
&= 2\psi^{-1}\bar{\gamma}^{k\ell}\left(\bar{\gamma}_{j\ell}\,\bar{D}_i\psi + \bar{\gamma}_{i\ell}\,\bar{D}_j\psi - \bar{\gamma}_{ij}\,\bar{D}_\ell\psi\right)\\
&= 2\bar{\gamma}^{k\ell}\left(\bar{\gamma}_{j\ell}\,\bar{D}_i(\log\psi) + \bar{\gamma}_{i\ell}\,\bar{D}_j(\log\psi) - \bar{\gamma}_{ij}\,\bar{D}_\ell(\log\psi)\right)\\
&= 4\delta_{(i}{}^k\,\bar{D}_{j)}(\log\psi) - 2\bar{\gamma}_{ij}\,\bar{D}^k(\log\psi). \qquad \text{(B.11)}
\end{aligned}$$

We now apply (B.10) to (B.9b) and expand:

$$\begin{aligned}
R_{ij} &= \bar{R}_{ij} - 2\,\bar{D}_{[i}\mathfrak{C}^k{}_{k]j} + 2\,\mathfrak{C}^\ell{}_{j[i}\,\mathfrak{C}^k{}_{k]\ell}\\
&= \bar{R}_{ij} - \left(\bar{D}_i\mathfrak{C}^k{}_{jk} - \bar{D}_k\mathfrak{C}^k{}_{ij}\right) + \left(\mathfrak{C}^\ell{}_{ij}\,\mathfrak{C}^k{}_{\ell k} - \mathfrak{C}^\ell{}_{jk}\,\mathfrak{C}^k{}_{i\ell}\right)\\
&= \bar{R}_{ij} - \bar{D}_i\left[\frac{1}{2}\bar{\gamma}_{jk}\,\bar{D}^k(\log\chi) - \delta_{(j}{}^k\,\bar{D}_{k)}(\log\chi)\right]\\
&\quad + \bar{D}_k\left[\frac{1}{2}\bar{\gamma}_{ij}\,\bar{D}^k(\log\chi) - \delta_{(i}{}^k\,\bar{D}_{j)}(\log\chi)\right]\\
&\quad + \left[\frac{1}{2}\bar{\gamma}_{ij}\,\bar{D}^\ell(\log\chi) - \delta_{(i}{}^\ell\,\bar{D}_{j)}(\log\chi)\right]\left[\frac{1}{2}\bar{\gamma}_{\ell k}\,\bar{D}^k(\log\chi) - \delta_{(\ell}{}^k\,\bar{D}_{k)}(\log\chi)\right]\\
&\quad - \left[\frac{1}{2}\bar{\gamma}_{jk}\,\bar{D}^\ell(\log\chi) - \delta_{(j}{}^\ell\,\bar{D}_{k)}(\log\chi)\right]\left[\frac{1}{2}\bar{\gamma}_{i\ell}\,\bar{D}^k(\log\chi) - \delta_{(i}{}^k\,\bar{D}_{\ell)}(\log\chi)\right]\\
&= \bar{R}_{ij} - \frac{1}{2}\bar{D}_i\bar{D}_j(\log\chi) + \frac{1}{2}\bar{D}_i\bar{D}_j(\log\chi) + \frac{3}{2}\bar{D}_i\bar{D}_j(\log\chi)\\
&\quad + \frac{1}{2}\bar{\gamma}_{ij}\,\bar{D}_k\bar{D}^k(\log\chi) - \frac{1}{2}\bar{D}_i\bar{D}_j(\log\chi) - \frac{1}{2}\underbrace{\bar{D}_j\bar{D}_i(\log\chi)}_{=\,\bar{D}_i\bar{D}_j(\log\chi)\text{ since }\log\chi\text{ is a scalar}}\\
&\quad + \frac{1}{4}\bar{\gamma}_{ij}\,\bar{D}_k(\log\chi)\bar{D}^k(\log\chi) - \frac{1}{4}\bar{\gamma}_{ij}\,\bar{D}_k(\log\chi)\bar{D}^k(\log\chi) - \frac{3}{4}\bar{\gamma}_{ij}\,\bar{D}_k(\log\chi)\bar{D}^k(\log\chi)\\
&\quad - \frac{1}{4}\bar{D}_i(\log\chi)\bar{D}_j(\log\chi) - \frac{1}{4}\bar{D}_i(\log\chi)\bar{D}_j(\log\chi) + \frac{1}{4}\bar{D}_i(\log\chi)\bar{D}_j(\log\chi)\\
&\quad + \frac{3}{4}\bar{D}_i(\log\chi)\bar{D}_j(\log\chi) + \frac{3}{4}\bar{D}_i(\log\chi)\bar{D}_j(\log\chi) + \frac{1}{4}\bar{D}_i(\log\chi)\bar{D}_j(\log\chi)\\
&\quad - \frac{1}{4}\bar{D}_i(\log\chi)\bar{D}_j(\log\chi) + \frac{1}{4}\bar{\gamma}_{ij}\,\bar{D}_k(\log\chi)\bar{D}^k(\log\chi) + \frac{1}{4}\bar{D}_i(\log\chi)\bar{D}_j(\log\chi)\\
&\quad + \frac{1}{4}\bar{\gamma}_{ij}\,\bar{D}_k(\log\chi)\bar{D}^k(\log\chi) - \frac{1}{4}\bar{D}_i(\log\chi)\bar{D}_j(\log\chi) - \frac{1}{4}\bar{D}_i(\log\chi)\bar{D}_j(\log\chi)\\
&\quad + \frac{1}{4}\bar{D}_i(\log\chi)\bar{D}_j(\log\chi) - \frac{1}{4}\bar{D}_i(\log\chi)\bar{D}_j(\log\chi) - \frac{3}{4}\bar{D}_i(\log\chi)\bar{D}_j(\log\chi)\\
&= \bar{R}_{ij} + \frac{1}{2}\left(\bar{D}_i\bar{D}_j(\log\chi) + \bar{\gamma}_{ij}\,\bar{D}_k\bar{D}^k(\log\chi)\right) + \frac{1}{4}\left(\bar{D}_i(\log\chi)\bar{D}_j(\log\chi) - \bar{\gamma}_{ij}\,\bar{D}_k(\log\chi)\bar{D}^k(\log\chi)\right).
\end{aligned}$$

Thus we have found that the 3D Ricci tensor can be split as

$$\boxed{\begin{aligned} R_{ij} &= \bar{R}_{ij} + R^{\chi}_{ij} && \text{(B.12a)}\\ \bar{R}_{ij} &= \partial_k \bar{\Gamma}^k_{ij} - \partial_j \bar{\Gamma}^k_{ik} + \bar{\Gamma}^k_{\ell k}\,\bar{\Gamma}^{\ell}_{ij} - \bar{\Gamma}^k_{\ell j}\,\bar{\Gamma}^{\ell}_{ik} && \text{(B.12b)}\\ R^{\chi}_{ij} &= \frac{1}{2}\left(\bar{D}_i\bar{D}_j(\log\chi) + \bar{\gamma}_{ij}\,\bar{D}_k\bar{D}^k(\log\chi)\right) && \text{(B.12c)}\\ &\quad + \frac{1}{4}\left(\bar{D}_i(\log\chi)\bar{D}_j(\log\chi) - \bar{\gamma}_{ij}\,\bar{D}_k(\log\chi)\bar{D}^k(\log\chi)\right). \end{aligned}}$$

Then, raising an index and contracting, we get

$$\begin{aligned} \gamma^{ij}R_{ij} &= \gamma^{ij}\left(\bar{R}_{ij} + R^{\chi}_{ij}\right) = \chi\bar{\gamma}^{ij}\left(\bar{R}_{ij} + R^{\chi}_{ij}\right)\\ R &= \chi\bar{R} + \chi[\frac{1}{2}\left(\bar{D}_k\bar{D}^k(\log\chi) + 3\,\bar{D}_k\bar{D}^k(\log\chi)\right)\\ &\quad + \frac{1}{4}\left(\bar{D}_k(\log\chi)\bar{D}^k(\log\chi) - 3\,\bar{D}_k(\log\chi)\bar{D}^k(\log\chi)\right)]\\ &= \chi\bar{R} + 2\,\chi\bar{D}_k\bar{D}^k(\log\chi) - \frac{1}{2}\,\chi\bar{D}_k(\log\chi)\bar{D}^k(\log\chi). \end{aligned}$$

Hence we have derived a conformal decomposition for the Ricci scalar as well,

$$\boxed{R = \chi\bar{R} + 2\,\chi\bar{D}^2(\log\chi) - \frac{1}{2}\,\chi\bar{D}_k(\log\chi)\bar{D}^k(\log\chi).} \qquad \text{(B.13)}$$

where $\bar{D}^2 = \bar{D}_k\bar{D}^k$ the conformal Laplace operator. We may further expand this expression as follows:

$$\begin{aligned} R &= \chi\bar{R} + 2\,\chi\bar{\gamma}^{ij}\bar{D}_i(\bar{D}_j(\log\chi)) - \frac{1}{2}\,\chi\bar{\gamma}^{ij}\bar{D}_i(\log\chi)\bar{D}_j(\log\chi)\\ &= \chi\bar{R} + 2\,\chi\bar{\gamma}^{ij}\bar{D}_i(\chi^{-1}\bar{D}_j\chi) - \frac{1}{2}\,\chi\cdot\chi^{-2}\bar{\gamma}^{ij}\bar{D}_i\chi\bar{D}_j\chi\\ &= \chi\bar{R} + 2\,\chi\bar{\gamma}^{ij}\left(\chi^{-1}\bar{D}_i\bar{D}_j\chi - \chi^{-2}\bar{D}_i\chi\bar{D}_j\chi\right) - \frac{1}{2}\,\chi^{-1}\bar{D}_k\chi\bar{D}^k\chi\\ &= \chi\bar{R} + 2\,\bar{D}^2\chi - \frac{5}{2}\,\chi^{-1}\bar{D}_k\chi\bar{D}^k\chi. \end{aligned} \qquad \text{(B.14)}$$

Appendix C

Numerical Methods

In this appendix we fill in some detail of a handful of numerical methods that we used in this thesis (the presentation is terse; it merely serves as a brief under-the-hood peek). Partial differential equations (PDE's) cannot be implemented using a computer in such raw form, as the computer would not be able to understand what the concept of a derivative is; hence we must settle for just an *approximation* of these derivatives. In typical Finite Difference Methods (FDM) fashion, we present some field/function and a discrete lattice, and then we evaluate certain combinations of values of this field at each lattice node in order to approximate its derivatives. (This approximation is usually referred to as the Finite Difference Approximation, or FDA.)

Let Φ be a field, sufficiently smooth so that it admits a Taylor series expansion about some point x. Then we write

$$\Phi(x+\Delta x) = \sum_{n=0}^{\infty} \partial_x^n \Phi(x) \frac{\Delta x^n}{n!} = \Phi(x) + \partial_x \Phi \Delta x + \partial_x^2 \Phi \frac{\Delta x^2}{2} + \partial_x^3 \Phi \frac{\Delta x^3}{6} + \dots \tag{C.1}$$

or

$$\Phi(x-\Delta x) = \sum_{n=0}^{\infty} \partial_x^n \Phi(x) \frac{(-1)^n \Delta x^n}{n!} = \Phi(x) - \partial_x \Phi \Delta x + \partial_x^2 \Phi \frac{\Delta x^2}{2} - \partial_x^3 \Phi \frac{\Delta x^3}{6} + \dots \tag{C.2}$$

Note that from either (C.1) or (C.2) we can get an expression for the first derivative of Φ, by isolating the second term on the RHS and then dividing by Δx. For instance, for (C.1),

$$\partial_x \Phi = \frac{\Phi(x+\Delta x) - \Phi(x)}{\Delta x} - \partial_x^2 \Phi \frac{\Delta x}{2} - \partial_x^3 \Phi \frac{\Delta x^2}{6} - \dots \tag{C.3}$$

Now the green part of equation (C.3) must be truncated at some point, since the computer is not capable of dealing with infinite sums; whence we write

$$\partial_x \Phi = \frac{\Phi(x+\Delta x) - \Phi(x)}{\Delta x} + O(\Delta x). \tag{C.4}$$

Similarly, from (C.2),

$$\partial_x \Phi = \frac{\Phi(x) - \Phi(x-\Delta x)}{\Delta x} + O(\Delta x). \tag{C.5}$$

Moreover, substracting (C.2) from (C.1), we have

$$\partial_x \Phi = \frac{\Phi(x+\Delta x) - \Phi(x-\Delta x)}{2\Delta x} + O(\Delta x). \tag{C.6}$$

In the limit where $\Delta x \to 0$, all three expressions (C.4)–(C.6) will converge to the derivative.

Using standard FDM notation, we write $x_i \equiv x_0 + i\Delta x$ and $\Phi_i \equiv \Phi(x_i)$. Then, if Δx is small but finite, equations (C.4) – (C.6) can be used to obtain approximations of the derivate $\partial_x \Phi$ about the grid point x_i of the form

$$\partial_x \Phi|_{x_i} \approx \frac{\Phi_{i+1} - \Phi_i}{\Delta x} \tag{C.7a}$$

$$\partial_x \Phi|_{x_i} \approx \frac{\Phi_i - \Phi_{i-1}}{\Delta x} \tag{C.7b}$$

$$\partial_x \Phi|_{x_i} \approx \frac{\Phi_{i+1} - \Phi_{i-1}}{2\Delta x}. \tag{C.7c}$$

The three expressions (C.7) are referred to as the ***forward***, ***backward***, and ***centred*** finite difference approximations, respectively, of $\partial_x \Phi$ evaluated at x_i. We shall use the latter in our work.

Now we also need to find a discrete expression for second derivatives. Write (C.1) and (C.2) in terms of the second derivative term:

$$\partial_x^2 \Phi = 2\frac{\Phi(x + \Delta x) - \Phi(x) - \partial_x \Phi \Delta x}{\Delta x^2} + O(\Delta x)$$

$$\partial_x^2 \Phi = 2\frac{\Phi(x - \Delta x) - \Phi(x) + \partial_x \Phi \Delta x}{\Delta x^2} + O(\Delta x).$$

Now adding these two equations, we get

$$\partial_x^2 \Phi = \frac{\Phi(x + \Delta x) - 2\Phi(x) + \Phi(x - \Delta x)}{\Delta x^2} + O(\Delta x). \tag{C.8}$$

Then, taking Δx to be small but finite, we can approximate the second derivate $\partial_x^2 \Phi$ about the grid point x_i:

$$\partial_x^2 \Phi|_{x_i} \approx \frac{\Phi_{i+1} - 2\Phi_i + \Phi_{i-1}}{\Delta x^2}. \tag{C.9}$$

Thus far we have only used three-point stencils to derive all the FDA's, and it turns out sometimes the necessity arises to use a more accurate scheme, such as an FDA based on a five-point stencil (see Fig C.1 on the right). In this case the derivative approximations are more accurate because more nodes are being used (four neighbouring points as opposed to just the two immediate neighbours, as in the previously derived formulæ. Using these extra nodes, we Taylor-expand

$$\Phi(x \pm 2\Delta x) \approx \Phi(x) \pm \partial_x \Phi(2\Delta x) + \partial_x^2 \Phi \frac{(2\Delta x)^2}{2} \pm \partial_x^3 \Phi \frac{(2\Delta x)^3}{6} + \dots \tag{C.10}$$

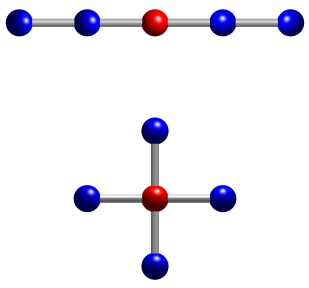

FIGURE C.1: Five-point stencil in one (top) and two (bottom) dimensions. [Image from Wikipedia]

Substracting the positive and negative versions of this expansion yields

$$\Phi(x+2\Delta x)-\Phi(x-2\Delta x)\approx\partial_x\Phi(4\Delta x)+\partial_x^3\Phi\frac{8\Delta x^3}{3}+\dots \tag{C.11}$$

We can then get rid of the $\partial_x^3\Phi$ term by multiplying $8\times$ ((C.1) $-$ (C.2)) and then substracting (C.11):

$$8\Phi(x+\Delta x)-8\Phi(x-\Delta x)-\Phi(x+2\Delta x)+\Phi(x-2\Delta x)\approx\partial_x\Phi(12\Delta x)+\dots \tag{C.12}$$

This leaves us with an expression for a five-point stencil approximation of the first derivative:

$$\partial_x\Phi\approx\frac{8(\Phi_{i+1}-\Phi_{i-1})-\Phi_{i+2}+\Phi_{i-2}}{12\Delta x}. \tag{C.13}$$

Similar derivations yield five-point stencil FDA's for higher derivatives:

$$\partial_x^2\Phi\approx\frac{16(\Phi_{i+1}+\Phi_{i-1})-30\Phi_i-\Phi_{i+2}-\Phi_{i-2}}{12\Delta x^2} \tag{C.14}$$

$$\partial_x^3\Phi\approx\frac{\Phi_{i+2}-\Phi_{i-2}+2(\Phi_{i-1}-\Phi_{i+1})}{2\Delta x^3} \tag{C.15}$$

$$\partial_x^4\Phi\approx\frac{\Phi_{i+2}+\Phi_{i-2}+6\Phi-4(\Phi_{i+1}+\Phi_{i-1})}{\Delta x^4}. \tag{C.16}$$

We make use of the latter FDA in the von Neumann analysis of our code (§ 2.1.1).

C.1 Simpson's Method

We need to evaluate, numerically, a double integral

$$S_E=\int_{\tau_{\min}}^{\tau_{\max}}\int_{x_{\min}}^{x_{\max}}\mathcal{L}\,\mathrm{d}x\,\mathrm{d}\tau. \tag{C.17}$$

We will tackle this integration via a $2D$ Simpson method. In $1D$, according to *Simpson's composite* $1/3$ *rule*, an integral

$$I=\int_a^b f(x)\,\mathrm{d}x$$

is approximated by partitioning the interval $[a,b]$ into N evenly spaced segments $a=x_0<x_1<\dots<x_N=b$ with spacing $\mathrm{h}\equiv(b-a)/N$, and then putting

$$I\approx\frac{\mathrm{h}}{3}\left[f_0+4\sum_{\substack{i=1\\ i\text{ is odd}}}^{N-1}f_i+2\sum_{\substack{i=2\\ i\text{ is even}}}^{N-2}f_i+f_N\right], \tag{C.18}$$

where as usual we wrote $f_k\equiv f(x_k)$, and we point out the requirement that in order for (C.18) to work N must be even. Alternatively, note that we may write this in vector form as

$$I\approx\frac{\mathrm{h}}{3}\boldsymbol{s}\boldsymbol{f}^T, \tag{C.19}$$

where $\boldsymbol{s} = [1\,4\,2\,4\cdots 2\,4\,1]$ and $\boldsymbol{f} = [f_0 \cdots f_N]$ are vectors of length $N+1$. In the $2D$ extension of this method both $\boldsymbol{s}$ and $\boldsymbol{f}$ become $(N+1)\times(N+1)$ matrices, $\boldsymbol{S}$ and $\boldsymbol{F}$. The latter is the Lagrangian that we want to integrate (= $\mathcal{L}$ in (C.17)), whilst the fomer is acquired by multiplying the Simpson coefficients at each grip point; for instance, if $N = 4$,

$$\boldsymbol{S} = \begin{pmatrix} 1\times 1 = 1 & 4\times 1 = 4 & 2\times 1 = 2 & 4\times 1 = 4 & 1\times 1 = 1 \\ 1\times 4 = 4 & 4\times 4 = 16 & 2\times 4 = 8 & 4\times 4 = 16 & 1\times 4 = 4 \\ 1\times 2 = 2 & 4\times 2 = 8 & 2\times 2 = 4 & 4\times 2 = 8 & 1\times 2 = 2 \\ 1\times 4 = 4 & 4\times 4 = 16 & 2\times 4 = 8 & 4\times 4 = 16 & 1\times 4 = 4 \\ 1\times 1 = 1 & 4\times 1 = 4 & 2\times 1 = 2 & 4\times 1 = 4 & 1\times 1 = 1 \end{pmatrix}.$$

The pattern is now clear for general N:

$$\boldsymbol{S} = \begin{pmatrix} 1 & 4 & 2 & 4 & \cdots & 2 & 4 & 1 \\ 4 & 16 & 8 & 16 & \cdots & 8 & 16 & 4 \\ 2 & 8 & 4 & 8 & \cdots & 4 & 8 & 2 \\ 4 & 16 & 8 & 16 & \cdots & 8 & 16 & 4 \\ \vdots & \vdots & \vdots & \vdots & \vdots & \vdots & \vdots & \vdots \\ 2 & 8 & 4 & 8 & \cdots & 4 & 8 & 2 \\ 4 & 16 & 8 & 16 & \cdots & 8 & 16 & 4 \\ 1 & 4 & 2 & 4 & \cdots & 2 & 4 & 1 \end{pmatrix}. \tag{C.20}$$

Thus we approximate the $2D$ integral (C.17) via the Frobenius inner product [1]

$$S_E \approx \frac{\mathrm{h}^2}{9}\boldsymbol{S} \otimes_F \mathcal{L} \equiv \frac{\mathrm{h}^2}{9}\sum_{i=\tau_{\min}}^{\tau_{\max}}\sum_{j=x_{\min}}^{x_{\max}} \boldsymbol{S}_{ij}\,\mathcal{L}_{ij}, \tag{C.21}$$

where $\boldsymbol{S}_{ij}$ is understood to be the (i,j)-component of (C.20) and $\mathcal{L}_{ij}$ is the FDA of the Lagrangian $\mathcal{L}$. Our user-defined **C++** function for this $2D$ Simpson implementation is shown on listing C.1.

```
// 2D Simpson's Rule
double Simpson2D (vector<vector<double>> Fij,  double step_size, int taumax
    , int xmax){
    // Initialize variables
    vector<double> Si {};
    vector<double> Action_Vec {};
    double actionvals {};
    double Action {};
    double Total_Action {};
    //initialize 2D  vector Sij to have size 121 x 121
    vector<vector<double>> Sij (taumax+1, vector<double> ( xmax+1, 0.0 ) );

    for (int i {0}; i <= taumax; i++){
        for (int j {0}; j <= xmax; j++){
            if (i == 0 || i == taumax) {
               if (j == 0 || j == xmax)
                  Sij.at(i).at(j) = 1.0;
               else if (j % 2 != 0)
```

[1] This is, of course, assuming the grid spacing h is uniform and equal in both the x and y directions.

```
                    Sij.at(i).at(j) = 4.0;
                else
                    Sij.at(i).at(j) = 2.0;
            }
            else if (j == 0 || j == xmax) {
                if (i % 2 != 0)
                    Sij.at(i).at(j) = 4.0;
                else
                    Sij.at(i).at(j) = 2.0;
            }
            else {
                if ( (i % 2 != 0) && (j % 2 != 0) )
                    Sij.at(i).at(j) = 16.0;
                else if ( ((i % 2 != 0) && (j % 2 == 0)) || ((i % 2 == 0)
                        && (j % 2 != 0)) )
                    Sij.at(i).at(j) = 8.0;
                else
                    Sij.at(i).at(j) = 4.0;
            }
            actionvals = (Sij.at(i).at(j)) * (Fij.at(i).at(j));
            Si.push_back(actionvals);
        }   //end of main 'j' loop
        Action = accumulate(Si.begin(), Si.end(), 0.0 );
        Action_Vec.push_back(Action);
        Si.clear();
    }    //end of main 'i' loop
    Total_Action = (pow(step_size,2)/9.0) *
             ( accumulate(Action_Vec.begin(), Action_Vec.end(), 0.0 ) );
    Action_Vec.clear();

    return Total_Action;
}
```

Listing C.1: Our user-defined $2D$ Simpson function.

C.2 Least Squares Fitting (LSF)

We begin with a set of n data points $P_0, \ldots, P_{n-1}$, where $P_i = (x_i, y_i)$. The procedure then is to find a line $y = mx + b$ (m being the slope and b the y-intercept) which best fits the data set (note that this is a classical $\max/\min$ calculus problem). The vertical distance from $P_i = (x_i, y_i)$ to the line $y = mx + b$ is $|y_i - (mx_i + b)|$. However, since we are heading toward a calculus style $\max/\min$ process, the absolute value is an inconvenience. To get around this, we instead square each of these terms and then add them all to get a function σ which depends on m and b:

$$\sigma(m, b) = \sum_i [y_i - (mx_i + b)]^2. \tag{C.22}$$

Next we apply standard $\max/\min$ techniques to σ. Differentiating,

$$\frac{\partial \sigma}{\partial m} = \sum_i 2\,[y_i - (mx_i + b)](-x_i) = 2\sum_i [mx_i^2 + (b - y_i)x_i]$$
$$\frac{\partial \sigma}{\partial b} = 2\sum_i [y_i - (mx_i + b)],$$

and then setting these derivatives to zero,

$$0 = \sum_i [mx_i^2 + (b - y_i)x_i] = m\sum_i x_i^2 + b\sum_i x_i - \sum_i x_i y_i$$
$$0 = \sum_i [y_i - (mx_i + b)] = -m\sum_i x_i - nb + \sum_i y_i.$$

Thus we have a a 2×2 linear system with unknowns m and b,

$$\sum_i x_i y_i = m\sum_i x_i^2 + b\sum_i x_i \tag{C.23a}$$
$$\sum_i y_i = m\sum_i x_i + nb, \tag{C.23b}$$

or in matrix notation,

$$\begin{pmatrix} \sum_i x_i^2 & \sum_i x_i \\ \sum_i x_i & n \end{pmatrix} \begin{pmatrix} m \\ b \end{pmatrix} = \begin{pmatrix} \sum_i x_i y_i \\ \sum_i y_i \end{pmatrix}. \tag{C.23⊛}$$

Now, introducing

$$A \equiv \begin{pmatrix} x_0 & \cdots & x_{n-1} \\ 1 & \cdots & 1 \end{pmatrix}$$

it is immediate that

$$AA^T = \begin{pmatrix} x_0 & \cdots & x_{n-1} \\ 1 & \cdots & 1 \end{pmatrix} \begin{pmatrix} x_0 & 1 \\ \vdots & \vdots \\ x_{n-1} & 1 \end{pmatrix} = \begin{pmatrix} \sum_i x_i^2 & \sum_i x_i \\ \sum_i x_i & n \end{pmatrix},$$

and

$$A \begin{pmatrix} y_0 \\ \vdots \\ y_{n-1} \end{pmatrix} = \begin{pmatrix} \sum_i x_i y_i \\ \sum_i y_i \end{pmatrix}.$$

Hence we may rewrite the 2×2 system (C.23⊛) as

$$AA^T \begin{pmatrix} m \\ b \end{pmatrix} = A \begin{pmatrix} y_0 \\ \vdots \\ y_{n-1} \end{pmatrix}. \tag{C.23⊛}$$

We then use a numerical package to solve this linear system; in our work we used **Numpy**, in which the built-in function **`numpy.linalg.lstsq`** suffices (see listing C.2).

```
import pandas as pd
import numpy as np

#import data using panda
x_pd = pd.read_csv("~/PATH to lambda csv. file", header = None)
y_pd = pd.read_csv("~/PATH to alpha csv. file", header = None)

#convert panda data to numpy data
x = np.array(x_pd[0])
y = np.array(y_pd[0])

#define A transpose
Atr = np.vstack([x, np.ones(len(x))]).T

#get slope m and y-intercept b (from y = mx + b)
m, b = np.linalg.lstsq(Atr, y, rcond=None)[0]
```

LISTING C.2: Linear LSF code to get the line $y = mx + b$ that best fits our data of α as a function of λ.

For the sake of completion let us just point out that the generalisation of the above procedure to a fitting with an m-degree polynomial is straightforward. The coefficient matrix A takes the form

$$A \equiv \begin{pmatrix} x_0^m & \cdots & x_{n-1}^m \\ \vdots & \vdots & \vdots \\ x_0 & \cdots & x_{n-1} \\ 1 & \cdots & 1 \end{pmatrix},$$

and instead of two independent variables m and b, we have $m+1$ variables $a_0, \ldots, a_m$, so that

$$AA^T \begin{pmatrix} a_m \\ \vdots \\ a_0 \end{pmatrix} = A \begin{pmatrix} y_0 \\ \vdots \\ y_{n-1} \end{pmatrix}. \tag{C.23◎}$$

The concept of LSF extends well beyond polynomials. For instance, we may also apply a LSF to our ansatz (2.45) from Chapter 2,

$$S_E = \frac{\alpha}{T}.$$

Applying the same procedure as above, we start from a function σ which depends only on α:

$$\sigma(\alpha) = \sum_i \left(y_i - \frac{\alpha}{x_i} \right)^2,$$

where the x_i are the temperature (T) values and y_i are the action (S_E) values on our data. Next we apply standard max/min techniques to σ. Differentiating,

$$\frac{\partial \sigma}{\partial \alpha} = \sum_i 2 \left(y_i - \frac{\alpha}{x_i} \right) \left(-\frac{1}{x_i} \right) = 2 \sum_i \left(\frac{\alpha}{x_i^2} - \frac{y_i}{x_i} \right)$$

and now setting to zero,

$$0 = 2\sum_i \left(\frac{\alpha}{x_i^2} - \frac{y_i}{x_i} \right) \implies \sum_i \frac{y_i}{x_i} = \sum_i \frac{\alpha}{x_i^2},$$

we find α from the equation

$$\alpha = \frac{\sum_i \frac{y_i}{x_i}}{\sum_i x_i^{-2}},$$

which is precisely Equation (2.46) that we used on Chapter 2. For this LSF there is no need to use some numerical package, since there is no matrix multiplication/inversion involved. Our own code to find α is shown on listing C.3.

```
// functor for getting sum of previous result and square inverse of current
    element
template<typename T>
struct invsqr{
    T operator()(const T& Left, const T& Right) const{
        return (Left + pow(Right*Right, -1) );
    }
};

// S_E = alpha/T
double S_Ansatz (vector <double> temp, vector <double> action){

    // Initialize variables
    double xval_invsqr {};
    double yval_over_xval {};
    vector <double> y_over_x {};
    double alpha {};

    for (int i{0}; i <= temp.size()-1; i++) {
        y_over_x.push_back( (action.at(i))/(temp.at(i)));
    }

    yval_over_xval = accumulate(y_over_x.begin(), y_over_x.end(), 0.0 );
    y_over_x.clear();
    xval_invsqr = accumulate(temp.begin(), temp.end(), 0.0, invsqr<double
    >() );

    alpha = yval_over_xval/xval_invsqr;
    return alpha;
}
```

Listing C.3: LSF for ansatz (2.45) to determine α.

Index

Bibliography

[1] Mario Gutierrez Abed and Ian G. Moss. "Bubble nucleation at zero and nonzero temperatures". In: (June 2020). arXiv: 2006.06289 [hep-th].

[2] Miguel Alcubierre. *Introduction to 3+1 numerical relativity*. International series of monographs on physics. Oxford: Oxford Univ. Press, 2008. URL: https://cds.cern.ch/record/1138167.

[3] Miguel Alcubierre and Bernd Brügmann. "Simple excision of a black hole in (3+1)-numerical relativity". In: *Phys. Rev.* D63 (2001), p. 104006. DOI: 10.1103/PhysRevD.63.104006. arXiv: gr-qc/0008067 [gr-qc].

[4] Miguel Alcubierre et al. "Gauge conditions for long term numerical black hole evolutions without excision". In: *Phys. Rev.* D67 (2003), p. 084023. DOI: 10.1103/PhysRevD.67.084023. arXiv: gr-qc/0206072 [gr-qc].

[5] Daniela Alic et al. "Conformal and covariant formulation of the Z4 system with constraint-violation damping". In: *Phys. Rev. D* 85 (6 Mar. 2012), p. 064040. DOI: 10.1103/PhysRevD.85.064040. URL: https://link.aps.org/doi/10.1103/PhysRevD.85.064040.

[6] Greg W. Anderson and Lawrence J. Hall. "Electroweak phase transition and baryogenesis". In: *Phys. Rev. D* 45 (8 Apr. 1992), pp. 2685–2698. DOI: 10.1103/PhysRevD.45.2685. URL: https://link.aps.org/doi/10.1103/PhysRevD.45.2685.

[7] Asimina Arvanitaki et al. "String axiverse". In: *Phys. Rev. D* 81 (12 June 2010), p. 123530. DOI: 10.1103/PhysRevD.81.123530. URL: https://link.aps.org/doi/10.1103/PhysRevD.81.123530.

[8] Thomas W. Baumgarte and Stuart L. Shapiro. *Numerical Relativity: Solving Einstein's Equations on the Computer*. Cambridge University Press, 2010. DOI: 10.1017/CBO9781139193344.

[9] J.K. Beem. *Global Lorentzian Geometry*. Chapman & Hall/CRC Pure and Applied Mathematics. CRC Press, 2017. ISBN: 9781351444705. URL: https://books.google.com/books?id=c803DwAAQBAJ.

[10] Sebastiano Bernuzzi and David Hilditch. "Constraint violation in free evolution schemes: Comparing the BSSNOK formulation with a conformal decomposition of the Z4 formulation". In: *Phys. Rev. D* 81 (8 Apr. 2010), p. 084003. DOI: 10.1103/PhysRevD.81.084003. URL: https://link.aps.org/doi/10.1103/PhysRevD.81.084003.

[11] Titus Beu. *Introduction to Numerical Programming: A Practical Guide for Scientists and Engineers Using Python and C/C++*. Aug. 2014. ISBN: 9781466569676.

[12] Thomas P. Billam et al. "Simulating seeded vacuum decay in a cold atom system". In: *Phys. Rev. D* 100 (6 Sept. 2019), p. 065016. DOI: 10.1103/PhysRevD.100.065016. URL: https://link.aps.org/doi/10.1103/PhysRevD.100.065016.

[13] C. Bona and C. Palenzuela. “Dynamical shift conditions for the Z4 and BSSN formalisms”. In: *Phys. Rev. D* 69 (10 May 2004), p. 104003. DOI: 10.1103/PhysRevD.69.104003. URL: https://link.aps.org/doi/10.1103/PhysRevD.69.104003.

[14] C. Bona et al. “General-covariant evolution formalism for numerical relativity”. In: *Phys. Rev. D* 67 (10 May 2003), p. 104005. DOI: 10.1103/PhysRevD.67.104005. URL: https://link.aps.org/doi/10.1103/PhysRevD.67.104005.

[15] Carles Bona et al. “A New formalism for numerical relativity”. In: *Phys. Rev. Lett.* 75 (1995), pp. 600–603. DOI: 10.1103/PhysRevLett.75.600. arXiv: gr-qc/9412071 [gr-qc].

[16] Jonathan Braden et al. “New Semiclassical Picture of Vacuum Decay”. In: *Phys. Rev. Lett.* 123 (3 July 2019), p. 031601. DOI: 10.1103/PhysRevLett.123.031601. URL: https://link.aps.org/doi/10.1103/PhysRevLett.123.031601.

[17] Curtis G. Callan and Sidney Coleman. “Fate of the false vacuum. II. First quantum corrections”. In: *Phys. Rev. D* 16 (6 Sept. 1977), pp. 1762–1768. DOI: 10.1103/PhysRevD.16.1762. URL: https://link.aps.org/doi/10.1103/PhysRevD.16.1762.

[18] Manuela Campanelli et al. “Accurate evolutions of orbiting black-hole binaries without excision”. In: *Phys. Rev. Lett.* 96 (2006), p. 111101. eprint: arXiv:gr-qc/0511048.

[19] Chiara Caprini et al. “General Properties of the Gravitational Wave Spectrum from Phase Transitions”. In: *Phys. Rev.* D79 (2009), p. 083519. DOI: 10.1103/PhysRevD.79.083519. arXiv: 0901.1661 [astro-ph.CO].

[20] Matthew W. Choptuik. “Universality and scaling in gravitational collapse of a massless scalar field”. In: *Phys. Rev. Lett.* 70 (1 Jan. 1993), pp. 9–12. DOI: 10.1103/PhysRevLett.70.9. URL: https://link.aps.org/doi/10.1103/PhysRevLett.70.9.

[21] Katy Clough. “Scalar Fields in Numerical General Relativity: Inhomogeneous inflation and asymmetric bubble collapse”. PhD thesis. Cham: King’s Coll. London, 2017. DOI: 10.1007/978-3-319-92672-8. arXiv: 1704.06811 [gr-qc].

[22] Katy Clough et al. “Robustness of Inflation to Inhomogeneous Initial Conditions”. In: *JCAP* 1709.09 (2017), p. 025. DOI: 10.1088/1475-7516/2017/09/025. arXiv: 1608.04408 [hep-th].

[23] Sidney Coleman. “Fate of the false vacuum: Semiclassical theory”. In: *Phys. Rev. D* 15 (10 May 1977), pp. 2929–2936. DOI: 10.1103/PhysRevD.15.2929. URL: https://link.aps.org/doi/10.1103/PhysRevD.15.2929.

[24] Heling Deng and Alexander Vilenkin. “Primordial black hole formation by vacuum bubbles”. In: *JCAP* 1712.12 (2017), p. 044. DOI: 10.1088/1475-7516/2017/12/044. arXiv: 1710.02865 [gr-qc].

[25] O. Fialko et al. “Fate of the false vacuum: Towards realization with ultra-cold atoms”. In: *EPL (Europhysics Letters)* 110.5 (June 2015), p. 56001. DOI: 10.1209/0295-5075/110/56001. URL: https://doi.org/10.1209%2F0295-5075%2F110%2F56001.

[26] Y. Fourès-Bruhat. “Théorème d’existence pour certains systèmes d’équations aux dérivées partielles non linéaires”. In: *Acta Math.* 88 (1952), pp. 141–225. DOI: 10.1007/BF02392131. URL: https://doi.org/10.1007/BF02392131.

[27] Éric Gourgoulhon. $3+1$ *Formalism in General Relativity: Bases of Numerical Relativity*. Springer, 2012.

[28] Carsten Gundlach and Jose M. Martin-Garcia. "Critical phenomena in gravitational collapse". In: *Living Rev. Rel.* 10 (2007), p. 5. DOI: 10.12942/lrr-2007-5. arXiv: 0711.4620 [gr-qc].

[29] Carsten Gundlach et al. "Constraint damping in the Z4 formulation and harmonic gauge". In: *Classical and Quantum Gravity* 22.17 (Aug. 2005), pp. 3767–3773. DOI: 10.1088/0264-9381/22/17/025. URL: https://doi.org/10.1088%2F0264-9381%2F22%2F17%2F025.

[30] Mark Hannam et al. "Wormholes and trumpets: The Schwarzschild spacetime for the moving-puncture generation". In: *Phys. Rev. D* 78 (2008), p. 064020. DOI: 10.1103/PhysRevD.78.064020. arXiv: 0804.0628 [gr-qc].

[31] S. W. Hawking, I. G. Moss, and J. M. Stewart. "Bubble Collisions in the Very Early Universe". In: *Phys. Rev.* D26 (1982), p. 2681. DOI: 10.1103/PhysRevD.26.2681.

[32] Mark Hindmarsh et al. "Gravitational waves from the sound of a first order phase transition". In: *Phys. Rev. Lett.* 112 (2014), p. 041301. DOI: 10.1103/PhysRevLett.112.041301. arXiv: 1304.2433 [hep-ph].

[33] Leanne D. Duffy Karl van Bibber. "Axions as Dark Matter Particles". arXiv:0904.3346v1. Apr. 2009.

[34] Pablo Laguna, Hannu Kurki-Suonio, and Richard A. Matzner. "Inhomogeneous inflation: The initial-value problem". In: *Phys. Rev. D* 44 (10 Nov. 1991), pp. 3077–3086. DOI: 10.1103/PhysRevD.44.3077. URL: https://link.aps.org/doi/10.1103/PhysRevD.44.3077.

[35] Mikko Laine and Aleksi Vuorinen. *Basics of Thermal Field Theory*. Vol. 925. Springer, 2016. DOI: 10.1007/978-3-319-31933-9. arXiv: 1701.01554 [hep-ph].

[36] A. Lichnerowicz. "L'intégration des équations de la gravitation relativiste et le problème des n corps". In: *J. Math. Pures Appl.* 23 (1944), p. 37.

[37] Andrei D. Linde. "Decay of the False Vacuum at Finite Temperature". In: *Nucl. Phys. B* 216 (1983). [Erratum: Nucl.Phys.B 223, 544 (1983)], p. 421. DOI: 10.1016/0550-3213(83)90072-X.

[38] Ariel M©gevand and Santiago Ramrez. "Bubble nucleation and growth in very strong cosmological phase transitions". In: *Nuclear Physics B* 919 (2017), pp. 74–109. ISSN: 0550-3213. DOI: https://doi.org/10.1016/j.nuclphysb.2017.03.009. URL: http://www.sciencedirect.com/science/article/pii/S0550321317300895.

[39] Florent Michel and Ian G. Moss. "Relativistic collapse of axion stars". In: *Phys. Lett.* B785 (2018), pp. 9–13. DOI: 10.1016/j.physletb.2018.07.063. arXiv: 1802.10085 [gr-qc].

[40] C. W. Misner, K. S. Thorne, and J. A. Wheeler. *Gravitation*. Ed. by Misner, C. W., Thorne, K. S., & Wheeler, J. A. 1973.

[41] Kyohei Mukaida and Masaki Yamada. "False Vacuum Decay Catalyzed by Black Holes". In: *Phys. Rev.* D96.10 (2017), p. 103514. DOI: 10.1103/PhysRevD.96.103514. arXiv: 1706.04523 [hep-th].

[42] T. Nakamura. "3D numerical relativity." In: *Relativistic Cosmology*. Ed. by M. Sasaki. 1994, pp. 155–182.

[43] Harald P. Pfeiffer and James W. York Jr. "Extrinsic curvature and the Einstein constraints". In: *Phys. Rev.* D67 (2003), p. 044022. DOI: 10.1103/PhysRevD.67.044022. arXiv: gr-qc/0207095 [gr-qc].

[44] Frans Pretorius. "Evolution of binary black hole spacetimes". In: *Phys. Rev. Lett.* 95 (2005), p. 121101. DOI: 10.1103/PhysRevLett.95.121101. eprint: arXiv:gr-qc/0507014.

[45] Frans Pretorius. "Numerical relativity using a generalized harmonic decomposition". In: *Classical and Quantum Gravity* 22.2 (Jan. 2005), pp. 425–451. DOI: 10.1088/0264-9381/22/2/014. URL: https://doi.org/10.1088%2F0264-9381%2F22%2F2%2F014.

[46] H. Ringström. *The Cauchy Problem in General Relativity*. ESI lectures in mathematics and physics. European Mathematical Society, 2009. ISBN: 9783037190531. URL: https://books.google.co.uk/books?id=Bn%5C_cC7QwQ0MC.

[47] Nicolas Sanchis-Gual et al. "Fully covariant and conformal formulation of the Z4 system in a reference-metric approach: Comparison with the BSSN formulation in spherical symmetry". In: *Phys. Rev. D* 89 (10 May 2014), p. 104033. DOI: 10.1103/PhysRevD.89.104033. URL: https://link.aps.org/doi/10.1103/PhysRevD.89.104033.

[48] Olivier Sarbach et al. "Hyperbolicity of the BSSN system of Einstein evolution equations". In: *Phys. Rev.* D66 (2002), p. 064002. DOI: 10.1103/PhysRevD.66.064002. arXiv: gr-qc/0205064 [gr-qc].

[49] P. Sikivie. "Dark Matter Axions". arXiv:0909.0949v1. Sept. 2009.

[50] R.M. Wald. *General Relativity*. University of Chicago Press, 1984. ISBN: 9780226870328. URL: https://books.google.co.uk/books?id=ibSdQgAACAAJ.

[51] J. W. York Jr. "Kinematics and dynamics of general relativity". In: *Sources of Gravitational Radiation*. Ed. by L. L. Smarr. Cambridge and New York: Cambridge University Press, 1979, pp. 83–126.

[52] James W. York. "Conformal "Thin-Sandwich" Data for the Initial-Value Problem of General Relativity". In: *Phys. Rev. Lett.* 82 (7 Feb. 1999), pp. 1350–1353. DOI: 10.1103/PhysRevLett.82.1350. URL: https://link.aps.org/doi/10.1103/PhysRevLett.82.1350.

[53] James W. York. "Conformally invariant orthogonal decomposition of symmetric tensors on Riemannian manifolds and the initial-value problem of general relativity". In: *Journal of Mathematical Physics* 14.4 (1973), pp. 456–464. DOI: 10.1063/1.1666338. eprint: https://doi.org/10.1063/1.1666338. URL: https://doi.org/10.1063/1.1666338.

[54] James W. Jr. York. "Covariant decompositions of symmetric tensors in the theory of gravitation". en. In: *Annales de l'I.H.P. Physique théorique* 21.4 (1974), pp. 319–332. URL: http://www.numdam.org/item/AIHPA_1974__21_4_319_0.